



Since January 2020 Elsevier has created a COVID-19 resource centre with free information in English and Mandarin on the novel coronavirus COVID-19. The COVID-19 resource centre is hosted on Elsevier Connect, the company's public news and information website.

Elsevier hereby grants permission to make all its COVID-19-related research that is available on the COVID-19 resource centre - including this research content - immediately available in PubMed Central and other publicly funded repositories, such as the WHO COVID database with rights for unrestricted research re-use and analyses in any form or by any means with acknowledgement of the original source. These permissions are granted for free by Elsevier for as long as the COVID-19 resource centre remains active.

# 8

# Pathology of Pulmonary Infection

RICHARD L. KRADIN, EUGENE J. MARK

## Introduction

- Approach to Sampling for Infection
- Transbronchial Biopsy
- Fine-Needle Aspiration Biopsy
- Transbronchial Needle Aspiration Biopsy
- Video-Assisted and Open Thoracoscopic Biopsy

## Handling Lung Biopsies

### Pulmonary Injury in Infection

- Pulmonary Host Response
- Diffuse Alveolar Damage
- RNA Viruses
- DNA Viruses
- Other Atypical Pneumonias
- Bacterial Infections
- Mycobacterial Infection
- Fungal Infection Due to Yeasts
- Hyphate Fungi
- Dematiaceous (Pigmented) Fungi
- Parasites

### Microbes Associated With Bioterrorism

- Anthrax
- Yersinia pestis* (Plague Pneumonia)
- Francisella tularensis* (Tularemia Pneumonia)

### Pleural Infection

## Introduction

In its role as a portal between the ambient environment and the internal milieu, the lung is also the most frequent site of serious infection. A variety of factors predispose to pulmonary infection, including distortions in lung anatomy, decreased mucociliary clearance, and abnormal cellular and humoral immunity. Iatrogenic immunosuppression and that resulting from human immunodeficiency virus type 1 (HIV-1) infection have led to the emergence of opportunistic infections that can present diagnostic challenges for the surgical pathologist.

Because a variety of microbes can potentially infect the lung and the histopathology of noninfectious conditions frequently mimic infection, the differential diagnosis of pulmonary infection is often broad. Although in many cases the clinical history,

radiographic findings, and the noninvasive sampling of secretions can establish the cause of infection, lung biopsy is required at times. How to approach the sampling of the lung in infection is an area of some complexity, so that it is incumbent upon both clinicians and pathologists to recognize the advantages and limitations of the currently available methods.

## Approach to Sampling for Infection

The optimal approach to sampling the lung for infection depends primarily on whether disease is localized or diffuse (Box 8.1). In immunosuppressed patients, diffuse pulmonary infiltrates due to infection can often be diagnosed by sputum induction or bronchoalveolar lavage (BAL). This is particularly the case when the microbial burden is also large. Noninvasive approaches are less sensitive than biopsy in diagnosing localized infections, and they cannot distinguish a colonizing commensal from an invasive pathogen.<sup>1</sup> In addition, the lung biopsy affords an opportunity to evaluate host immunocompetence with accuracy that cannot be achieved by noninvasive or minimally invasive methods. Lung biopsy may also be required to exclude infection definitively and to establish noninfective diagnoses (e.g., acute lung injury due to chemotherapy).

Pathologists prefer to examine generous samplings of lung because diagnoses based on such biopsies are more accurate, yield a greater degree of information with respect to host immunity, and may reveal other potentially treatable disorders.<sup>2</sup>

## Transbronchial Biopsy

The lung has approximately the surface area of a tennis court; thus sampling error is an unavoidable pitfall in diagnostic pulmonary pathology. The transbronchial biopsy (TBB) preferentially samples peribronchiolar lung tissue, yielding tissue fragments of 1 to 3 mm in diameter.<sup>3</sup> However, peripherally located lung lesions often cannot be accessed by this approach.

TBB is generally adequate for diagnosing diffuse pulmonary infections and peribronchiolar granulomatous diseases, such as sarcoidosis and lymphangitic spread of tumor or tuberculosis, but at times the findings of a TBB can be nonspecific and misleading. For example, “organizing pneumonia” in a TBB may represent a nonspecific reaction adjacent to focus of infection or malignancy, a nonspecific manifestation of chemotherapy effect, aspiration, or cryptogenic disease. For this reason, the findings gleaned from a TBB must always be thoughtfully correlated with clinical and radiographic findings.<sup>4</sup>

### • BOX 8.1 Approach to the Isolation of Pulmonary Microorganisms

Expectorated sputum  
 Induced sputum  
 Bronchoalveolar lavage  
 Fine-needle aspirate (1 mm)  
 Bronchial biopsy (1-3 mm)  
 Transbronchial biopsy (1-3 mm)  
 Transbronchial needle biopsy (1 mm)  
 Video-assisted thoracoscopic biopsy (2-3 cm)  
 Open-lung biopsy (2-3 cm)  
 Surgical lobectomy  
 Autopsy

### Fine-Needle Aspiration Biopsy

Computed tomography (CT)-guided fine-needle aspiration biopsies have a high yield in the diagnosis of peripheral nodular infiltrates.<sup>5</sup> Biopsies can be semiliquid or include a 1-mm core of tissue. When performed with the assistance of a cytotechnologist, rapid diagnoses can be proffered by examining stained smears directly at the bedside. Fine-needle aspirates are useful in diagnosing localized infections, and cytopathologists can also suggest the pattern of inflammation based on the types of inflammatory cell subsets in the sample and the presence or absence of necrosis.

### Transbronchial Needle Aspiration Biopsy

Transbronchial needle aspiration biopsy of regional lymph node groups is often a low-yield procedure because nonspecific reactive regional lymphadenitis is common in the presence of pulmonary infection.<sup>6</sup> The procedure is prone to artifacts that may present diagnostic difficulties for the surgical pathologist. However, when adopted judiciously, this approach may be adequate for the diagnosis of infection, as in one series in which approximately 50% of cases of tuberculous lymphadenitis were accurately diagnosed.

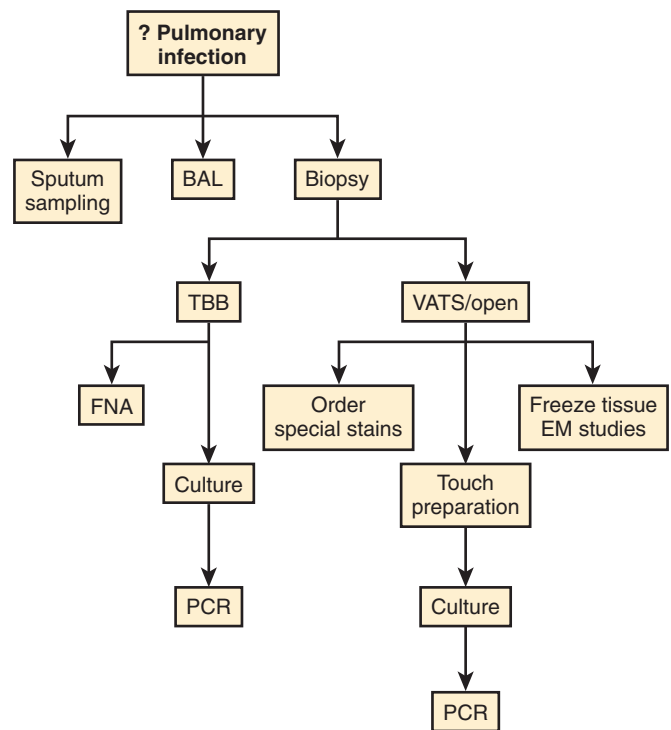
The technique of endobronchial ultrasound-guided transbronchial and needle biopsies has become standard procedure in many centers. This approach increases the diagnostic yield for localized lesions and allows for mediastinoscopic evaluation. It may be particularly helpful in patients with lung tuberculosis with mediastinal adenopathy.<sup>7</sup>

### Video-Assisted and Open Thoracoscopic Biopsy

Video-assisted thoracoscopic surgical (VATS) lung biopsy has replaced open thoracotomy biopsy as the optimal approach for obtaining large samples of lung.<sup>8</sup> The procedure is associated with modest and acceptable morbidity, has the advantage of allowing direct access to widely separated lung segments, and provides generously sized wedge biopsies of 2 to 3 cm. Consequently, VATS should be considered a first line approach when a timely accurate diagnosis is essential.

### Handling Lung Biopsies

Appropriate handling of the lung biopsy is essential for obtaining the highest diagnostic yield<sup>9</sup> (Fig. 8.1). Sampling the lung for microbiologic culture should ideally take place under sterile



• **Figure 8.1** Approach to the handling of lung biopsies. BAL, Bronchoalveolar lavage; EM, electron microscopy; FNA, fine needle aspiration; PCR, polymerase chain reaction; TBB, transbronchial biopsy; VATS, video-assisted thoracoscopic surgical.

conditions in the operating room, but the pathologist processing the biopsy should try to ascertain that all necessary diagnostic tests have been ordered and be prepared to harvest additional samples for testing that may have been overlooked. When preparing tissue for microbiologic isolation, the lung should be minced rather than crushed because hyphate fungi (e.g., *Zygomycoses* spp.) may fail to grow in culture following maceration.<sup>10</sup> A pathologist should not place a lung biopsy directly into fixative, without first considering a diagnosis of infection. If questions arise as to which tests to order or how best to transport the specimen to the laboratory, discussions with the hospital microbiology laboratory staff or a hospital infectious disease specialist will be of assistance.

The examination of touch imprints of lung tissue is a simple and rapid way of identifying pathogens. Touch imprints can be prepared from foci of pulmonary consolidation, necrosis, or supuration and rapidly stained for bacteria, mycobacteria, and fungi in the surgical pathology suite or the microbiology laboratory. Concomitantly biopsies may be harvested for ultrastructural analysis, polymerase chain reaction (PCR) assays, or research purposes. For large biopsies, it may be possible to inflate the lung with 5% formalin via a small (23 to 25) gauge needle to optimize subsequent histologic examination.

## Pulmonary Injury in Infection

### Pulmonary Host Response

The diagnosis of infection requires both an interpretation of the morphologic changes evoked by the pathogen and the identification of a pathogen in situ. The pattern of pulmonary inflammation often suggests the route of entry of an infectious agent and may help to narrow the diagnostic possibilities. It is necessary to be

familiar with the multiplicity of response patterns evoked by infection and to recognize that these can vary depending on the route of entry, pathogen load, and the competence of host defenses. For example, whereas herpesvirus 1 can produce a miliary pattern of fibrinoid necrosis in an immunosuppressed patient with viremia, it can also cause ulceration of the tracheo-bronchial mucosa in a chronically intubated patient.

Microbes are rarely identified randomly or diffusely in infections; rather, they tend to be compartmentalized, so that substantial effort may be wasted in searching for them where they are not likely to be found. Mycobacteria and fungi are usually localized in areas of necrosis; *Rickettsia* spp. and *Bartonella* spp. largely target the microvasculature; viruses tend to attack the airways; thus the surgical pathologist must both be acquainted with the pulmonary microanatomy and with the preferential localization of microbes in pulmonary tissues.

### Anatomy of Pulmonary Defense

The lung is an elastic organ composed of dichotomously branching conducting airways terminating in alveolated surfaces.<sup>11</sup> It has a dual blood supply; the pulmonary circulation arises from the cardiac right ventricle and carries deoxygenated blood at low arterial pressures to the alveolar surfaces; the bronchial circulation arises from branches of the aorta and nourishes both the airways and the connective tissue stroma with oxygenated blood. All new growths within the lung, including regions of infective bronchiectasis, lung abscess, and tuberculous cavities, will evoke neoangiogenesis from the bronchial microcirculation.

Two systems of pulmonary lymphatic channels drain the lung either centrifugally towards the hilum, or centripetally along the convexities of the pleural surfaces before coursing to the hilar lymph nodes. From the lymph nodes, organisms can enter the systemic circulation and spread widely throughout the body. For example, group A streptococci spp. will rapidly invade pulmonary lymphatics and course to the pleura to produce an empyema.

### Pulmonary Defenses

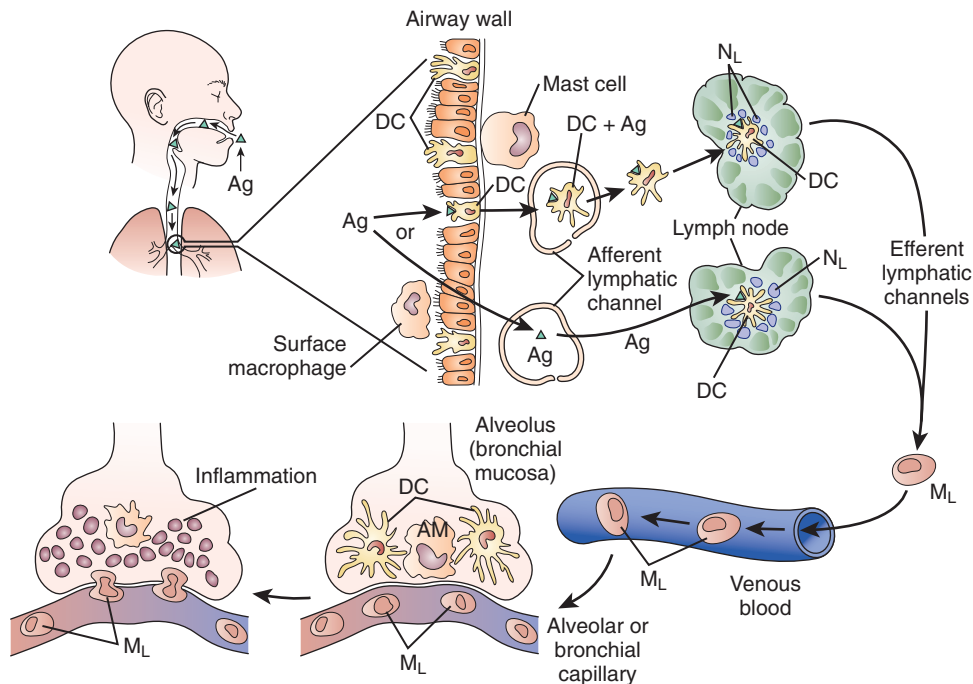
Most microbes are small (<5  $\mu\text{M}$ ) and can penetrate to the distal gas-exchanging surfaces of the lung, although the majority are excluded by the defenses of the upper airways or deposit along the conducting airways to be cleared by the mucociliary escalator. Humoral factors, including secretory immunoglobulin A (sIgA) and defensins released by airway cells, limit microbial penetration into tissues. Airway mucosal dendritic cells (DCs) trap microbial antigens and transport them to regional lymph nodes, where they are processed and present to both T and B lymphocytes, evoking adaptive immunity (Fig. 8.2).<sup>12</sup>

Ulceration or thickening of the gas-exchange surface limits diffusion of oxygen and carbon dioxide. For this reason, the alveolus is under normal conditions maintained sterile by resident macrophages that scavenge inhaled particulates and secrete monokines, including interleukin (IL)-10 and transforming growth factor (TGF)- $\beta$ , that locally suppress inflammation and promote immunotolerance.

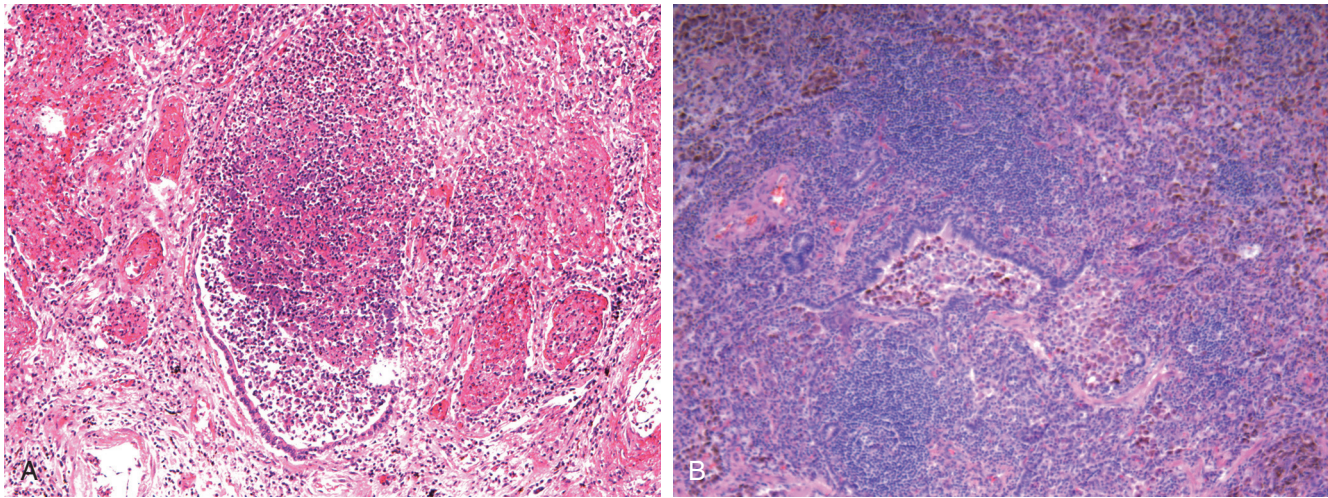
When the alveolar lining is injured or when the number of invading organisms exceeds the phagocytotic capacities of resident macrophages, neutrophils and exudate monocytes are recruited to sites of lung infection.<sup>13</sup> Even small numbers of virulent pathogens can greatly amplify inflammation via the release of chemokines, cytokines, and complement by host immune cells. These defenses promote the clearance of infection but can also damage the lung. Lung biopsies afford the pathologist a unique opportunity to assess these dynamic responses directly, in addition to identifying a causative pathogen.

### Patterns of Lung Injury Due to Infection

A number of generic patterns of inflammation may be evoked by infection, but how they are distributed is often specific to the involved tissue (Box 8.2). Clinicians and radiologists have developed classification systems with respect to pulmonary infection



• **Figure 8.2** Pulmonary immune anatomy. Ag, Antigen; DC, dendritic cells; NL, lymph node; ML, macrophage.



• **Figure 8.3** A, Acute bronchiolitis showing neutrophilic exudate in the lumen of a small airway B, Chronic lymphocytic bronchiolitis.

### • BOX 8.2 Injury Patterns Seen in Lung Infection

Tracheobronchitis  
 Bronchiolitis (acute, chronic, necrotizing)  
 Bronchiectasis  
 Bronchopneumonia (acute, chronic, necrotizing)  
 Eosinophilic pneumonia  
 Pulmonary hemorrhage  
 Pulmonary edema  
 Diffuse alveolar damage  
 Pulmonary nodules and micronodules  
 Cavitory pneumonia  
 Vasculitis  
 Capillary dissemination  
 Lymphatic dissemination  
 Pulmonary hypertension  
 Pleuritis

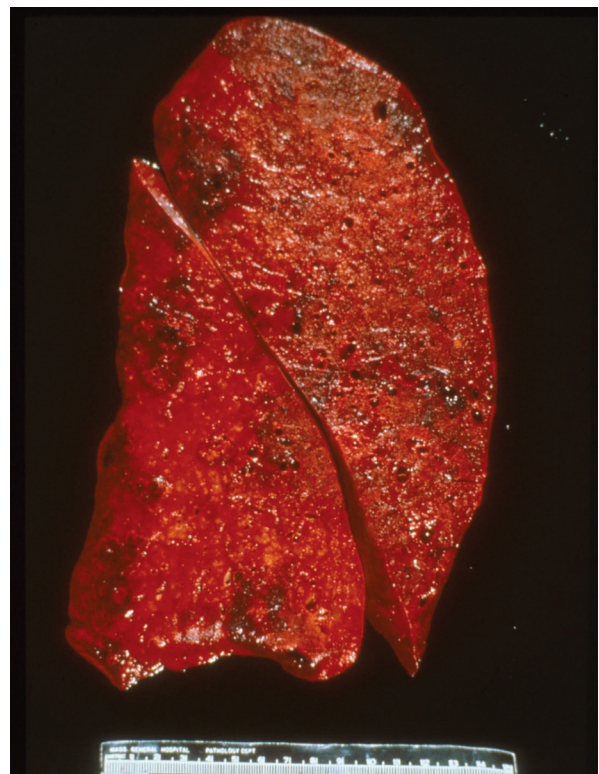
that are distinct from those of pathologists. For example, a variety of infectious agents yield a picture that clinicians generically term “atypical” interstitial pneumonia, to differentiate them from “typical” bacterial pneumonias.<sup>14</sup> However, the histopathology of an “atypical pneumonia” may be centered on the lung interstitium, small airways, or the alveolar spaces; and because this text is aimed primarily at surgical pathologists, pathologic schemas of classification will be adopted here, with reference to their clinical counterparts when appropriate.

#### Tracheobronchitis/Bronchiolitis and Miliary Infection

Many pathogens target the conducting airways to produce tracheobronchitis and bronchiolitis. Pathologic changes range from superficial erosion of the lining respiratory epithelium, to ulceration and repair. The type of inflammation will vary from intraluminal neutrophilic exudates (Fig. 8.3A) to airway cuffing by lymphocytes and histiocytes (see Fig. 8.3B), depending on the offending pathogen.

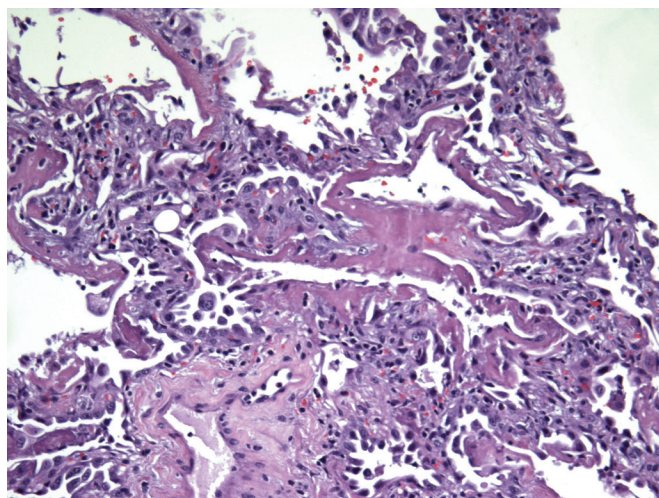
#### Diffuse Alveolar Damage

Disease of the gas-exchange alveolar surfaces can show a spectrum of changes, including acute ulceration and septal infiltration by

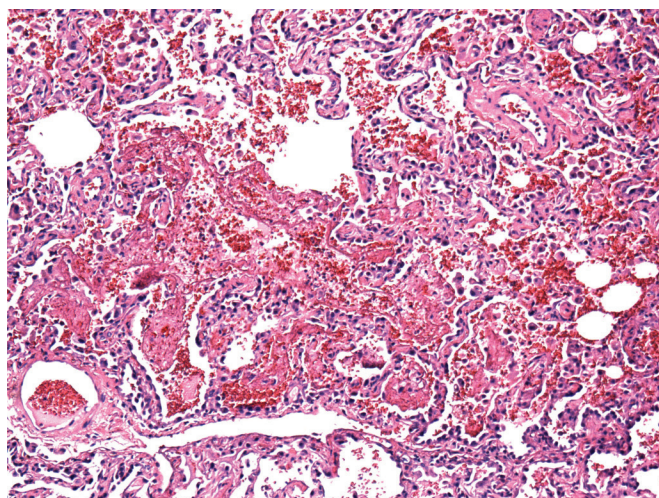


• **Figure 8.4** Consolidated lung with the beefy red appearance of diffuse alveolar damage in a patient who died of influenza pneumonia.

chronic inflammatory cells.<sup>15</sup> Diffuse alveolar damage (DAD) represents a global injury to the gas-exchange surfaces due to disruption of the blood–air barrier leading to exudative edema and fibrosis and resulting in severely impaired blood and tissue oxygenation (Fig. 8.4). The sine qua non of DAD is the *hyaline membrane* that is composed of necrotic alveolar lining cell debris and an extravascular fibrin coagulum apposed to an ulcerated alveolar wall, which yields a gel that entraps lung water (Fig. 8.5). Although DAD is the most frequent pathologic cause of the clinical entity, the adult respiratory distress syndrome (ARDS),



• **Figure 8.5** Hyaline membrane lining an alveolar duct in diffuse alveolar damage



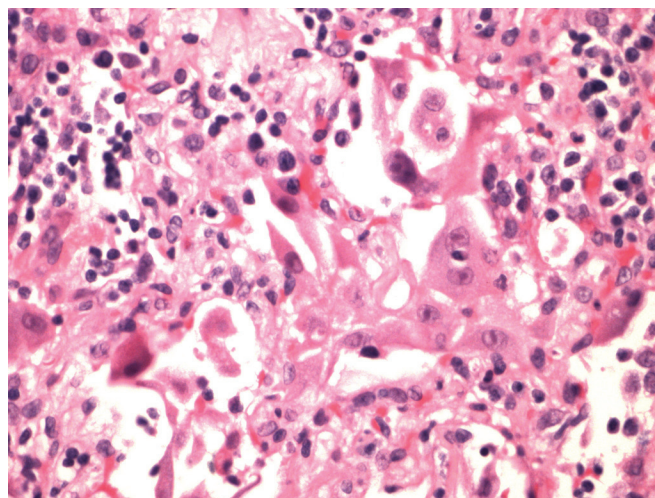
• **Figure 8.6** Lung in exudative phase of diffuse alveolar damage with hemorrhage and inflammation. This finding should not be overinterpreted as evidence of infection.

### • BOX 8.3 Causes of Diffuse Alveolar Damage

Pulmonary infection  
 Systemic infection with sepsis  
 Vasodilatory shock  
 Aspiration  
 Drugs  
 Radiation  
 Trauma  
 Accelerated phase of chronic interstitial pneumonia  
 Idiopathic

other diseases, including extensive bronchopneumonia and acute pulmonary hemorrhage, can also lead to ARDS (Box 8.3). The pathology of the exudative phase of DAD can focally mimic acute bacterial infection, and one must maintain a high threshold for making the diagnosis of acute infection in this setting (Fig. 8.6).

Viruses are the most common infectious cause of DAD, although bacteria, fungi, and parasites also produce diffuse lung



• **Figure 8.7** Lung in reparative phase of acute lung injury showing highly atypical alveolar lining cells with changes that mimic viral infection.

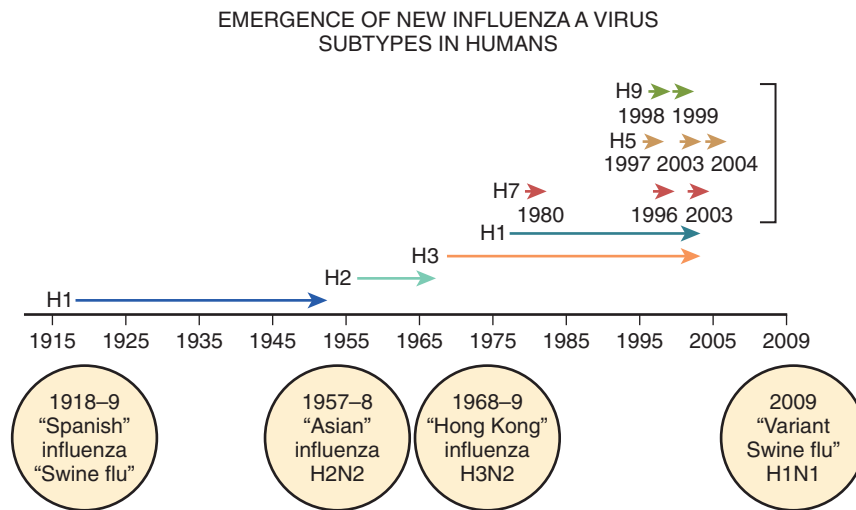
**TABLE 8.1** Changes Seen in Virus-Infected Lung Cells

Organism	Cytopathic Change
Influenza	No cytopathic change
SARS (Coronavirus)	No cytopathic change
Respiratory syncytial virus	Polykaryons, inconspicuous cytoplasmic inclusions
Parainfluenza	Polykaryons, intracytoplasmic inclusions
Measles	Polykaryons, intranuclear inclusions
Adenovirus	Intranuclear inclusions (smudge cells)
Herpesvirus	Intranuclear inclusions, polykaryons
Cytomegalovirus	Intranuclear and cytoplasmic inclusions
Varicella-Zoster	Intranuclear inclusions
EBV	No cytopathic change

EBV, Epstein-Barr virus; SARS, severe acute respiratory syndrome.

injury. DAD can result from sepsis that complicates either pulmonary or extrapulmonary infection. Whenever DAD is present, the surgical pathologist must examine the lung for evidence of viral-induced cytopathic changes. These vary with the type of viral infection, and some viruses do not produce cytopathic changes, so that viral infection is always in the differential diagnosis of DAD (Table 8.1). A common pitfall in diagnosis is to mistake the hyperplastic reparative alveolar type II cells of DAD that can exhibit prominent nucleoli with viral infected cells, particularly when examining rapidly frozen sections, in which these changes may be especially prominent (Fig. 8.7).

Due to the introduction of noninvasive and rapid PCR diagnoses of respiratory viruses from nasal swabs and respiratory secretions, it has become increasingly unusual to encounter these infections in the routine practice of surgical pathology, except at autopsy in lethal cases.



• **Figure 8.8** Neuraminidase and hemagglutinin expression of *Influenza* correlates with epidemic outbreaks.

## RNA Viruses

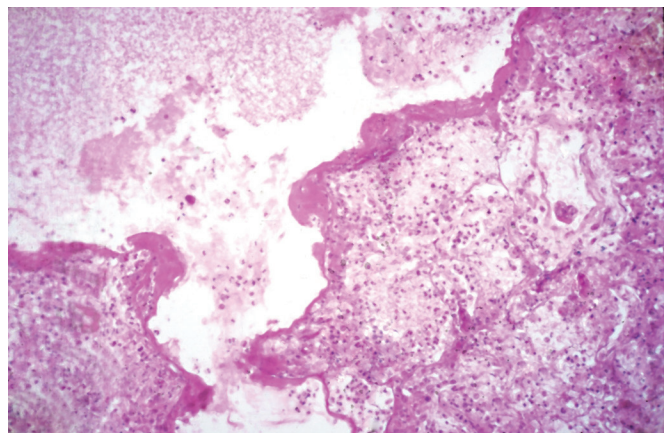
### Influenza

Influenza is a rod-shaped RNA virus that can cause either bronchiolitis or DAD without apparent cytopathic changes. Influenza infection recurs each year due to a high incidence of mutation of its hemagglutinin (H) and neuraminidase (N) antigens, and these determine its virulence. When mutations occur concomitantly in both the H and N antigens, pandemics with potentially high degrees of morbidity due to the lack of immunity may ensue (Fig. 8.8).<sup>16</sup> H1N1 influenza was responsible for an epidemic in this country, and sporadic cases have persisted. Patients dying with this infection were often relatively young and their lungs showed DAD with prominent areas of hemorrhage.<sup>17</sup> Currently, epidemiologists are carefully monitoring the evolution of an avian influenza in Southeast Asia for evidence of spread to humans.

Influenza is the most common cause of viral pneumonia, although most cases are subclinical. The virus most commonly causes a diffuse tracheobronchitis/bronchiolitis in which the normal ciliated respiratory epithelium is sloughed.<sup>18</sup> However, when DAD develops, it can carry a high mortality even in the absence of acute bacterial superinfection (Fig. 8.9).<sup>19</sup> The lungs in DAD due to influenza in patients with prolonged survival often develop prominent squamous metaplasia of bronchoalveolar lining cells (Fig. 8.10A). Although these findings are characteristic, they are also nonspecific, so that immunostains, in situ hybridization, electron microscopy, or viral antigen detection may be required to establish the diagnosis (see Fig. 8.10B). Superinfection by pyogenic bacteria, including *Haemophilus influenzae*, group A *Streptococcus*, and *Staphylococcus* are a well-recognized complication and may mask evidence of a healing influenza infection.

### Severe Acute Respiratory Syndrome

The epidemic of the zoonotic coronavirus infection termed severe acute respiratory syndrome (SARS) fortunately has not recurred, as the virus led to acute respiratory distress with high mortality. The lungs at autopsy showed DAD with scattered multinucleated giant cells of uncertain diagnostic significance. The virus otherwise produced no cytopathic changes and was essentially histologically indistinguishable from DAD due to influenza.<sup>20</sup>



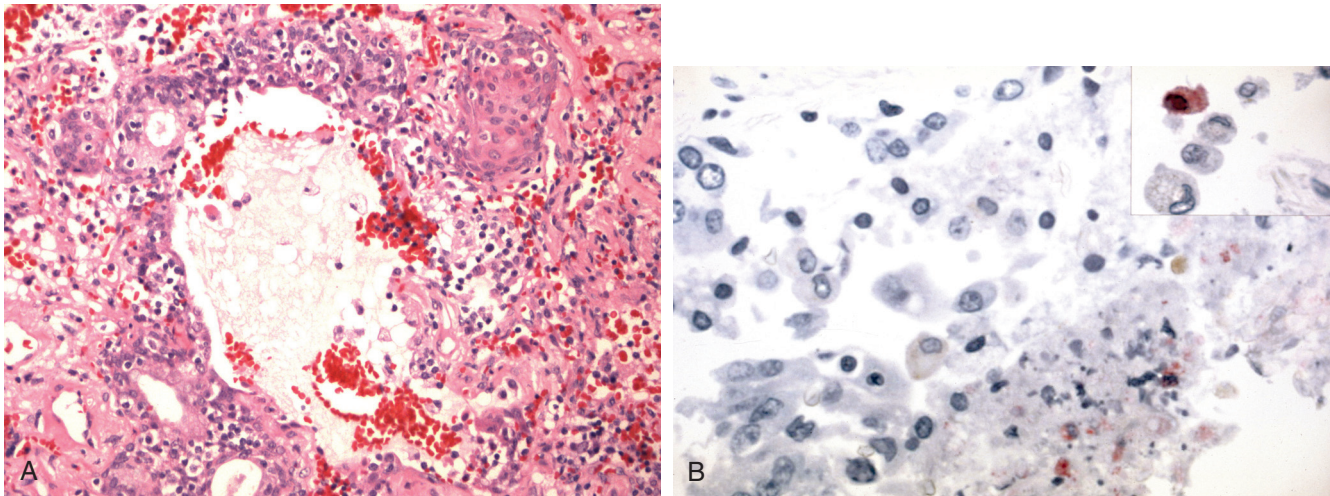
• **Figure 8.9** Lung from a patient who died in the 1918 influenza epidemic showing diffuse alveolar damage with no cytopathic changes.

### Middle East Respiratory Syndrome

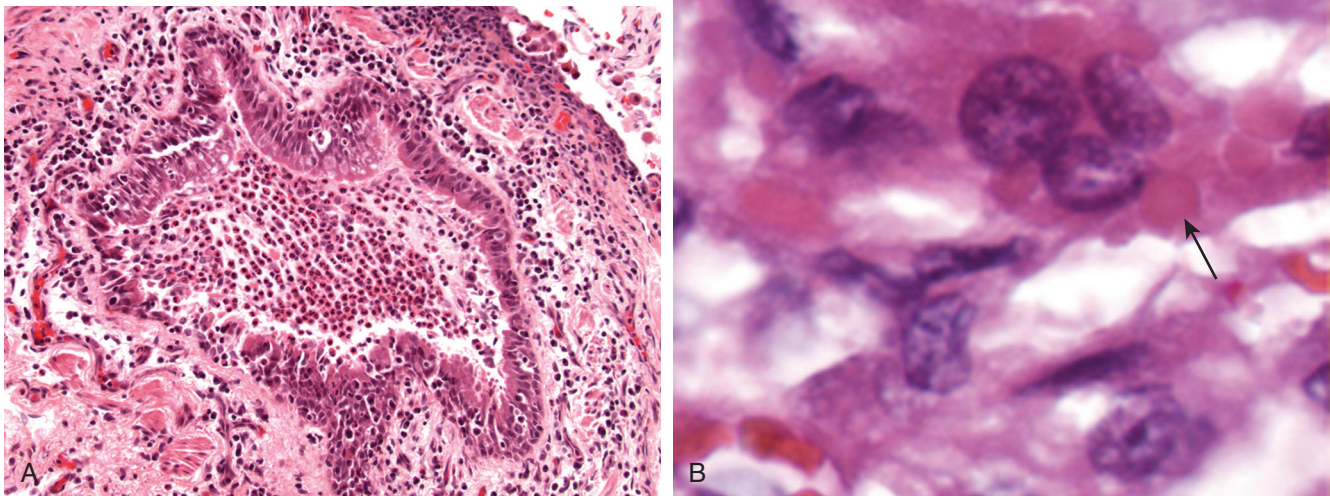
Like SARS, Middle East respiratory syndrome (MERS) is also caused by a coronavirus.<sup>21</sup> The first cases were reported in Saudi Arabia in the fall of 2012, but cases had occurred in Jordan earlier that year. All cases of MERS to date have been linked through travel to or residence in countries in and near the Arabian Peninsula. The largest known outbreak of MERS outside the Arabian Peninsula occurred in the Republic of Korea in 2015 and was associated with a traveler returning from the Arabian Peninsula. MERS-Coronavirus (CoV) spreads from ill people to others via close contact, such as caring for or living with an infected person, and patients have ranged in age from infants to nonagenarians. Unfortunately, the detailed histopathology of patients with MERS has not been reported but is likely to resemble that due to other coronaviruses.

### Respiratory Syncytial Virus

Respiratory syncytial virus (RSV) causes a benign respiratory infection in older children and has been recognized as a cause of adult community-acquired pneumonia, acute bronchiolitis, and



• **Figure 8.10** **A**, Lung in patient with diffuse alveolar damage due to influenza showing prominent squamous metaplasia of terminal airways. **B**, Immunostain confirms the presence of influenza A.



• **Figure 8.11** **A**, Acute bronchiolitis in respiratory syncytial virus (RSV). **B**, Multinucleated epithelial cells in RSV contain inconspicuous eosinophilic cytoplasmic inclusions (*arrow*).

DAD in the immunosuppressed host.<sup>22</sup> The infection targets the respiratory lining epithelium producing syncytial giant cells with nonprominent eosinophilic inclusions (Fig. 8.11). Human metapneumovirus produces changes comparable to RSV and must be included in its differential diagnosis.

### Parainfluenza

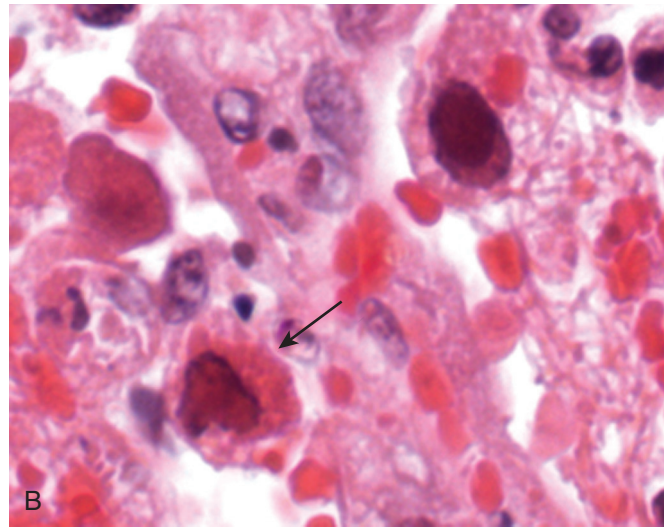
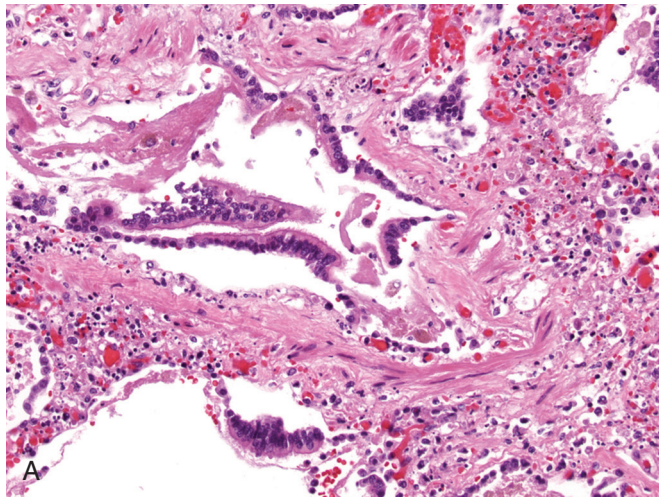
Parainfluenza causes a benign upper respiratory infection in children that rarely progresses to DAD, although severe disease may develop in the immunosuppressed host. Like RSV, parainfluenza produces bronchiolitis and DAD with syncytial giant cells and epithelial cell intracytoplasmic inclusions.<sup>23</sup> However, the

latter are both more frequent and larger than those seen in RSV (Fig. 8.12).

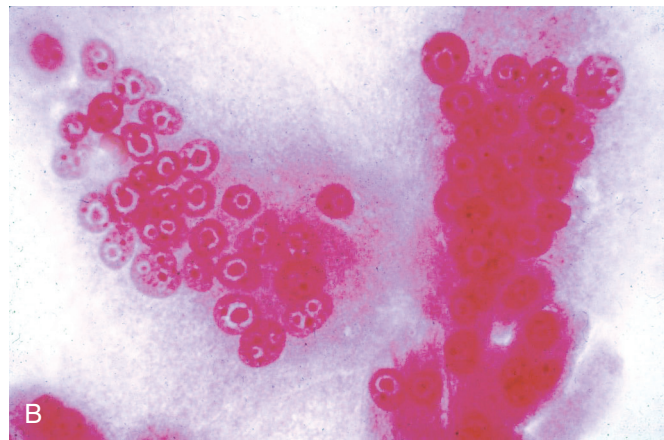
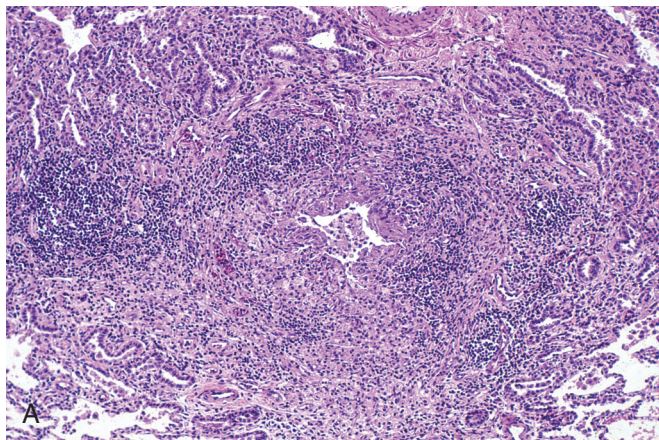
### Measles

Measles pneumonia is a rare and serious complication of the childhood viral exanthem. The pathology of pulmonary measles infection ranges from bronchiolitis (Fig. 8.13A) to DAD. The virus produces multikaryons with prominent glassy eosinophilic nuclear Cowdry type A inclusions (see Fig. 8.13B).<sup>24</sup> The differential diagnosis of giant cell pneumonia includes RSV and hard-metal pneumoconiosis; however, the giant cells in the latter disorders lack intranuclear inclusions, and hard-metal





• **Figure 8.12** A, Bronchiolitis in parainfluenza infection. B, Epithelial cell showing eosinophilic inclusions that are both larger and more frequent than in respiratory syncytial virus (*arrow*).



• **Figure 8.13** A, Chronic inflammation involving a small airway in a patient with measles. B, Multinucleated cell showing glassy nuclear Cowdry type A inclusions.

pneumoconiosis specifically lacks the exudative features of an acute infection.

## DNA Viruses

### Adenovirus

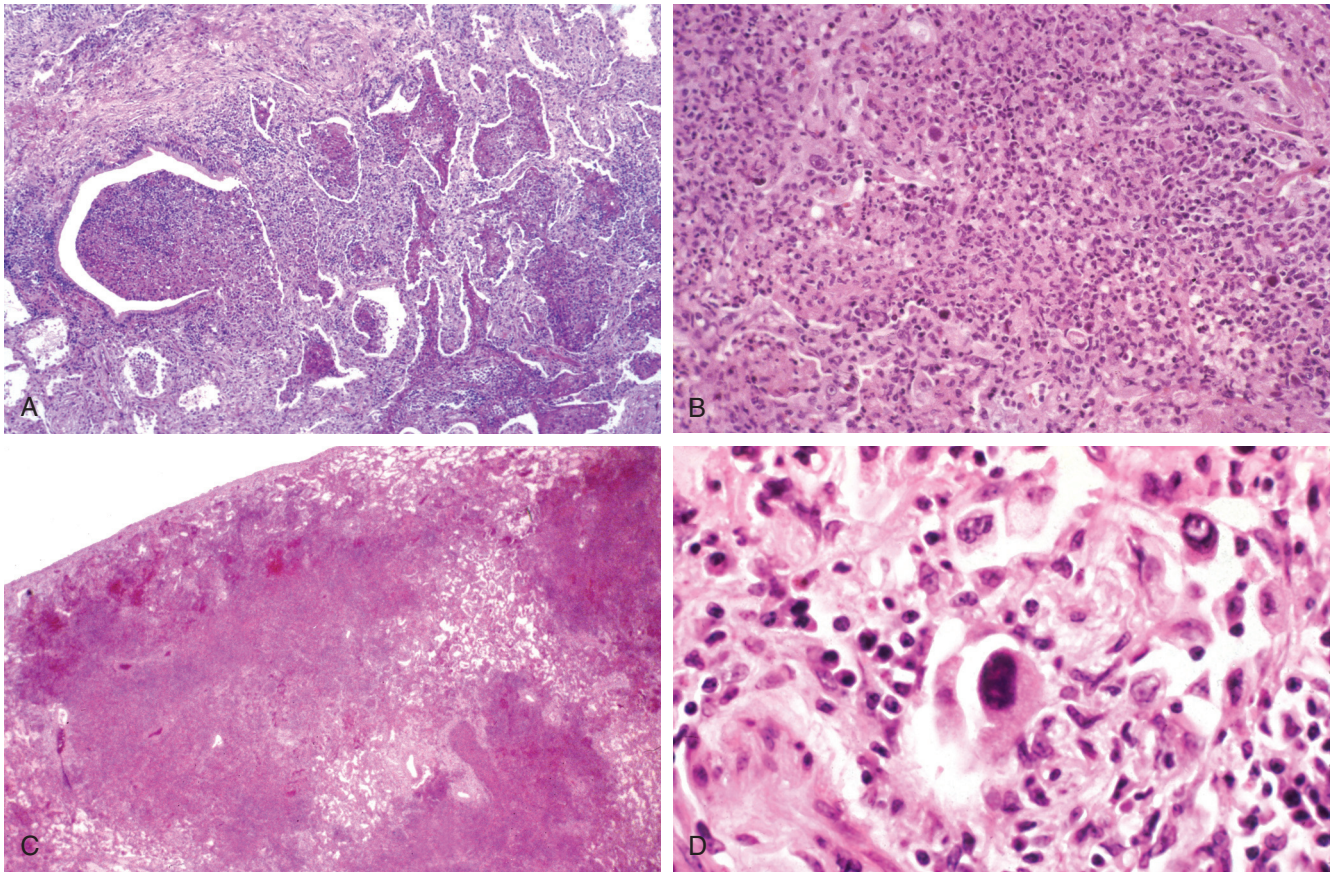
Adenovirus primarily affects the immunosuppressed host but can produce outbreaks in healthy subjects living at close quarters (e.g., military recruits). Adenovirus typically produces (1) ulcerative bronchiolitis with karyorrhexis (Fig. 8.14A), (2) neutrophilic pneumonia (see Fig. 8.14B), (3) acute intrapulmonary necrosis with hemorrhage (see Fig. 8.14C), or (4) DAD. Infected cells can exhibit amphophilic intranuclear inclusions with perinuclear clearing that mimic *herpesvirus* infection but more characteristically produce “smudge cells” (see Fig. 8.14C), showing hyperchromatic nuclei extruding beyond the confines of their nuclear membranes.<sup>25</sup>

The appearance of “smudge cells” can be mimicked by pulmonary cytotoxic drug injury or by epithelial repair in the early proliferative phase of DAD. For this reason and because of the potential overlap with herpesvirus-induced cytopathic changes, the diagnosis of adenovirus infection should always be confirmed

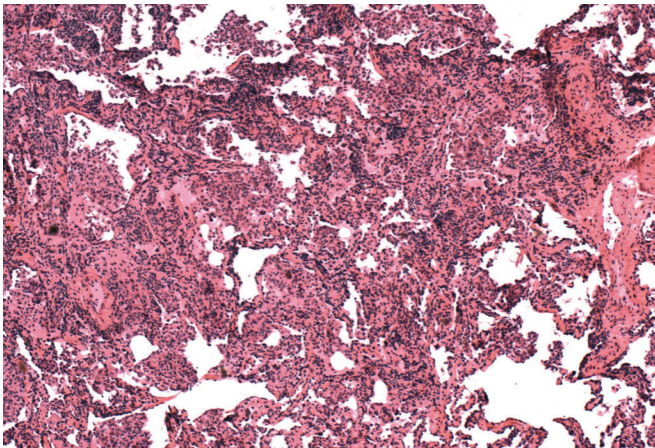
by immunohistochemical staining, ultrastructural examination, or viral isolation.

### Cytomegalovirus

Cytomegalovirus (CMV) occurs at the extremes of age or as a result of immunosuppression, and it is a common infection in HIV/acquired immune deficiency syndrome (AIDS).<sup>26</sup> The number of cells showing cytopathic changes can vary considerably and parallels the severity of infection. CMV primarily targets pulmonary macrophages and endothelial cells, but virtually any cell can show cytopathic features. The most common distribution is blood-borne miliary disease (Fig. 8.15), but bronchiolitis and DAD also occur. The diagnostic features of infection are (1) cytomegaly, (2) intranuclear inclusions with characteristic Cowdry type B inclusions (Fig. 8.16A), and (3) ill-defined amphophilic intracytoplasmic inclusions that are seen with hematoxylin and eosin (H&E), periodic acid–Schiff (PAS), and Gomori methenamine silver (GMS) stains (see Fig. 8.16B). In patients receiving prophylactic treatment with antivirals, CMV infection may fail to exhibit cytopathic changes. However, immunostains and in situ hybridization will continue to identify intracellular CMV antigens (see Fig. 8.16C).<sup>27</sup>



• **Figure 8.14** A, Ulcerative bronchiolitis in adenovirus infection. B, Neutrophilic pneumonia due to adenovirus. C, Necrotizing hemorrhagic pneumonia. D, “Smudge cell” showing extrusion of nuclear contents beyond the confines of the nuclear membrane.



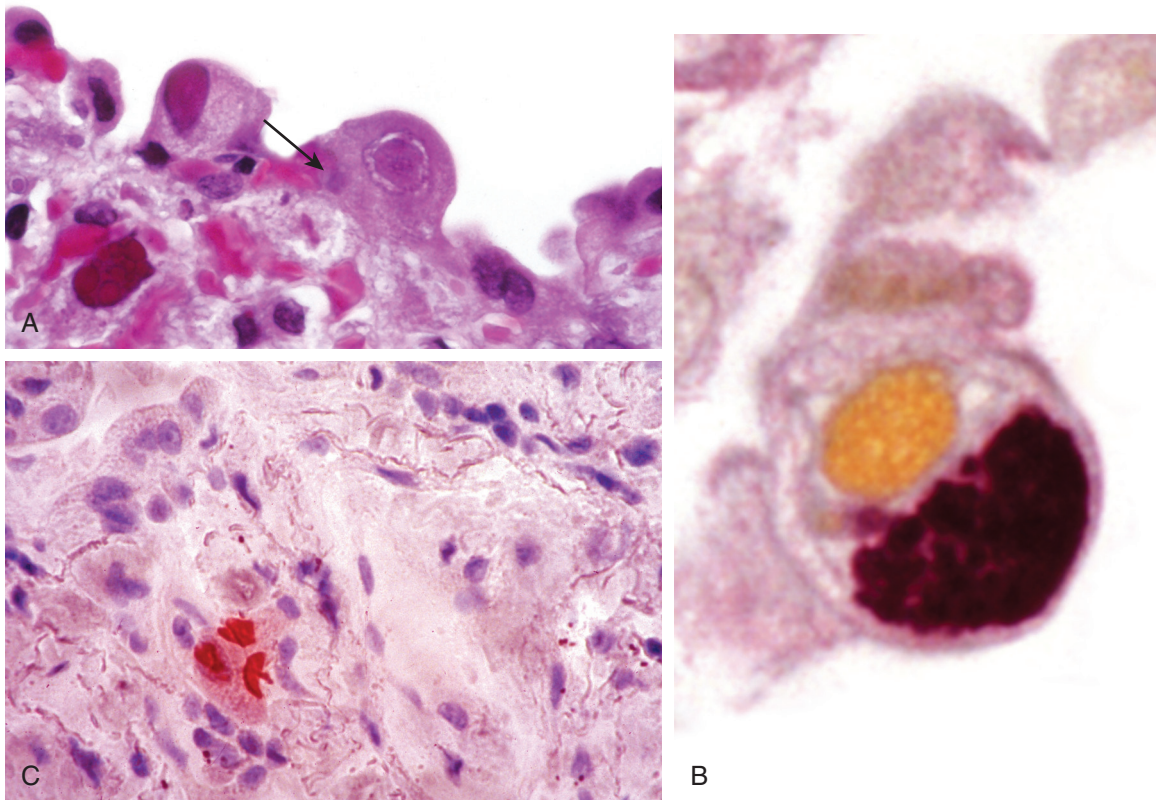
• **Figure 8.15** Focus of miliary infection in cytomegalovirus.

CMV is a frequent copathogen in the immunosuppressed patient and a cause of immunosuppression in its own right. Patients with active pulmonary infections will generally have circulating CMV DNA as judged by PCR assay of peripheral blood. CMV infection can also be seen together with other viral infections, *Pneumocystis jiroveci*, or opportunistic fungal infections (Fig. 8.17).

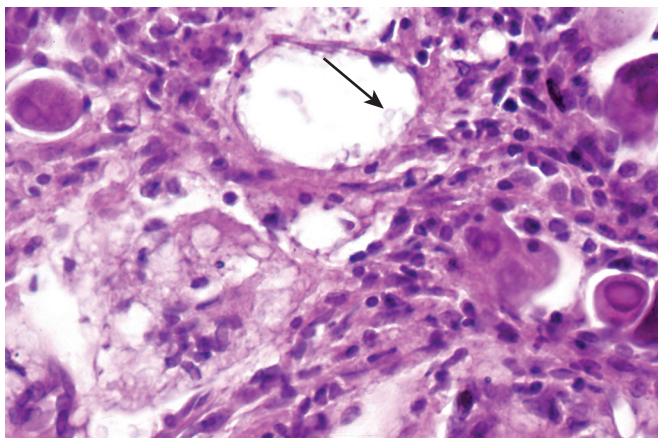
### Herpesvirus

Herpesvirus types 1 and 2 both infect the lung.<sup>28</sup> The incidence of herpesvirus infection increases with immunosuppression and when mucosal barrier defenses have been breached. Herpesvirus characteristically elicits a prominent neutrophilic response that mimics pyogenic bacterial infection, but foci of necrosis, cell karyorrhexis, and piled up virus-infected cells with amphophilic nuclei confirm the diagnosis (Fig. 8.18). Diagnostic cytopathic changes include type A or type B Cowdry nuclear inclusions showing molding of adjacent cells with multikaryon formation (Fig. 8.19). Immunosuppressed patients with herpesvirus viremia develop miliary foci of hemorrhagic necrosis with prominent fibrinous exudates (Fig. 8.20A and B).<sup>29</sup> In a recently reported case, herpesvirus type 2 was demonstrated to occur as a superinfection in a patient recovering from a bacterial superinfection of influenza pneumonia (see Fig. 8.20C).<sup>30</sup>

Herpesvirus pulmonary infections also develop in patients with structural abnormalities of the airways or as complications of primary infections of the oropharynx and esophagus. Intubated patients receiving chronic ventilatory support are at increased risk due to local barotrauma from inflated endotracheal tubes. The respiratory mucosa is the primary target (Fig. 8.21). At times, extensive necrosis of an ulcerated airway suggests the diagnosis, but immunostaining for herpes viral antigen can demonstrate high background staining, obscuring the diagnosis.<sup>27</sup> When this is the case, examining paraffin-embedded tissues by electron microscopy can reveal diagnostic virions (Fig. 8.22A to C).



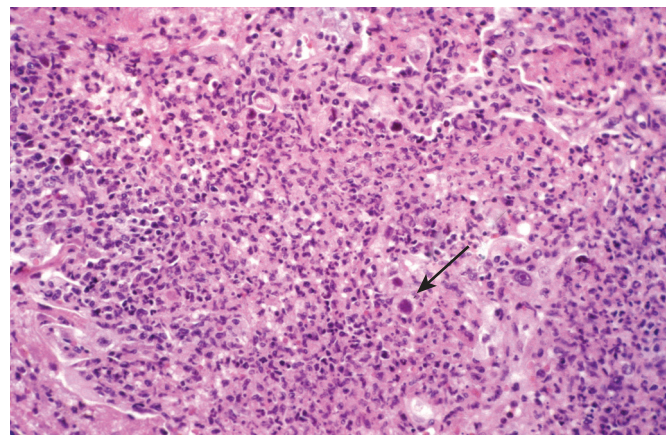
• **Figure 8.16** **A**, Alveolar type II lining cells with prominent cytomegaly, Cowdry type B inclusions, and cytoplasmic inclusions (*arrow*). **B**, Cytoplasmic inclusions stain positive with Gomori methenamine silver. **C**, Immunostain demonstrates cytomegalovirus antigen in a patient treated with gancyclovir.



• **Figure 8.17** Patient with cytomegalovirus infection and cryptococcal pneumonia (*arrow*) complicating human immunodeficiency virus/acquired immune deficiency syndrome.

### Varicella Zoster

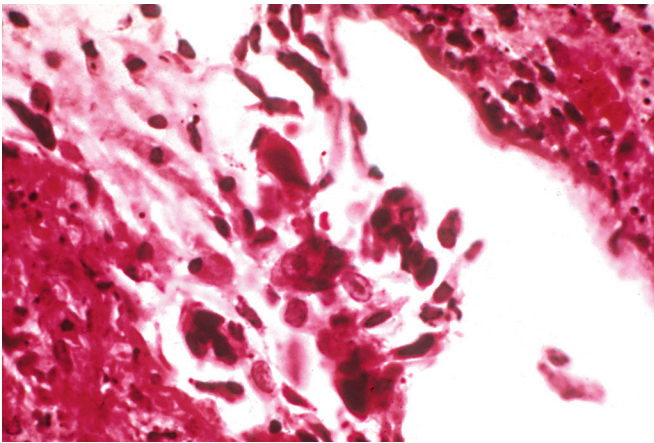
*Varicella zoster* pneumonia is a rare complication of the childhood chickenpox, and it is more commonly encountered as the consequence of reactivated virus in the immunocompromised host. Following nonlethal pulmonary infections in childhood, the lung shows multiple calcified miliary lesions. Cases coming to biopsy or autopsy show miliary nodules of hemorrhagic necrosis in lung and pleura or DAD (Fig. 8.23).<sup>31</sup> Infected cells with primarily Cowdry type A inclusions may be seen at the edges of the lesion, but they are harder to identify than in herpesvirus pneumonia.



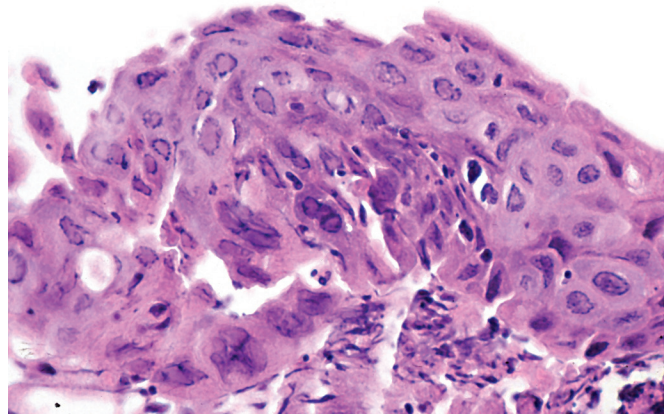
• **Figure 8.18** Neutrophilic bronchopneumonia due to herpesvirus 1. *Arrow* shows viral infected cell.

### Hantavirus

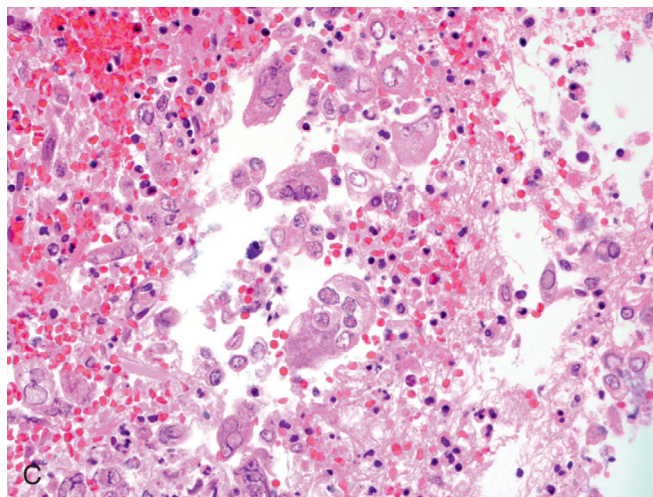
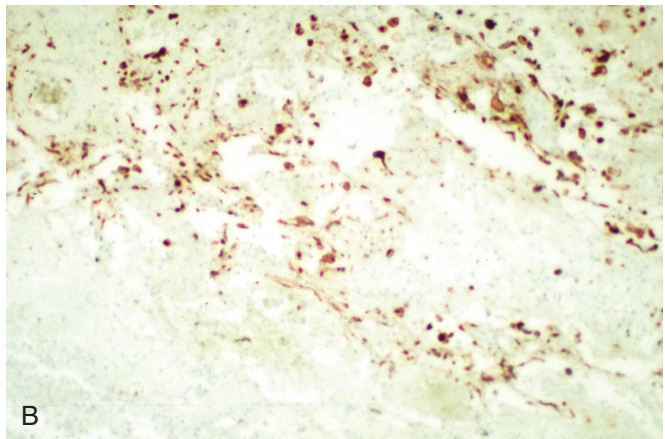
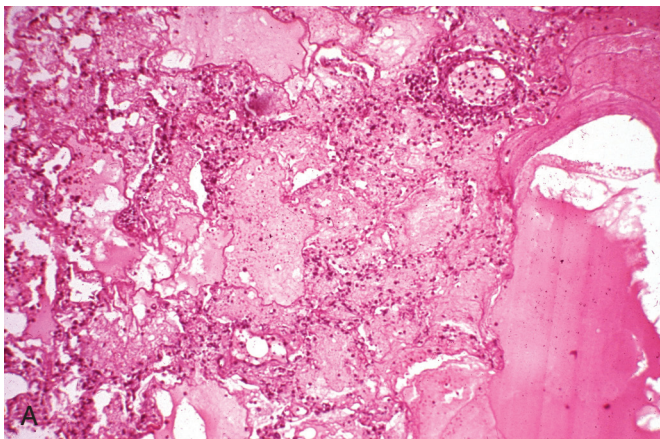
This virus produced an epidemic in the four corners region of the southwestern United States in 1993.<sup>32</sup> The infection is a zoonosis transmitted by infected rodent feces. The most common radiographic presentation is diffuse pulmonary edema with pleural effusions mimicking congestive heart failure. Histologically the lung shows pulmonary edema with scant poorly formed hyaline membranes (Fig. 8.24A), with atypical lymphocytes circulating within the pulmonary vasculature (see Fig. 8.24B).<sup>33</sup> Confirmation of the diagnosis requires specific immunohistochemistry,



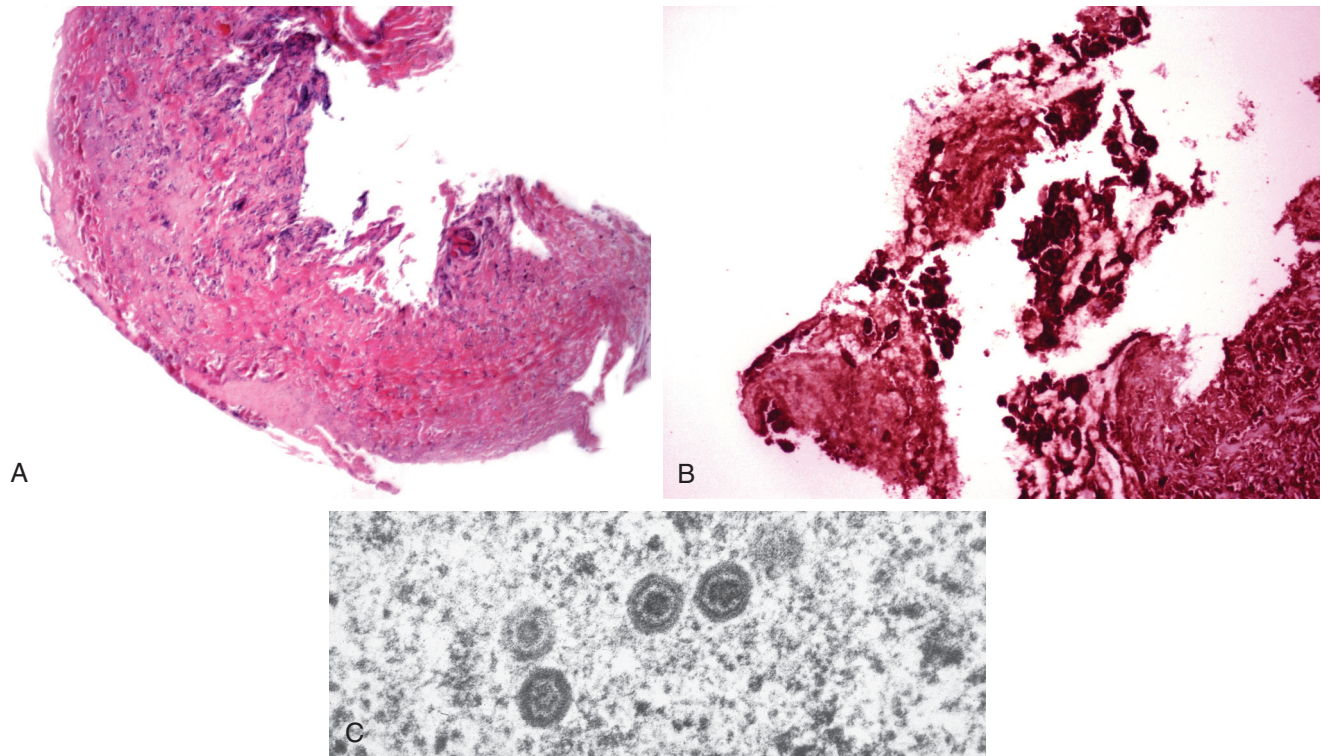
• **Figure 8.19** Nuclear inclusions in herpetic pneumonia.



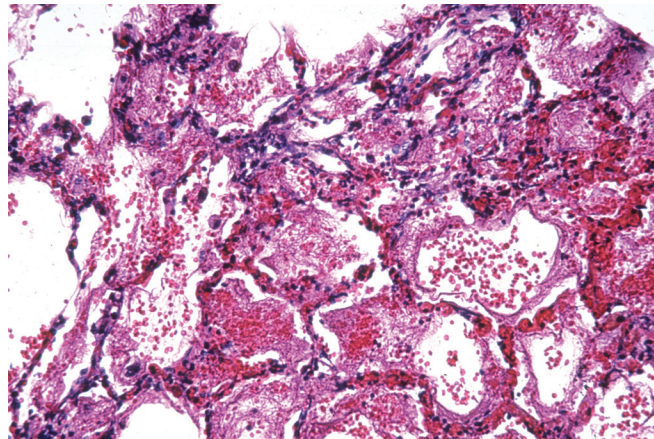
• **Figure 8.21** Herpetic inclusions in squamous respiratory epithelium of a chronically intubated patient.



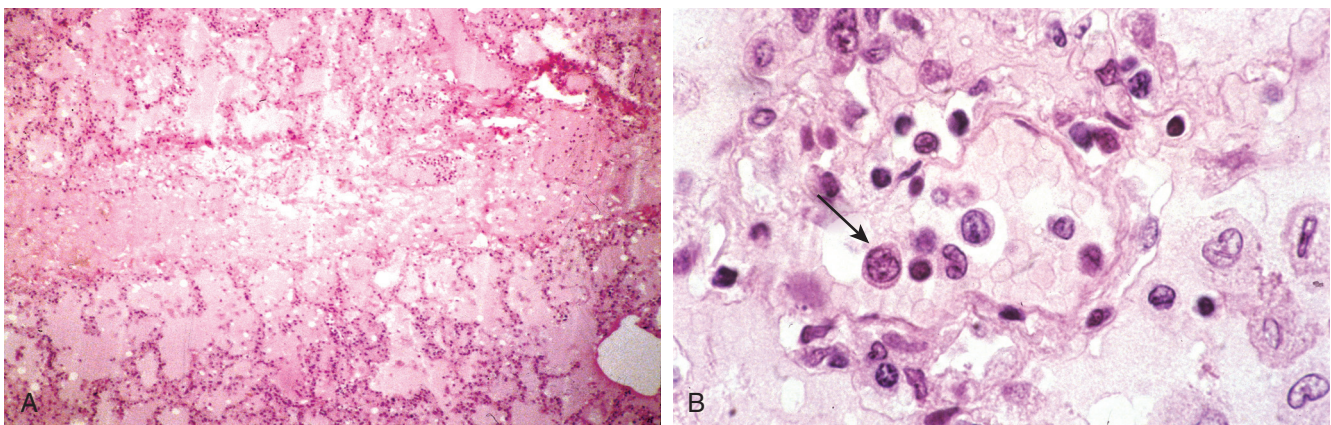
• **Figure 8.20** **A**, Hemorrhagic necrotizing pneumonia in an immunosuppressed patient with herpesvirus 1 viremia. **B**, Multiple infected cells immunostaining for herpesvirus 1. **C**, Herpesvirus type 2 complicating influenza pneumonia with collections of multinucleated cells with nuclear inclusions.



• **Figure 8.22** A, Ulcerated tracheal lesion showing (B) intense immunostaining for herpesvirus 1 with diagnosis (C) confirmed by ultrastructural examination demonstrating diagnostic virions.



• **Figure 8.23** Hemorrhagic pneumonia due to Varicella-Zoster virus.



• **Figure 8.24** A, Pulmonary edema in patient with hantavirus infection. B, Pulmonary vessel with intraluminal atypical lymphocytes. Arrow shows circulating atypical lymphocyte.

serologic evidence of hantavirus-specific IgM, PCR, or ultrastructural identification of the causative virions.

## Other Atypical Pneumonias

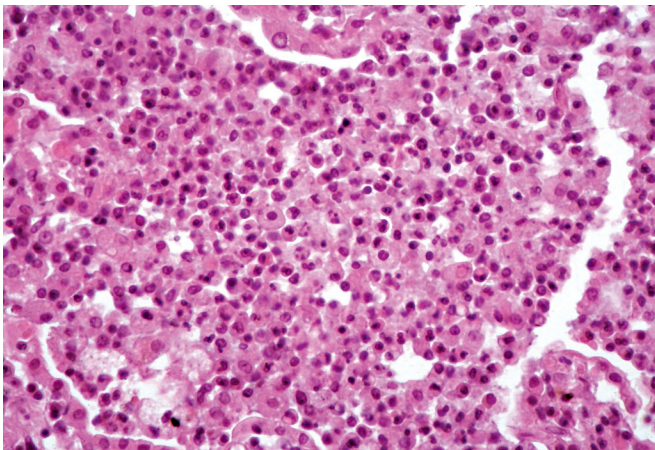
### *Mycoplasma Pneumonia*

*Mycoplasma* are the smallest (0.2 to 0.8  $\mu\text{M}$ ) free-living bacteria, but they lack a true cell wall. They are facultative anaerobes, except for *Mycoplasma pneumoniae*, the most common pulmonary pathogen, which is a strict aerobe. *Mycoplasma pneumoniae* occurs worldwide with no increased seasonal activity, but epidemics predictably occur every 4 to 8 years. Although primarily an infection of young adults, it can attack older adults. The most common clinical syndrome is tracheobronchitis, with one-third of patients developing a mild but persistent pneumonia.

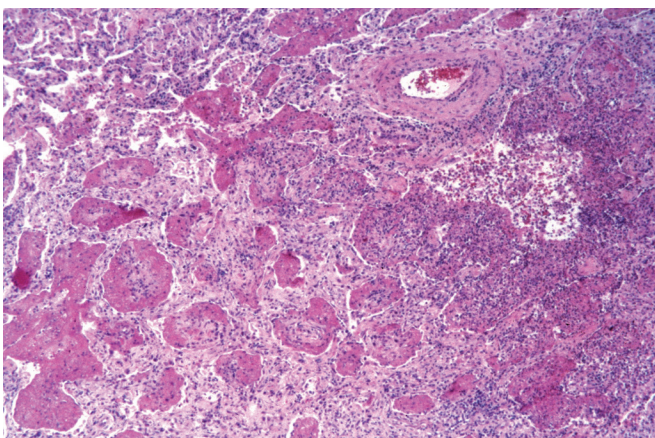
*Mycoplasma pneumoniae* is rarely biopsied, because positive cold agglutinin and specific complement fixation antigen assays will establish the diagnosis. Biopsied cases show lymphocytic or neutrophilic bronchiolitis with alveolar wall inflammation and fibrinous exudates (Fig. 8.25).<sup>34</sup> Similar changes are seen in both *Chlamydia* (Fig. 8.26) and *Coxiella pneumoniae*.

### Epstein-Barr Virus

*Epstein-Barr virus* (EBV) has been implicated in disorders ranging from the mononucleosis syndrome to malignant lymphoid



• **Figure 8.25** Histiocytic and fibrinous exudates in *Mycoplasma pneumoniae*.



• **Figure 8.26** Prominent fibrinous and histiocytic exudates due to *Chlamydia* spp.

neoplasia.<sup>35</sup> The mononucleosis syndrome includes pharyngitis, lymphadenitis, and hepatosplenomegaly. Pulmonary involvement can occur as part of the syndrome, but it is unusual and rarely biopsied. EBV pneumonia shows patchy peribronchiolar and interstitial polyclonal lymphoid infiltrates with scant interstitial and intra-alveolar fibrin exudates (Fig. 8.27). The diagnosis is generally established serologically by EBV antigen titers but can be confirmed by in situ hybridization.

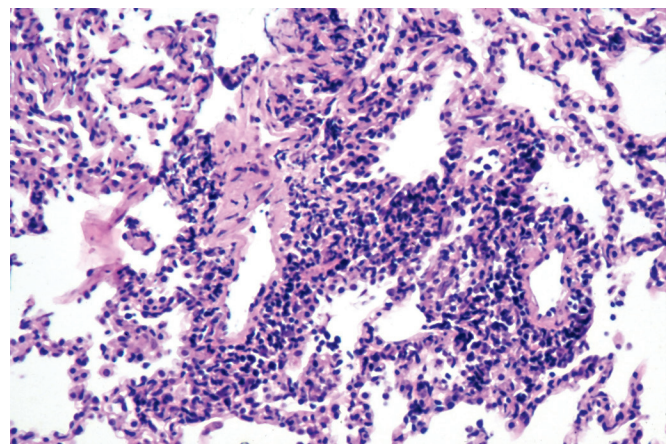
### *Pneumocystis jiroveci*

For years, the organism formerly known as *Pneumocystis carinii* was thought to be a protozoon; however, it is now confidently classified as a fungus. Originally described as a plasma-cell interstitial pneumonia in malnourished children, it was subsequently seen in patients with hematologic malignancies and in those receiving chemotherapy or chronic corticosteroids. In the 1980s pneumocystis pneumonia became a signal infection in establishing the diagnosis of AIDS. It was encountered in epidemic proportions until prophylactic use of trimethoprim-sulfa (*Bactrim*) became a routine aspect of HIV/AIDS management. *P. jiroveci* is currently most often diagnosed by sputum induction, and lung biopsy is reserved for diagnostic challenges.<sup>36</sup>

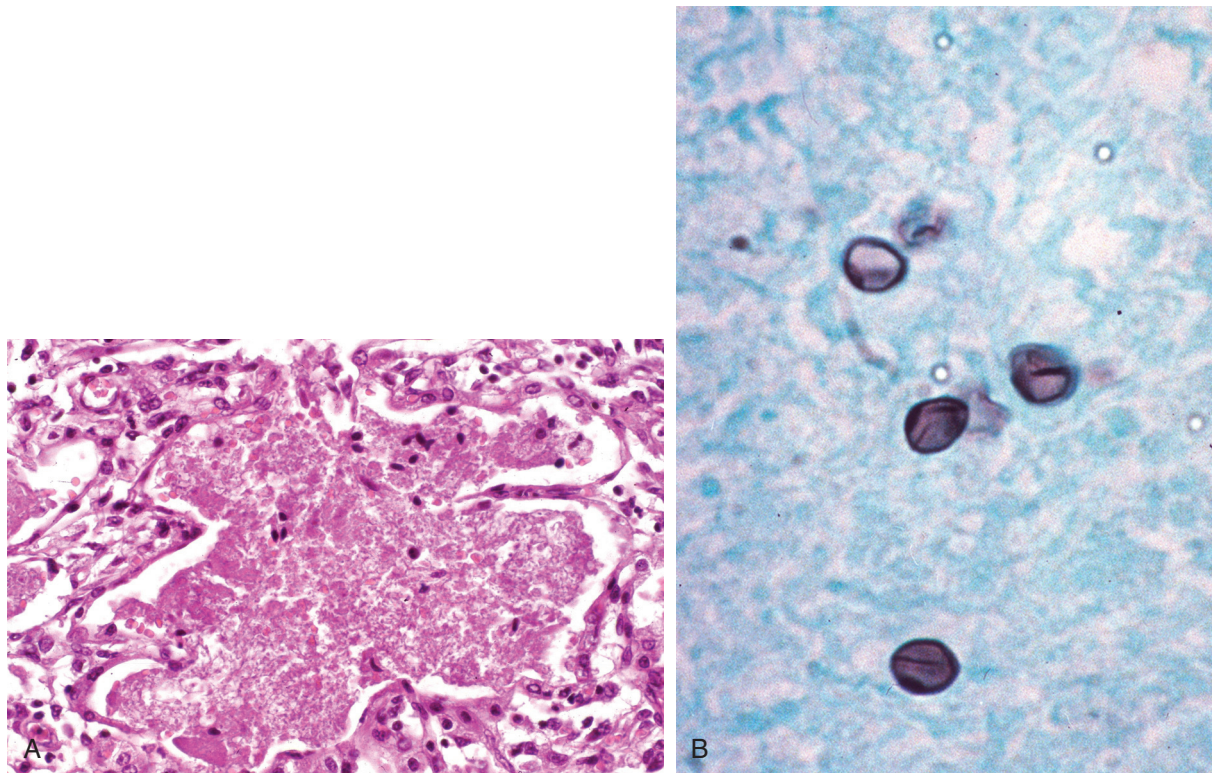
Although the disease presents radiographically as an atypical “interstitial” pneumonia, interstitial inflammation is not its most striking pathologic feature. In pneumocystis pneumonia the alveoli are filled with a frothy eosinophilic exudate that mimics exudative pulmonary edema or alveolar lipoproteinosis (Fig. 8.28A). The pulmonary interstitium shows a mild plasma cell–rich pneumonitis and prominent alveolar type II cell hyperplasia.

The diagnosis is confirmed by the presence of oval-, helmet-, or crescent-shaped GMS-positive “cysts,” 4 to 6  $\mu\text{M}$  in greatest dimension, within the alveolar froth (see Fig. 8.28B).<sup>37</sup> *Pneumocystis* is distinguished from GMS-positive fungal yeast forms by the absence of budding, pericapsular accentuation, and a so-called intracytoplasmic dot, in the former. However, when these features are absent and when the organism load in the biopsy is low, it may be difficult to confidently exclude *Histoplasma* or *Cryptococcus*. In these cases, specific immunohistochemistry can confirm the diagnosis.

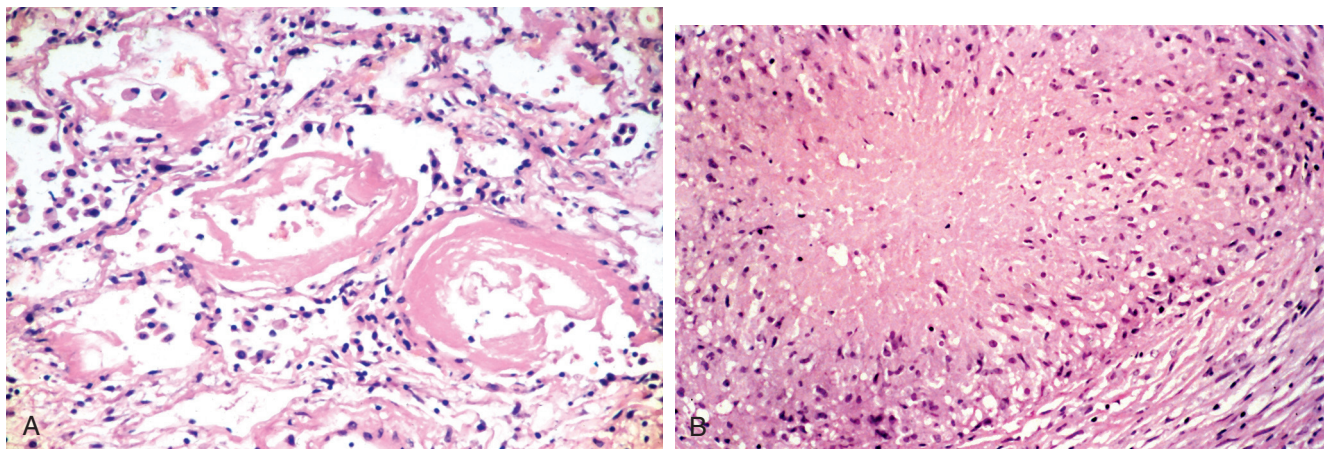
Multiple patterns of unusual host reactions to *P. jiroveci* have been recognized.<sup>38</sup> These include DAD (Fig. 8.29A), solitary necrotizing granulomas (see Fig. 8.29B), miliary infection, lymphoid interstitial pneumonia, and regional lymphadenitis.



• **Figure 8.27** Dense lymphoid infiltrate in patient with Epstein-Barr virus pneumonia.



• **Figure 8.28** A, Alveolar eosinophilic exudate in pneumocystis pneumonia showing (B) Gomori methenamine silver–positive cyst forms with pericapsular accentuation.



• **Figure 8.29** (A) Diffuse alveolar damage and (B) Necrotizing granulomatous inflammation due to pneumocystis.

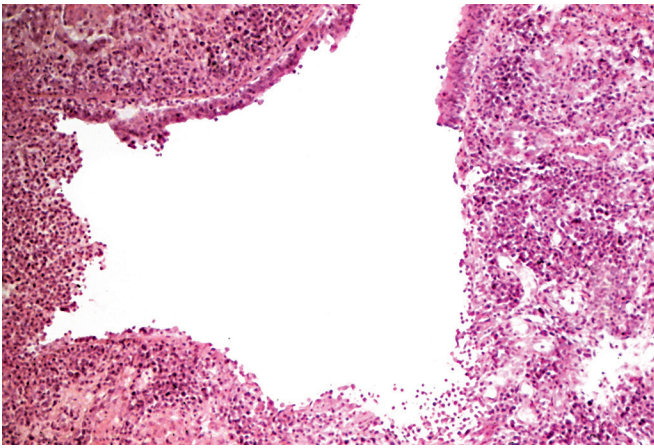
Microcalcifications may be seen in areas of infection, and thin-walled cyst formation may develop.

### Bronchiectasis

Bronchiectasis is one of the major manifestations of pulmonary infection. Dilatation and anatomic distortion of conducting airways can result from acute and chronic airway injury from airway infection (wet bronchiectasis) or from adjacent parenchymal scarring (“dry” or traction bronchiectasis). A number of infections can damage the large airways and lead to bronchiectasis. Reversible cylindrical bronchiectasis may appear radiographically in patients, following an acute bacterial pneumonia. Because this

change often resolves, biopsies of suspicious bronchiectatic regions should be deferred until a period of weeks has elapsed after an acute infection. Because regions of chronic bronchiectasis are fed by varicose bronchial arteries that often course directly beneath the airways surface, endoscopic biopsies of bronchiectatic areas are generally contraindicated.

Prior to the development of childhood vaccination, viral exanthems and *Bordetella pertussis* were common causes of bronchiectasis (Fig. 8.30). Cystic fibrosis, a genetic disorder of chloride transport, is currently a leading cause of severe bronchiectasis in young adults, as advances in management have resulted in patients surviving beyond childhood (Fig. 8.31).



• **Figure 8.30** Bronchiolitis secondary to *Bordetella pertussis* infection, once a common cause of bronchiectasis.



• **Figure 8.31** The lung in cystic fibrosis showing bronchiectasis and a cavitory abscess.

In bronchiectasis, the airways lose their cartilaginous support due to chronic inflammation and become dilated and prone to repeated bouts of mucoid impaction and infection.<sup>39</sup> The airways develop a spectrum of gross changes, ranging from cystic, varicose, to cylindrical dilatation, associated with distal peribronchiolar inflammation (Fig. 8.32A), and increasing degrees of parenchymal scarring with loss of gas-exchanging alveoli (see Fig. 8.32B). Although the large airways are invariably ectatic, the distal airways in bronchiectasis are generally narrowed by constrictive bronchiolitis.

Recurrent polymicrobial infections with necrotizing bronchopneumonia and abscess formation complicate bronchiectasis. Patients are also prone to develop infections due to antibiotic-

resistant mucoid forms of *Pseudomonas*, *Burkholderia* spp., *Stenotrophomonas maltophilia*, *Achromobacter xylosoxidans* (see Fig. 8.32C)<sup>40</sup> and *Staphylococcus* spp. Some patients with infective bronchiectasis develop allergic bronchopulmonary aspergillosis (ABPA) and superinfection with atypical mycobacteria.<sup>41</sup>

### Acute Bronchopneumonia

Acute bronchopneumonia is the most common distribution of pulmonary infection. Gram-positive and gram-negative bacteria, as well as some viruses, including herpesvirus and adenovirus, elicit primarily an exudation of neutrophils, whereas the cellular response to other viruses, fungi, mycoplasma, and chlamydia are primarily lymphohistiocytic. Bronchopneumonia generally results from microaspiration of pathogens that have colonized the oropharynx (Fig. 8.33A). At times the aspiration of colonized food particles can carry bacteria and fungi into the lung (see Fig. 8.33B). Terminal episodes of aspiration often show colonies of gram-positive *Aerococci*, previously referred to as “gaffky,” (see Fig. 8.33C) and their appearance is both common and characteristic in autopsy lungs.<sup>42</sup>

### Bacterial Infections

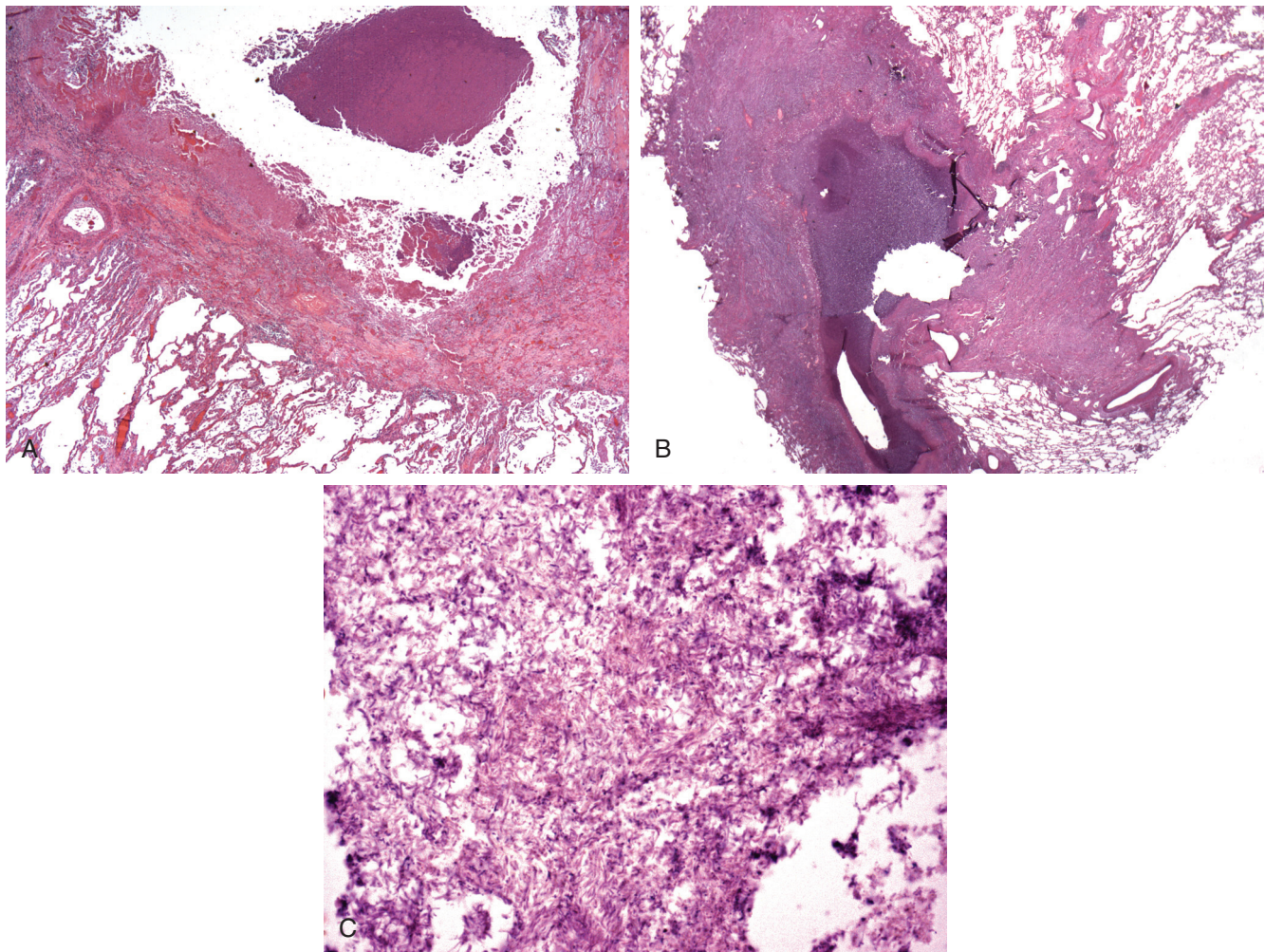
The pyogenic bacteria are distinguished by their propensity to evoke acute neutrophilic inflammation and “pus.” Pyogenic infections as well as other acute necrotizing bronchopneumonias progress to *organizing pneumonia*, characterized by a fibrohistiocytic response that obliterates small airways along with inflammation of the surrounding alveolar interstitium (Fig. 8.34). This reaction is nonspecific, and “organizing pneumonia” or “bronchiolitis obliterans with organizing pneumonia” is a rubric for the generic lesion that may be due to infection or noninfective inflammatory disorders or may be idiopathic.<sup>43</sup> It is important for the surgical pathologist to convey clearly to the treating clinicians that a diagnosis of “organizing pneumonia” does not indicate a specific etiology.

### Pneumococcal Pneumonia

Streptococcal pneumonia (pneumococcal pneumonia) is a community-acquired pneumonia that classically produces a lobar pneumonia healing by resolution (i.e., without necrosis or scarring).<sup>44</sup> In some cases, pneumococcal pneumonia complicates a resolving viral tracheobronchitis or influenza. In the age of antibiotic treatment, most cases do not progress to lobar involvement and are limited to acute nonnecrotizing bronchopneumonia. A large number of serotypes of streptococcal pneumonia have been isolated, and certain ones (e.g., type 3) can be virulent, producing necrotizing pneumonia, bacteremia, and death, despite prompt antibiotic treatment.

Although rarely biopsied, lobar pneumococcal pneumonia is still seen at autopsy. The early phase of the disease, the *red hepatization*, shows exudation of edema fluid with the diapedesis of red blood cells (Fig. 8.35A). The exudate spreads to fill an entire lung lobe via the pores of Kohn, interalveolar potential channels within the normal lung (see Fig. 8.35B). The acute cellular response is neutrophilic, but this is followed within days by alveolar filling with exudate macrophages that ingest the infected exudate, the *gray hepatization* (see Fig. 8.35C). Despite the extensive inflammatory changes, alveolar necrosis is absent—a finding best assessed by elastic stains—and the lung heals by *resolution* with minimal sequelae. The offending organisms are gram-positive, lancet-shaped cocci growing in pairs (diplococci) and in





• **Figure 8.32** A, Bronchiectasis in cystic fibrosis showing dilatation and destruction of airway wall. B, Dense peribronchiolar scar in bronchiectasis. C, Bronchiectatic airway with colonies of gram-negative bacilli identified by culture as *Burkholderia cepacia*.

short chains, and they can be identified by both tissue Gram and GMS stains (see Fig. 8.35D).

### Group A Streptococci

Group A streptococcal pneumonia occurs at the extremes of life or as a complication of resolving influenza infection.<sup>45</sup> It produces a rapidly progressing and life-threatening pneumonia with edema, hemorrhage, abscess formation, empyema, and septicemia. Group A streptococci evoke a brisk increase in pulmonary capillary permeability, yielding what can be mistaken for cardiogenic pulmonary edema on low-power microscopic examination (Fig. 8.36A). However, further scrutiny reveals necrotic macrophages and innumerable gram-positive bacteria in chains (see Fig. 8.36B). Pulmonary hemorrhage and abscess formation are frequently seen. Streptococci have a predilection to course along pulmonary lymphatic channels, recapitulating erysipeloid spread in the skin, to produce an early empyema (Fig. 8.37).

### Staphylococcus aureus

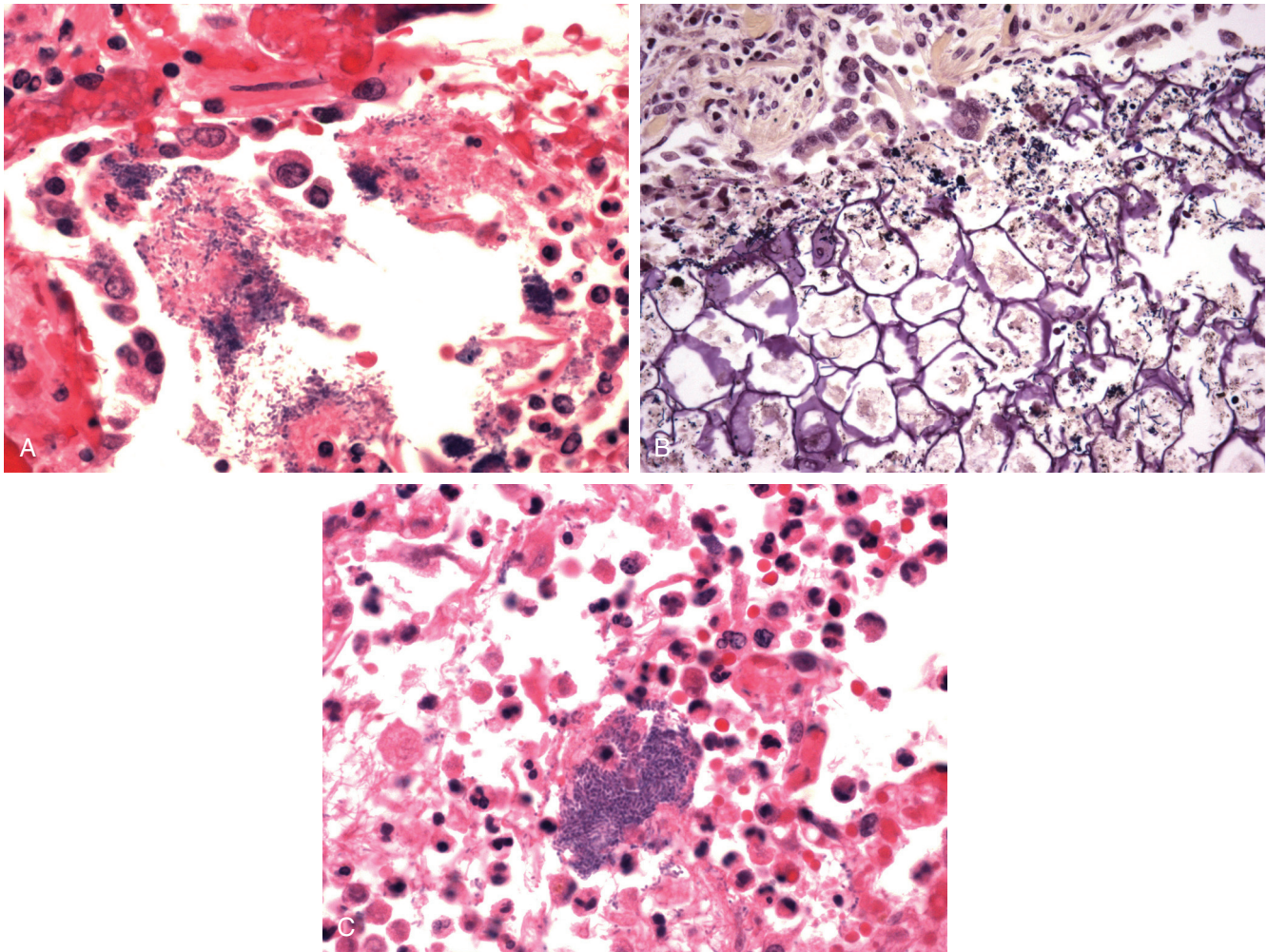
*S. aureus* has emerged as a frequently encountered life-threatening pulmonary pathogen. Previously seen as a community-acquired complication of influenza, staphylococcal infection is now a

primary cause of nosocomial pneumonia, and its evolving drug resistance accounts for methicillin-resistant *S. aureus* (MRSA) strains, which are of particular concern for hospital infection control epidemiologists.<sup>46</sup>

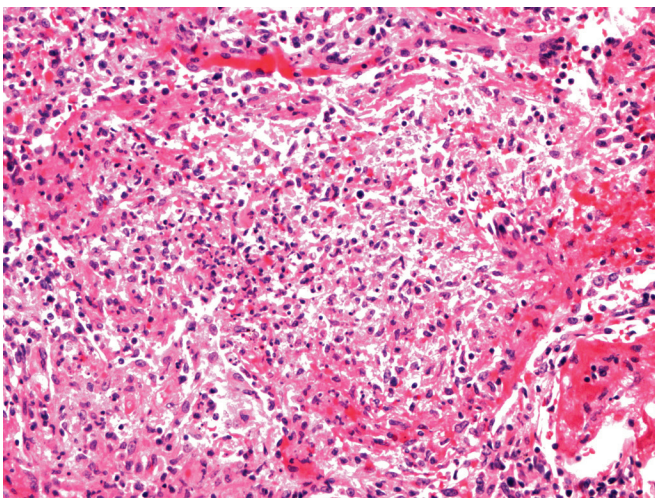
*S. aureus* spp. produce a necrotizing pyogenic pneumonia with abscess formation (Fig. 8.38A). The organisms grow in clusters as gram-positive microcolonies (see Fig. 8.38B). Infection heals by organization with scarring, and cystic pneumatoceles may develop. Some phage-infected strains of the organism produce an exotoxin that can activate the CD3 receptor to promote the release of the T lymphocyte's complement of lymphokines, leading to a *toxic shock syndrome* with sepsis physiology, DAD, and disseminated intravascular coagulation that leads to death if not treated promptly.

### Gram-Negative Bacteria

Most gram-negative bacilli produce a necrotizing bronchopneumonia with hemorrhage and abscess formation. Certain virulent gram-negative species, including *Klebsiella*, *Pseudomonas*, *Acinetobacter*, and *Burkholderia* spp., have a propensity to infect the pulmonary microvasculature, leading to necrosis, bacteremia, and septic shock.<sup>47</sup> The lung shows fibrinoid necrosis with colonies of



• **Figure 8.33** **A**, Acute bronchiolitis due to *Staphylococcus*. **B**, Lentil aspiration with colonies of gram-positive bacteria. **C**, Terminal aspiration showing intraluminal colony of gram-positive *Aerococcus* spp. (*Gaffkya*).



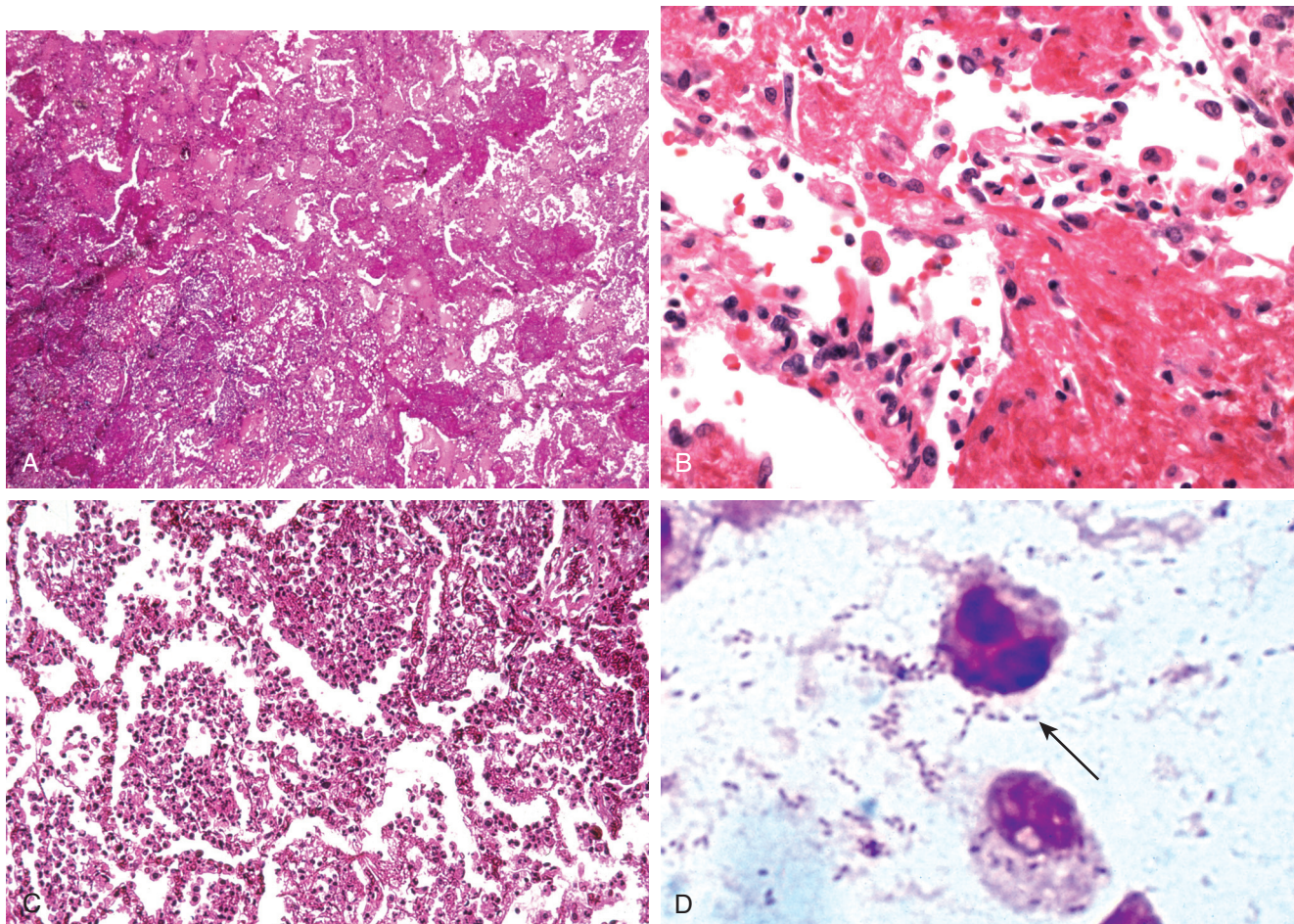
• **Figure 8.34** Organizing pneumonia showing macrophages and early fibrosis in respiratory bronchioles and alveoli.

gram-negative bacilli streaming along the vessel walls, where they create an ill-defined purplish hue in H&E-stained sections (Fig. 8.39A and B)

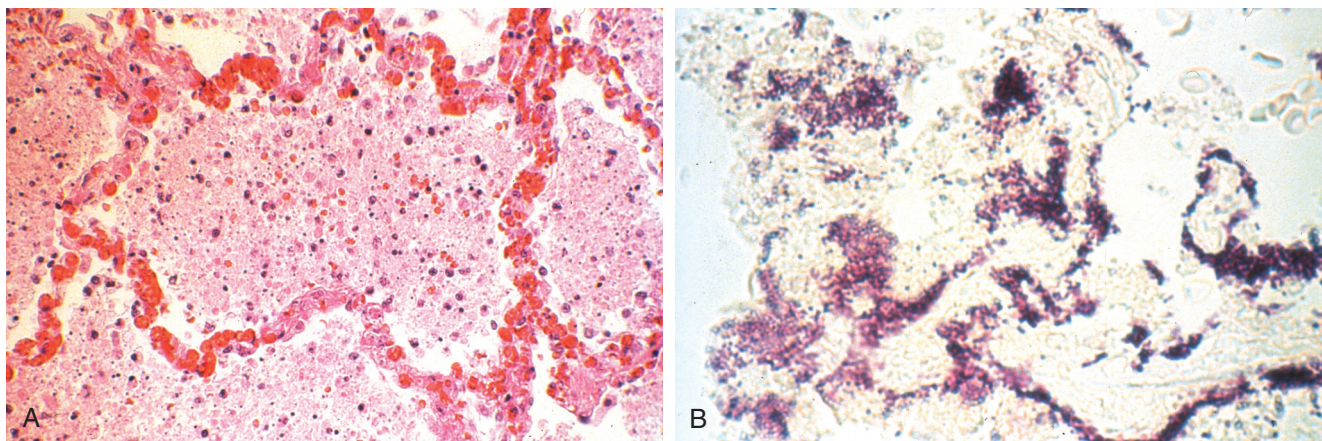
**Klebsiella.** *Klebsiella* pneumonia generally occurs in patients who are immunocompromised due to age, ethanol abuse, or diabetes mellitus. It is a common cause of ventilator-associated pneumonia (VAP).<sup>48</sup> Like the pneumococcus, *Klebsiella* spp. classically produce a lobar pneumonia with a slimy “mucoid” appearance and an unexplained predilection for the upper lobes (Fig. 8.40A). Infection produces hemorrhagic necrosis, microabscesses, and cavity formation. The organisms are short gram-negative bacilli that can be demonstrated with both tissue gram stain (see Fig. 8.40B) and GMS by virtue of their capsules. Less commonly, *Klebsiella* spp. produce a chronic necrotizing pneumonia with scarring and distortion of the pulmonary anatomy (see Fig. 8.40C).

#### Lung Abscess Due to Oropharyngeal Aspiration

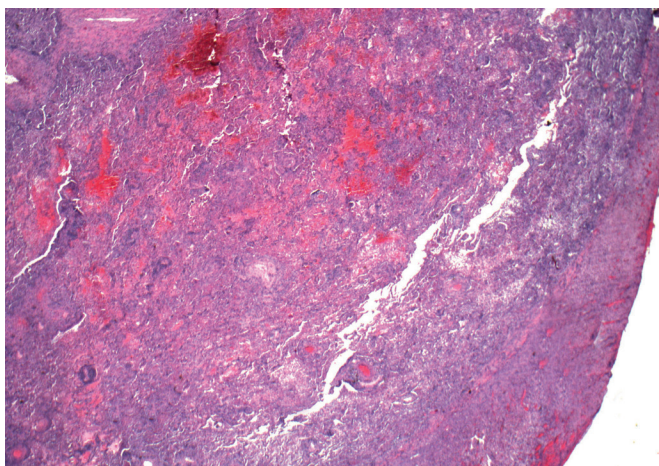
Lung abscess complicates the aspiration of polymicrobial oropharyngeal bacteria. The organisms isolated from a lung abscess include mixed gram-positive and gram-negative aerobic flora, as well as anaerobes. Patients with poor oral hygiene due to dental



• **Figure 8.35** **A**, In the red hepatization phase of pneumococcal lobar pneumonia, alveoli are filled by fibrin with diapedesis of red blood cells. **B**, The infected exudate extends throughout the lobe via the pores of Kohn, potential channels between adjacent alveoli. **C**, In the gray hepatization phase, alveoli are filled by leukocytes that scavenge bacteria and detritus prior to resolution of the infection. **D**, The pneumococcus is a lancet-shaped, gram-positive coccus that grows in pairs (diplococci) (arrow) and chains.



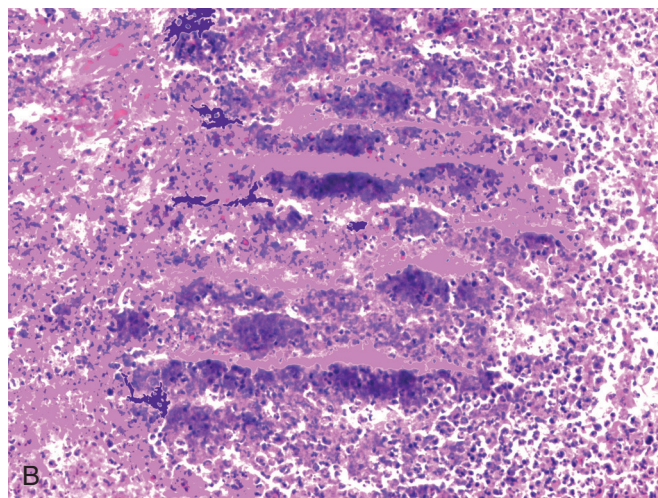
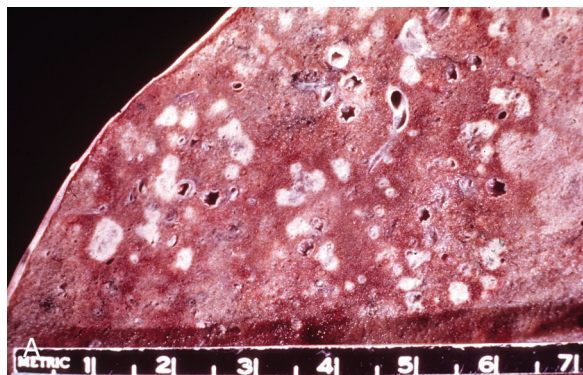
• **Figure 8.36** **A**, The alveolar spaces in streptococcal pneumonia show an eosinophilic exudate that mimics proteinaceous pulmonary edema at low power. **B**, Innumerable gram-positive cocci in chains are seen in the exudates and tend to invade lymphatics.



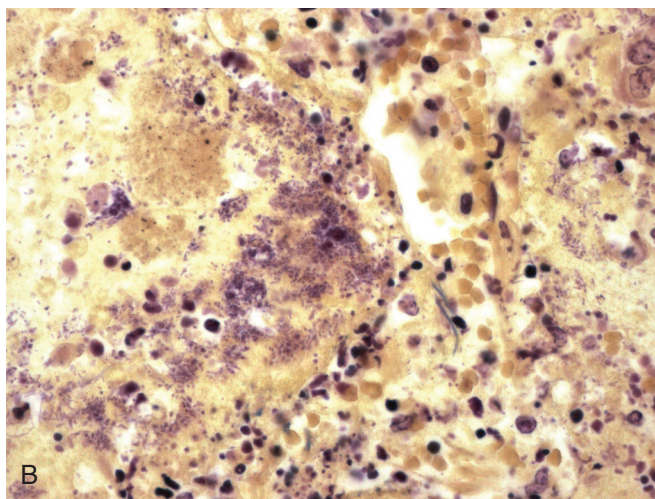
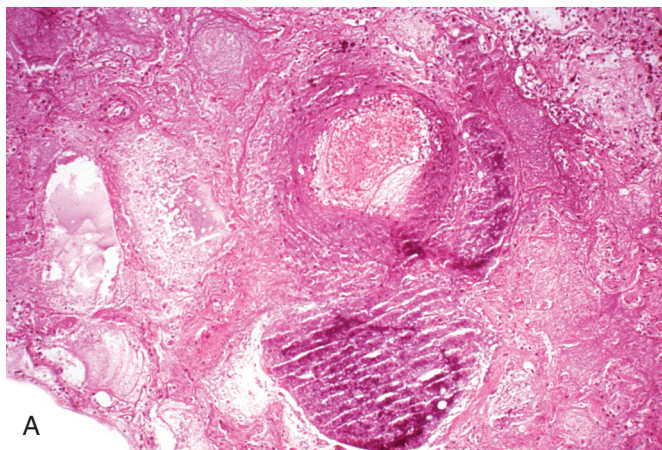
• **Figure 8.37** Abscess formation and empyema occur early in streptococcal pneumonia.

caries, those with gingival and tonsillar disease, and those with disorders that impair either consciousness or normal swallowing (e.g., ethanolism, seizure disorder, and cerebrovascular accidents) are at increased risk for aspiration pneumonia and lung abscess.<sup>49</sup> The disorder begins as a necrotizing bronchopneumonia in a dependent segment of the lung and progresses to produce a cavitary abscess communicating with a feeding adjacent airway. Most lung abscesses are diagnosed and treated noninvasively; however, failure to respond to medical treatment due to poor drainage and closure may prompt surgical excision.

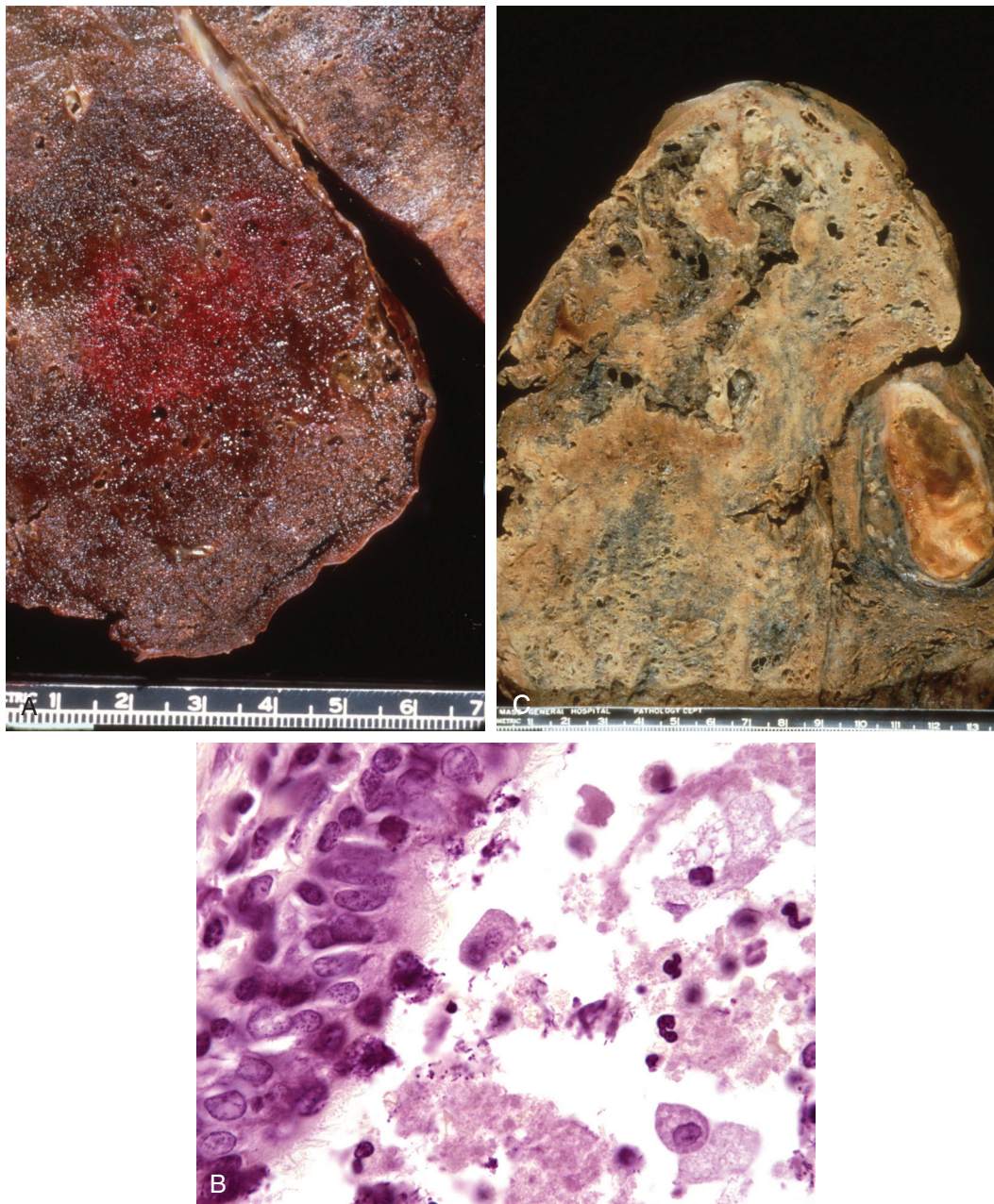
Microscopically the wall of the lung abscess is irregular with a shaggy, fibrinous lining (Fig. 8.41A) that may be difficult to distinguish from a necrobiotic rheumatoid nodule or Wegener granulomatosis. However, palisading granulomatous inflammation is not a prominent finding in lung abscess. The area around the cavity shows acute and organizing bronchopneumonia (see Fig. 8.41B). The activity of a lung abscess may be determined microscopically by examining its lining because actively infected cavities show a squamous epithelial lining, whereas healed cavities are lined by normal respiratory epithelium and may be mistaken for a focus of bronchiectasis.



• **Figure 8.38** A, Lung in staphylococcal pneumonia showing bronchopneumonia with abscess formation. B, Microabscess with gram-positive *S. aureus* in clusters.



• **Figure 8.39** A, Fibrinoid necrosis with dense bacterial growth visible in hematoxylin and eosin sections in *Pseudomonas* pneumonia. B, Clusters of gram-negative bacilli are identified.



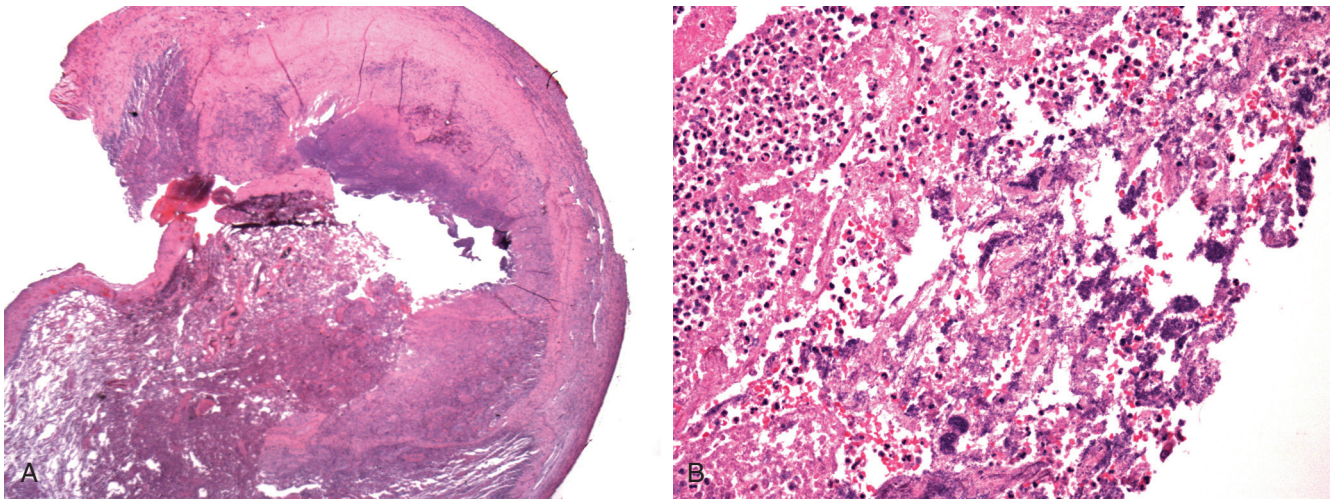
• **Figure 8.40** **A**, Hemorrhagic lobar pneumonia due to *Klebsiella pneumoniae*. The organism has a predilection for the upper lung lobes. **B**, *Klebsiella* is a small, nonmotile, gram-negative rod that also stains with Gomori methenamine silver. **C**, Chronic necrotizing pneumonia due to *Klebsiella* spp. with extensive scarification of necrotic lung.

### Actinomycosis

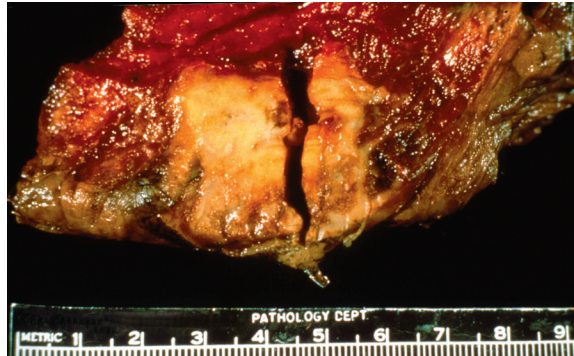
*Actinomyces* spp. are gram-positive filamentous bacteria that cause a chronic distal necrotizing pneumonia with a proclivity towards penetrating into the adjacent soft tissues of the chest wall.<sup>50</sup> *Actinomyces* are aspirated from the oropharynx, where they are commonly part of the tonsillar flora in younger patients or a pathogen related to poor oral hygiene and gingivitis in older adults. The risk factors for actinomycosis are similar to those of lung abscess. The infection extends into the pleura and then forms sinuses within the soft tissues of the chest wall that ultimately exit at the skin surface. The indurated pulmonary lesion may be mistaken clinically for an aggressive peripheral lung

malignancy, but its gross appearance at surgery is usually distinct (Fig. 8.42).

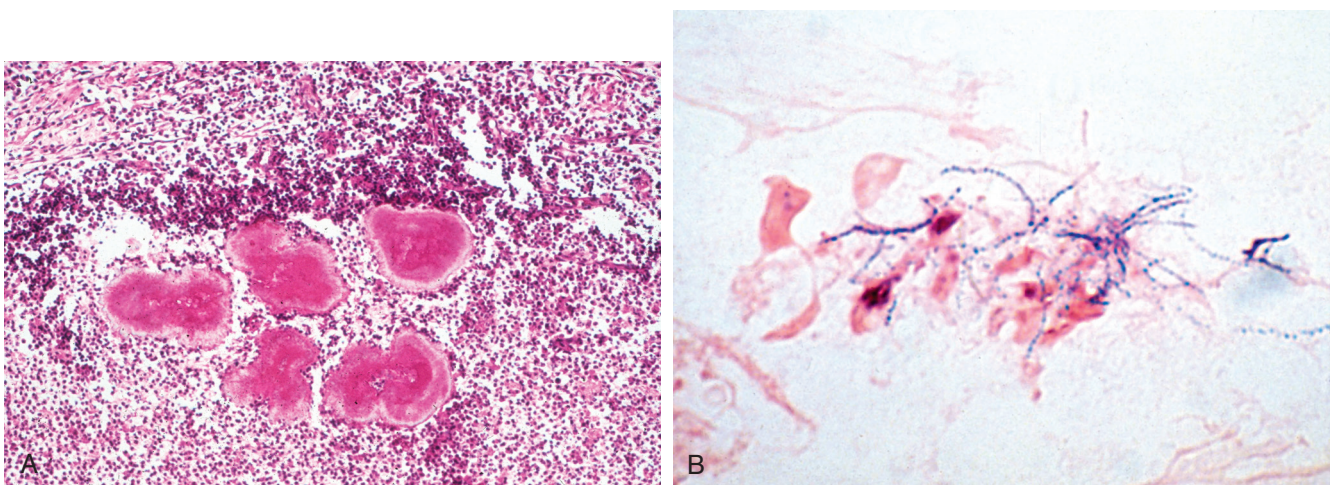
The histologic response evoked by actinomycosis is variegated, with microabscesses, polymorphous infiltrates of lymphocytes, histiocytes, plasma cells, giant cells, and fibrosis. At times, the extent of the fibroinflammatory response can lead one to consider a diagnosis of “inflammatory pseudotumor.” The correct diagnosis is established by the presence of “sulfur granules” (Fig. 8.43A)—bright yellow specks seen with the naked eye or with the aid of a hand lens—that microscopically represent colonies of tangled gram-positive, GMS-positive, beaded filamentous bacilli, (see Fig. 8.43B and C) coated by an eosinophilic matrix



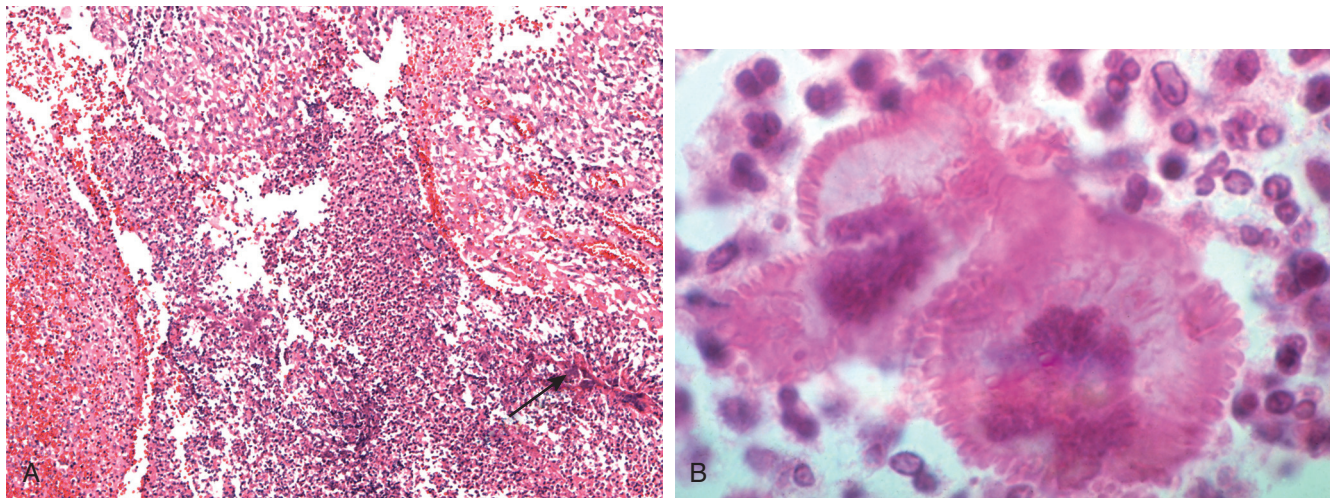
• **Figure 8.41** A, Shaggy fibrinous exudate lining wall of lung abscess due to aspiration of oropharyngeal mixed flora. B, Necrosis and bacteria in lung abscess.



• **Figure 8.42** Subpleural nodule of actinomycosis resected for suspicion of carcinoma. Note the yellow-tan appearance that suggests inflammation rather than malignancy.



• **Figure 8.43** A, Multiple actinomycotic sulfur granules within granulohistiocytic inflammatory response. B, Gram stain shows irregularly beaded filaments of *Actinomyces* spp. that also stain with Gomori methenamine silver (GMS). Recall that GMS stains all gram-positive organisms and with no specificity for actinomycosis.



• **Figure 8.44** **A**, Low-power view of botryomycosis in an infected airway. *Arrow* shows focus of botryomycosis at low power. **B**, High power of botryomycotic granule due to *S. aureus*.

of exudate plasma proteins termed the *Splendore-Hoeppli* reaction. Treatment includes long-term antibiotics and surgical resection.

The differential diagnosis of “sulfur granules” in the lung includes *botryomycosis*, a term used to describe a variety of infections by colonies of gram-positive cocci, either *Streptococcus* or *Staphylococcus* that grossly appear comparable to the sulfur granules caused by *Actinomyces*.<sup>51</sup> Distinguishing these entities depends on the morphology of the bacteria in the granules (i.e., cocci in botryomycosis versus filamentous bacteria in actinomycosis) (Fig. 8.44A and B).

### **Nocardia**

*Nocardia* spp. produces pneumonia primarily in the immunosuppressed host.<sup>52</sup> The organism shares morphologic and histochemical staining features with *Actinomyces*, but its clinical and histologic responses are usually easily distinguished. *Nocardia* produces a necrotizing pneumonia with granulohistiocytic inflammation (Fig. 8.45A), and special stains highlight tangles of gram-positive, GMS-positive filamentous organisms showing less beading than *Actinomyces* (see Fig. 8.45B). Sulfur granules are rarely seen in pulmonary infections. As distinct from *Actinomyces*, *Nocardia* are weakly acid fast and can be highlighted with modified Ziehl-Neelsen stains (e.g., Fite-Faraco) (see Fig. 8.45C). Nocardiosis is a recognized complication of pulmonary alveolar lipoproteinosis and has recently been observed in patients receiving therapies that interfere with the activities of tumor necrosis factor (TNF)- $\alpha$ .

### **Legionella**

*Legionella* spp. produce pulmonary infections ranging in severity from a mild respiratory illness to life-threatening pneumonia. Patients may suffer from a modest degree of immunosuppression due to diabetes and ethanolism. The organism can be inhaled from contaminated water and air conditioning sources, and these have been the sources of point outbreaks of infection.

The diagnosis of *Legionella* infection is currently established noninvasively by immunoassays; however, the disease may be identified histologically in biopsy or autopsy tissues. The infected lung characteristically shows a fibrinohistiocytic response with alveolar filling by fibrin and necrotic macrophages with a sparse

neutrophilic component (Fig. 8.46A), although its histology may also be indistinguishable from that of pyogenic infections.<sup>55</sup> It can be mimicked by acute fibrinous organizing pneumonia (AFOP), a recently recognized noninfective pattern of pulmonary injury (see Fig. 8.46B). Although *Legionella* is a gram-negative coccobacillus, it stains weakly with gram stains, and silver impregnation stains are required to blacken the organisms, which are often abundant in situ in the absence of prior treatment (Fig. 8.47A). *Legionella micdadei* is distinguished by its staining with modified Ziehl-Neelsen stains (see Fig. 8.47B).

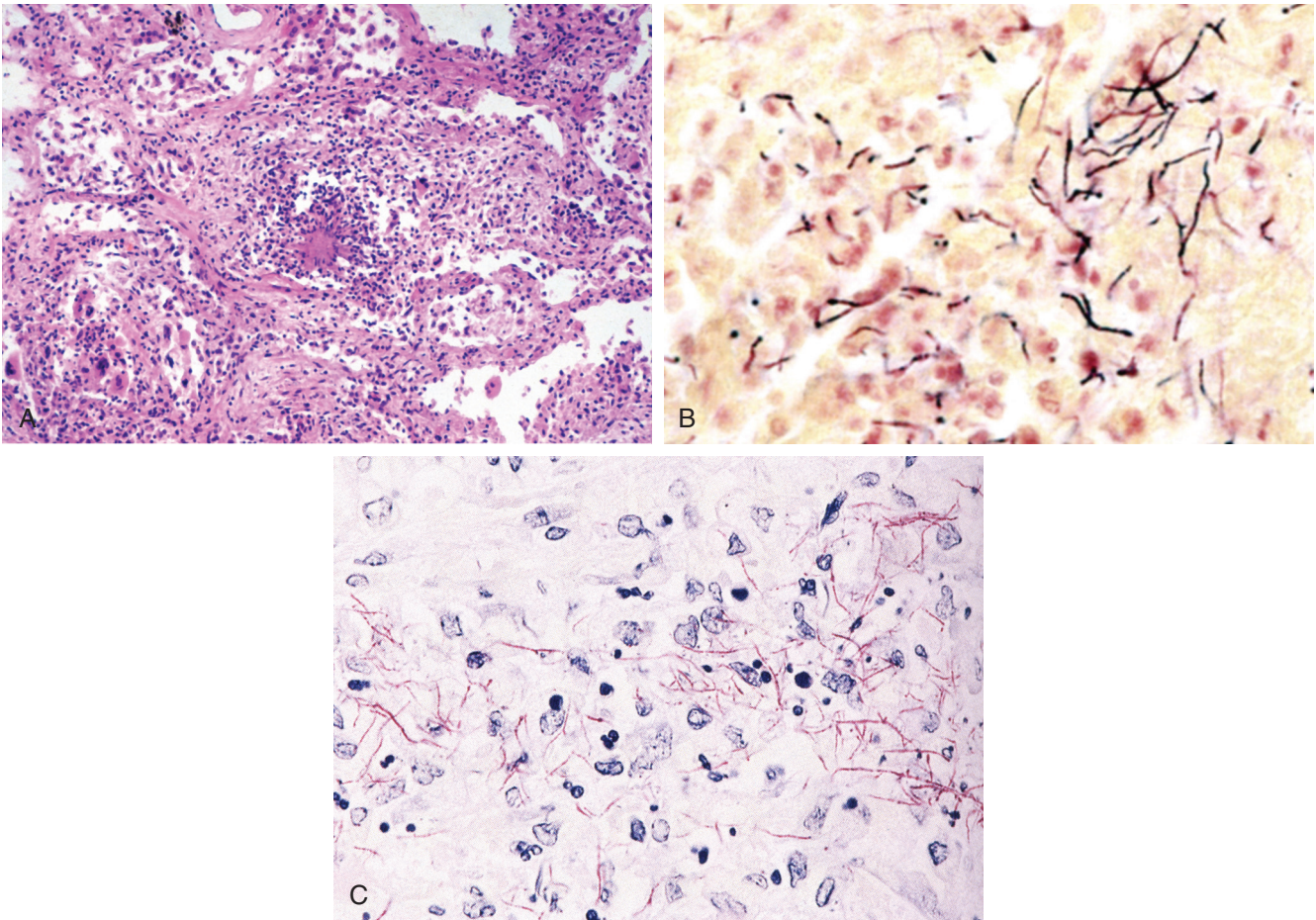
### **Rhodococcus equi**

*Rhodococcus pneumoniae* is a zoonotic infection that causes a nodular histiocytic and cavitary pneumonia in immunosuppressed patients, most commonly with HIV/AIDS (Fig. 8.48).<sup>54</sup> The causative gram-positive cocci are easily identified (Fig. 8.49A) and also stain positive with the modified Ziehl-Neelsen stain (see Fig. 8.49B). The inflammatory response shows *malakoplakia* (Fig. 8.50A), with formation of intracellular calcific concretions termed *Michaelis-Gutmann* bodies that, although nonspecific, are characteristically seen in the infection and can be highlighted by both PAS and iron stains (see Fig. 8.50B).<sup>55</sup>

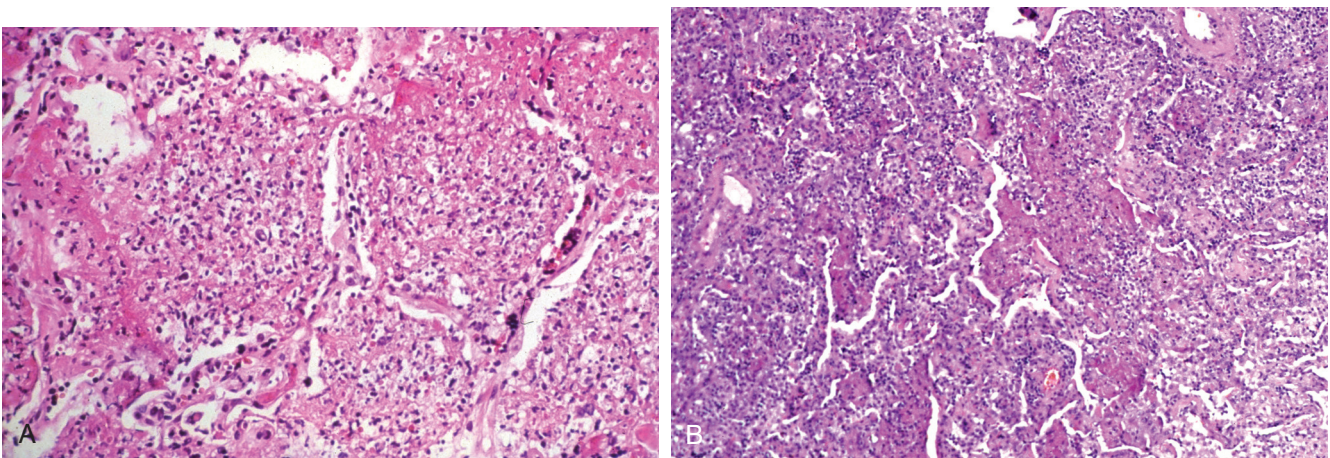
### **Tropheryma whipplei (Whipple Disease)**

Whipple disease is a rare disorder caused by the actinomycete *T. whipplei*. Whipple disease most commonly causes intestinal malabsorption, but pulmonary and neurologic disease also occurs. In an examination of the pulmonary microbiome in patients with HIV-1 infection, it was demonstrated that a large percentage of patients are colonized by *T. whipplei*.<sup>56</sup>

In the lung, Whipple disease can present as interstitial infiltrates, pleural effusions, or pulmonary hypertension.<sup>57</sup> The characteristic change in the disorder is the accumulation of foamy macrophages that show intense staining with PAS (Fig. 8.51). In some cases, microgranulomas that are histologically comparable to those seen in sarcoidosis may confuse the diagnosis (Fig. 8.52), together with the fact that the PAS staining in these granulomas may be equivocal. It is uncertain whether sarcoidosis is associated with Whipple disease or whether the sarcoidal granulomas are evidence of early infection. In these cases a small bowel biopsy will generally establish the diagnosis. Further confirmation can be

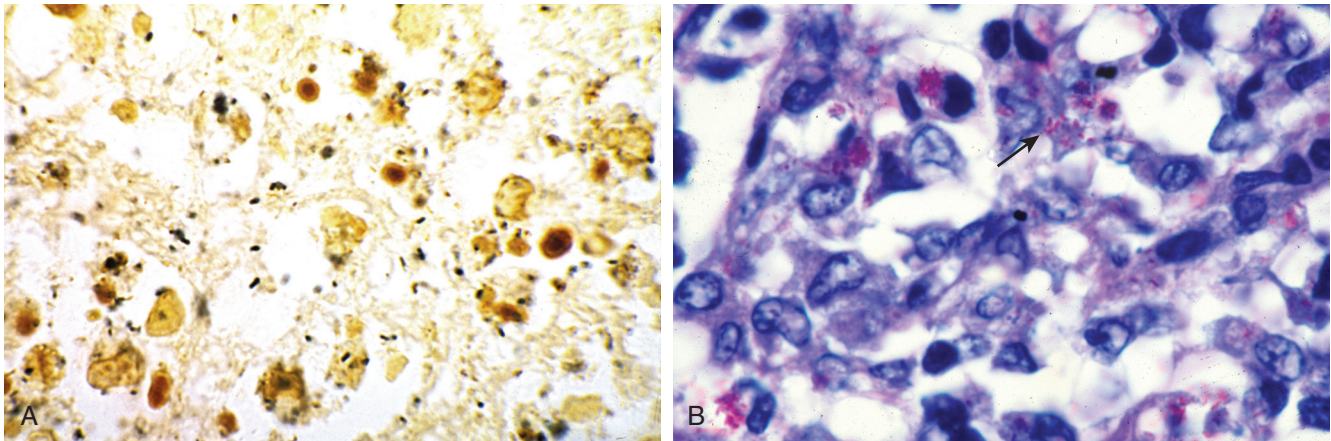


• **Figure 8.45** **A**, Necrotizing pneumonia due to *Nocardia asteroides* shows granulohistiocytic response. **B**, Like *Actinomyces*, *Nocardia* is a gram-positive filamentous bacillary actinomycetes that also stains with Gomori methenamine silver. **C**, Unlike *Actinomyces*, *Nocardia* is weakly acid-fast, and can be demonstrated with the Fite-Faraco stain.

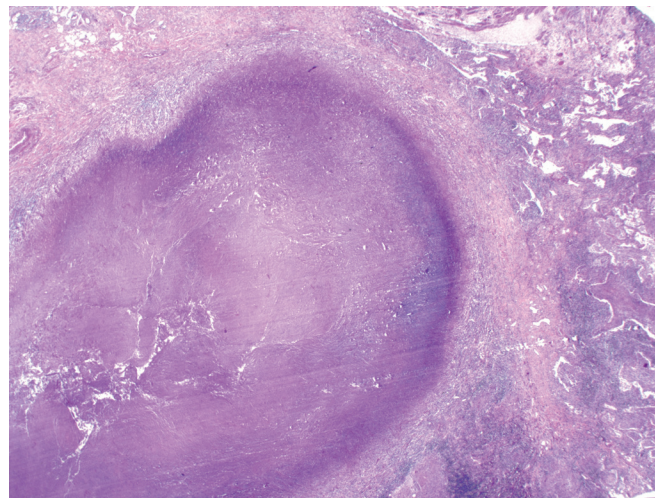


• **Figure 8.46** **A**, *Legionella* spp. characteristically produce a necrotizing bronchopneumonia with alveolar filling by fibrin and histiocytes. **B**, This appearance must be distinguished from acute fibrinous organizing pneumonia, in which the alveolar spaces are filled with fibrin, but this disorder is not due to infection.

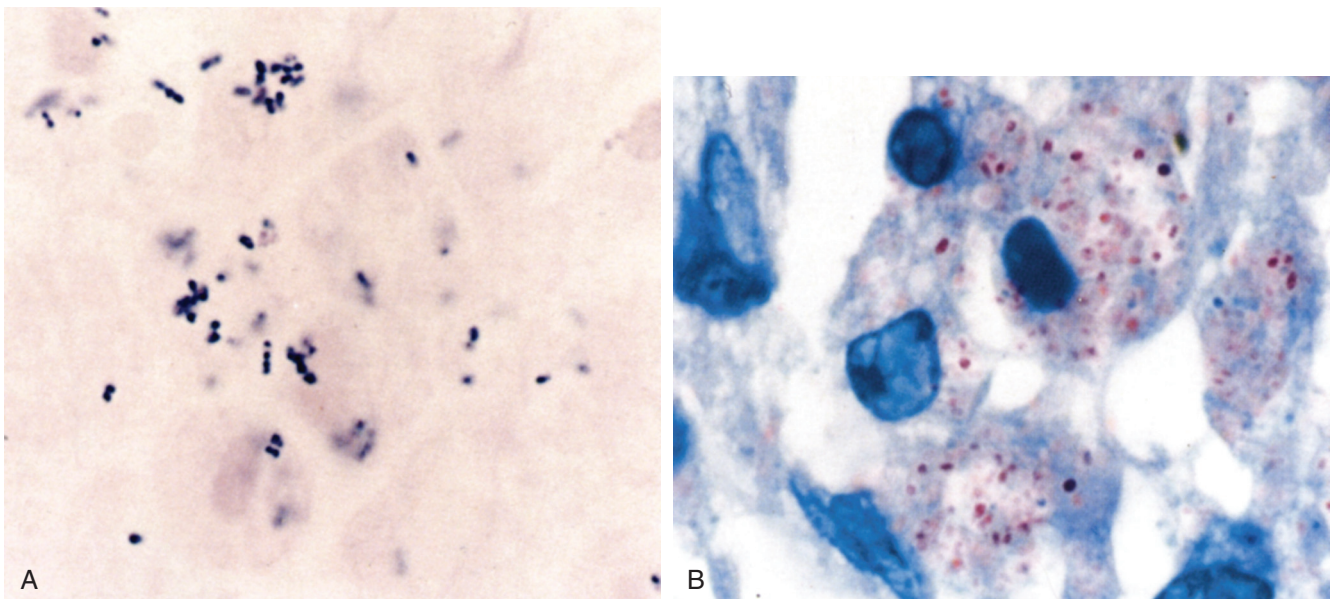




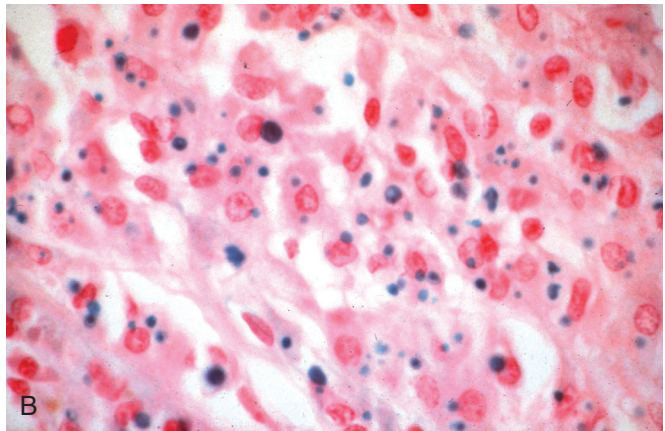
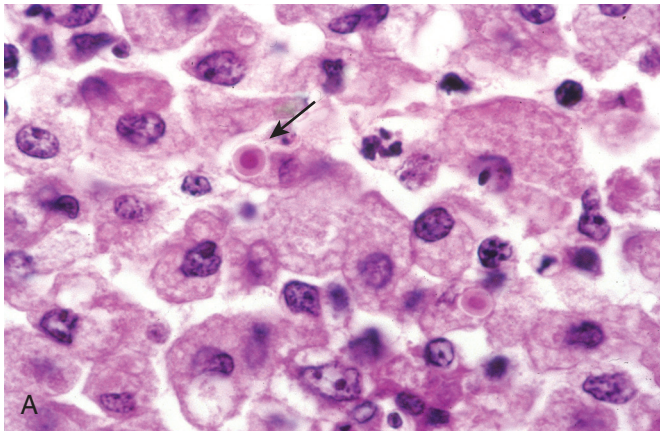
• **Figure 8.47** **A**, *Legionella* spp. are gram-negative coccobacilli but must be demonstrated by silver impregnation. **B**, *L. micdadei*, the Pittsburgh pneumonia agent, also stains with modified acid fast bacillus (AFB) stains. *Arrow* shows AFB-positive bacteria.



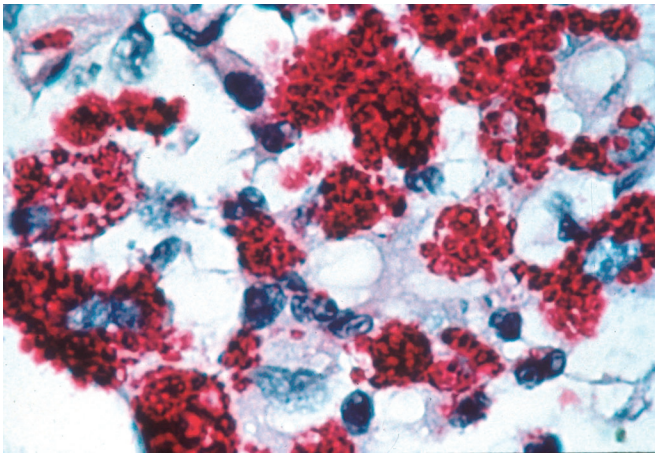
• **Figure 8.48** *Rhodococcus equi* causes a cavitory nodular pneumonia.



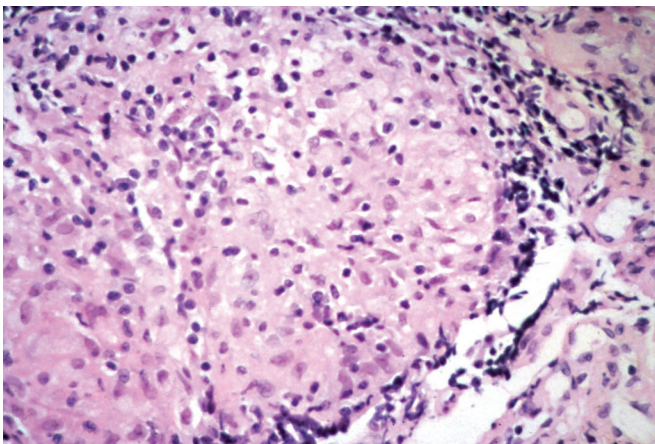
• **Figure 8.49** **A**, The causative gram-positive cocci also **(B)** stain with modified AFB preparations.



• **Figure 8.50** A, Malakoplakia with *Michaelis-Gutman* bodies, calcific concretions that are also positive in periodic acid–Schiff- and (B) iron-stained sections.



• **Figure 8.51** Macrophages staining intensely periodic acid–schiff-positive in Whipple disease.

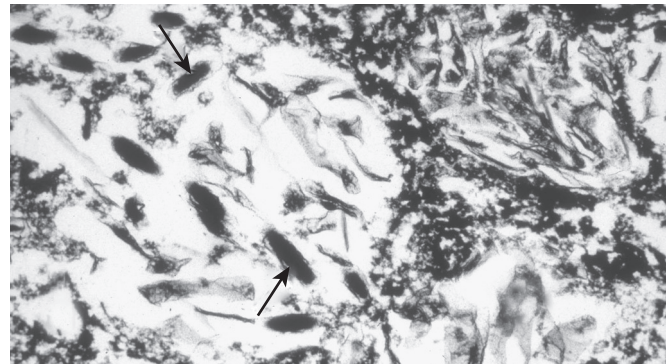


• **Figure 8.52** Nonnecrotizing granulomas mimicking sarcoidosis in Whipple disease.

achieved via ultrastructural examination demonstrating the bacillary organisms (Fig. 8.53) or by specific PCR.

### Granulomatous Pneumonia

Pathologists apply the term “granuloma” to a variety of histologic responses, including micronodular collections of tightly knit



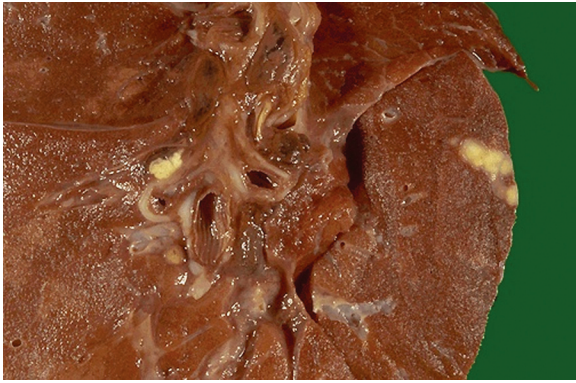
• **Figure 8.53** Ultrastructure demonstrates bacilli of *T. whipplei*. Arrows show “Whipple body” bacterium.

epithelioid macrophages (tuberculoid granulomas), necrotizing histiocytic reactions (necrotizing granuloma), and diffuse polymorphic infiltrates composed of lymphocytes, histiocytes, and plasma cells (granulomatous inflammation). The organisms that evoke these cellular responses are limited and include actinomycetes, mycobacteria, fungi, and helminths.

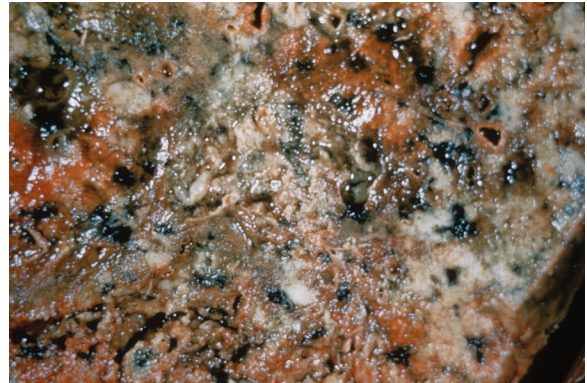
### Mycobacterial Infection

Pulmonary necrotizing granulomatous inflammation is most commonly caused by mycobacterial or fungal infections. Tuberculosis is caused by a gram-positive soil actinomycete. The disease was recognized in antiquity, and it continues to represent a major source of global morbidity and mortality, largely due to its recrudescence in the setting of poverty and HIV/AIDS.<sup>58</sup> The term *tuberculosis* is properly limited to infections caused by *Mycobacterium tuberculosis* and its genetically related congeners (e.g., *Mycobacterium bovis*) and is not the appropriate appellation for infections due to nontuberculous or “atypical” mycobacteria.

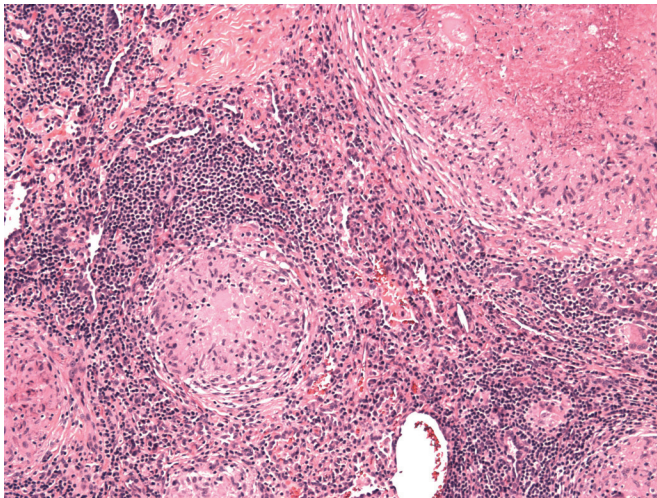
*M. tuberculosis* can affect the pulmonary airways, parenchyma, or pleura. Inhaled mycobacteria proliferate in the alveolar spaces and are then transported via lymphatics to regional hilar lymph nodes, from which they can enter the systemic circulation to spread to other organs. Progression of infection is limited by the acquisition of effective cell-mediated immunity.<sup>59</sup> The initial pulmonary focus of infection (*Ghon focus*) subsequently heals by fibrosis and may show dystrophic calcification. This Ghon focus together with the accompanying calcified site of infection in a



• **Figure 8.54** The *Ranke complex* includes the intrapulmonary *Ghon* focus of initial infection and the calcified hilar lymph node.



• **Figure 8.56** The cheesy gross appearance of a focus of caseous necrosis.



• **Figure 8.55** The tuberculoid granuloma is a collection of epithelioid histiocytes often with giant cells, surrounded by a lymphocytic infiltrate and fibrosis.

hilar lymph node are termed the *Ranke complex*, (Fig. 8.54) and the foci of primary disseminated infection are termed *Simon foci*. At all sites, the cellular response to *M. tuberculosis* is characterized by nodular collections of epithelioid macrophages with multinucleated giant cells, the tuberculoid granuloma or *tubercle*. These can undergo central necrosis due to a cell-mediated hypersensitivity response. Sites of tuberculous infection may also show neutrophilic and eosinophilic exudates, but these are generally not prominent features.

The mature tuberculoid granuloma is surrounded by a rim of T lymphocytes and contained by an outer zone of fibrosis (Fig. 8.55). The presence of tuberculoid granulomas can be a distinguishing feature clue in differentiating tuberculosis from other forms of necrotizing granulomatous inflammation (e.g., Wegener granulomatosis) in which tuberculoid granulomas are infrequent.

The term *caseous necrosis* properly refers to the “cheesy” appearance of the necrotic lesion on gross inspection. The histologic correlate is destruction of lung tissue (Fig. 8.56) with loss of the underlying reticulin stroma. However, as the latter finding is not apparent in H&E stained sections, it is best, in practice, to term tuberculous lesions as either “necrotizing” or “necrotizing,” and to avoid the terms “caseating” versus “noncaseating.”

#### • BOX 8.4 Acid-Fast Bacteria

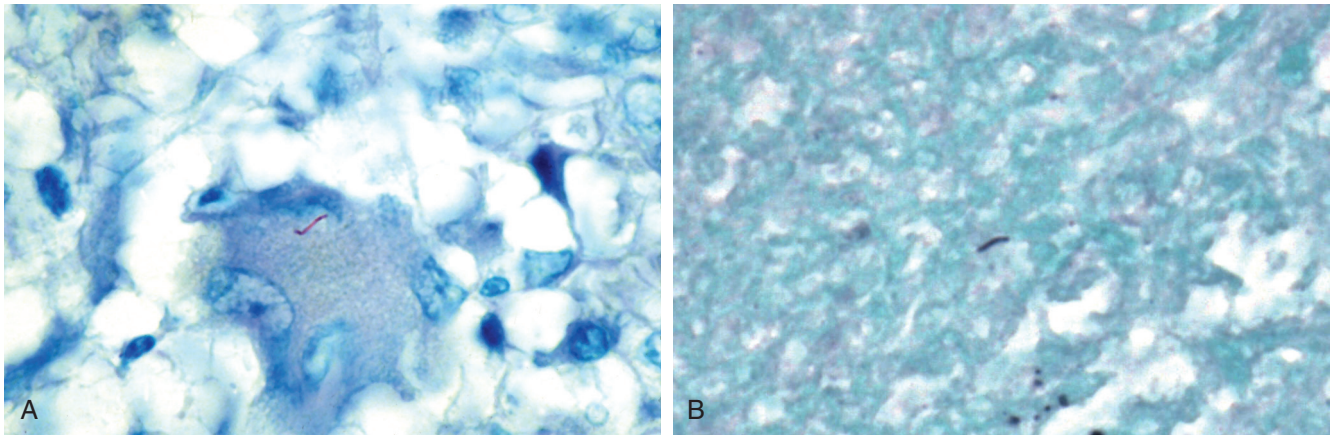
*Mycobacteria*  
*Nocardia*  
*Rhodococcus*  
*L. micdadei*

Because the response to mycobacterial infection reflects a component of immune hypersensitivity, even small numbers of organism can evoke substantial lung injury, and this complicates the task of identifying mycobacteria in situ. The organisms are best identified by their red color in acid-fast bacillus (AFB)-stained sections, such as with the Ziehl-Neelsen stain or its modifications (e.g., Fite-Faraco). Mycobacteria can show substantial morphologic variability. They are curvilinear, vary in length, and exhibit a characteristic “beaded” appearance attributable to non-homogeneous uptake of the AFB stain (Fig. 8.57A).

However, there is no reliable way to distinguish *M. tuberculosis* from “atypical” mycobacteria by histochemical staining. Because mycobacteria are weakly gram positive, they can also be demonstrated in GMS-stained sections, a finding that is nonspecific but can at times aid in the identification of the inconspicuous bacilli (see Fig. 8.57B). Because nonmycobacterial organisms can also be AFB positive, differential staining and culture results at times may be required to establish an accurate diagnosis (Box 8.4).

In practice the identification of *M. tuberculosis* by Ziehl-Neelsen staining is relatively insensitive, identifying mycobacteria in approximately 60% of culture-positive cases, so that the diagnosis may depend on isolating organisms in culture. In one study of more than 300 biopsies, mycobacteria were cultured from the biopsy specimens that contained necrotizing granulomas (38.2%), nonnecrotizing granulomas (32.4%), poorly formed granulomas (30.0%), or acute inflammation (15.8%). Tissues with fibrotic or hyalinized granulomas, nonspecific chronic inflammation, nonspecific reactive or reparative changes, no significant histologic abnormality, or malignancy failed to yield positive cultures. This study concluded that biopsy specimens with the latter diagnoses were inappropriate specimens for both mycobacterial culture and histochemical staining. Preliminary results with mycobacterial probes suggest that an in situ Affymetrix technique may increase the yield for detecting mycobacteria in lung biopsies.

Mycobacteria grow slowly in culture, and it can take weeks before they are eventually isolated. Consequently, ancillary



• **Figure 8.57** **A**, Mycobacterial tuberculosis, the “red snapper,” is a short beaded bacillus that can be equally well demonstrated with either the Ziehl-Neelsen stain or its weakly acid-fast modifications. **B**, Mycobacteria are apparent in Gomori methenamine silver-stained sections, but this finding is less specific than AFB staining.

### • BOX 8.5 Pulmonary Manifestations of Tuberculosis

Exposures with no disease (Ranke complex)  
 Caseating pneumonia  
 Acinar-nodose pneumonia  
 Nodular disease (tuberculoma)  
 Cavitory pneumonia  
 Tracheobronchitis  
 Miliary disease  
 Lymphadenitis and calcification  
 Pleuritis  
 Fibrothorax (late)

methods have been developed with the aim of increasing the likelihood of establishing a diagnosis in a timely fashion. Sensitive fluorescent staining techniques, including the auramine-rhodamine stain, are used routinely in some laboratories in examining smears and tissues. PCR methods have been developed that can identify *M. tuberculosis* and distinguish them from atypical mycobacteria, both in fresh tissues and into paraffin-embedded sections. The sensitivity and specificity of the latter approach is discussed elsewhere in this text.

#### Spectrum of Pulmonary Tuberculous Infection

Tuberculosis has protean manifestations in the lung (Box 8.5). Following most exposures, the primary infection is limited by the host's cellular immune system and the host remains asymptomatic, showing evidence of previous limited infection only via a positive tuberculin skin test. However, small numbers of mycobacteria can remain potentially viable, and active infection may ensue if cell-mediated immunity is diminished by age, the use of corticosteroids, diabetes, ethanolism, or by concomitant chronic infection. There is a marked increase in tuberculosis in patients with pulmonary silicosis, and establishing the presence of mycobacterial infection in a patient with progressive massive fibrosis due to silicosis can be difficult.

As previously noted, histologic examination of infection can provide an estimation of the adequacy of host immunity. The morphology of giant cells may be an indicator of whether host

cell-mediated immunity is adequate in containing tuberculous infection. Prior to the development of effective cell-mediated immunity, many giant cells in the lesions show nuclei that have aggregate towards one pole of the multikaryon (Fig. 8.58A), whereas when infection is effectively contained, Langhans giant cells with peripheral nuclei or giant cells with centrally placed nuclei predominate (see Fig. 8.58B). If cell-mediated immunity is profoundly diminished, granulomas may be poorly formed or absent.

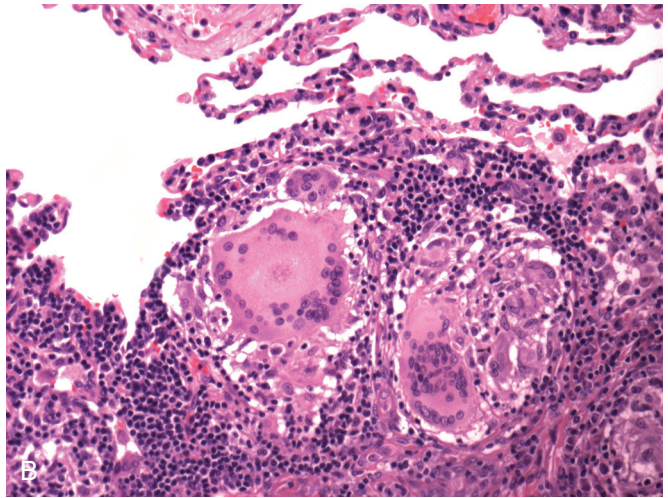
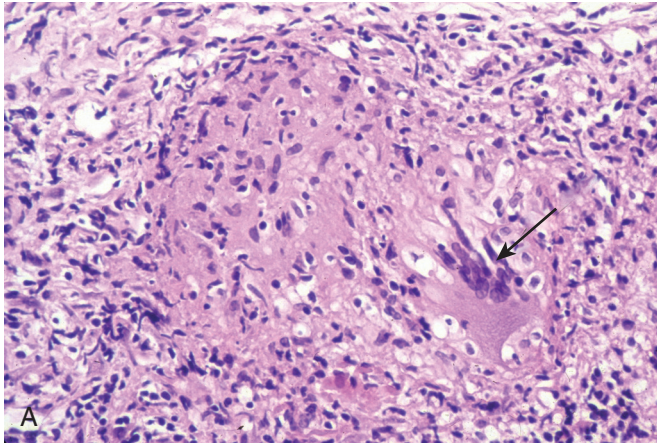
Failure to contain the primary infection leads to its progression. Primary tuberculosis may show necrotizing pneumonia (Fig. 8.59), regionally involved lymph nodes, and a granulomatous pleuritis with lymphocytic effusion. Dissemination of organisms via the bloodstream can yield miliary disease, in which innumerable foci of active infection with poorly formed granulomas are seen (Fig. 8.60 A to C).<sup>60</sup>

Tuberculous acinar-nodose bronchopneumonia results from mycobacterial infection extending along the pulmonary acinus (Fig. 8.61). Tuberculomas are defined foci of nodular tuberculous infection (Fig. 8.62). When these cavitate into an adjacent bronchus, it can lead to discharge of numerous bacilli with cough or expectoration (Fig. 8.63A). Although bacillary counts in cavitory lesions are generally high, even large cavities at times will fail to show a single identifiable organism by histochemical staining, and diagnosis must be made presumptively based on histologic appearance and empiric response to antituberculous medications.<sup>61</sup> The extension of cavitory disease to involve an accompanying pulmonary artery may produce a Rasmussen aneurysm and risk of vascular rupture leading to fatal hemoptysis (see Fig. 8.63B).

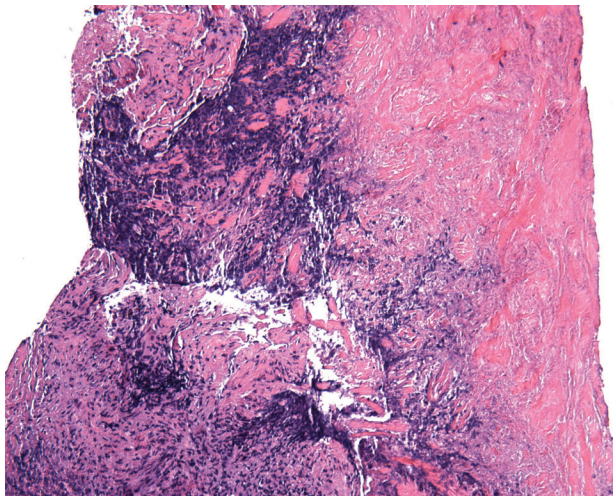
Mycobacteria can spread along the mucosal surfaces of the airways to produce ulcerated lesions in the larynx and tracheo-bronchial tree that can mimic Wegener granulomatosis (Fig. 8.64). However, as previously noted, the latter disorder rarely includes well-formed tuberculoid granulomas, and their presence favors the diagnosis of infection.

#### Reactivation Tuberculosis

Most clinically encountered cases of tuberculosis occurring in previously asymptomatic individuals with positive cutaneous responses to purified protein derivative (PPD) represent either



• **Figure 8.58** **A**, Polarized giant cells in early infection with *M. tuberculosis* (arrow). These cells may reflect host difficulties in containing the infection. **B**, Mature infection shows Langhans giant cells and giant cells with central nuclei.



• **Figure 8.59** Necrotizing pneumonia due to *M. tuberculosis*.

reactivation or reinfection. Reactivation indicates an acquired defect in cell-mediated immunity. Tuberculosis tends to reactivate in the upper lobes of the lung where ventilation/perfusion ratios are high. Histologically the lung shows necrotizing granulomas in areas of scarring and traction bronchiectasis (Fig. 8.65), due to the initial mycobacterial infection. In addition to reactivation of tuberculosis, the differential diagnosis of necrotizing granulomatous inflammation in this setting includes fungal infection and atypical mycobacterial infection, because both have a predilection to develop in areas of old pulmonary apical scarring. The distinction may be difficult in the case of atypical mycobacterial infection, as special stains cannot distinguish these possibilities, and culture or ancillary diagnostic tests are necessary (Fig. 8.66).

### Atypical Mycobacteria

A number of mycobacteria that are genetically distinct from *M. tuberculosis* can produce pulmonary infection.<sup>62</sup> These organisms vary in virulence, and this is often reflected in the histologic appearance of the infection (Box 8.6). *Mycobacterium avium-*

### • BOX 8.6 Classification of Mycobacteria

#### Tuberculosis Complex

*M. tuberculosis*  
*M. bovis*

#### Runyon Group I

*M. kansasii*  
*M. marinum*

#### Runyon Group II

*M. goodii*  
*M. scrofulaceum*

#### Runyon Group III

*M. intracellulare*  
*M. avium*  
*M. xenopi*

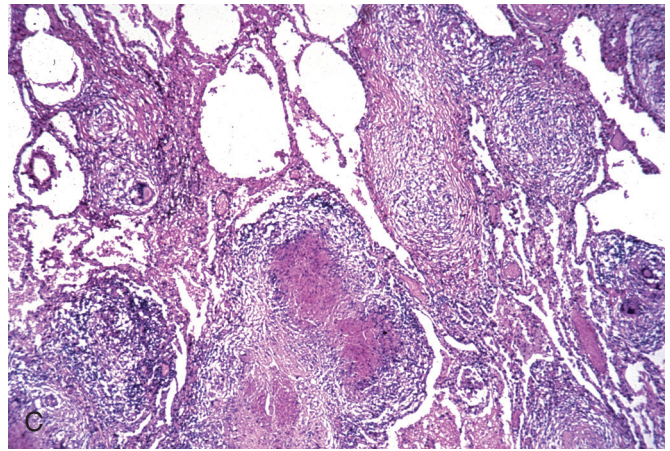
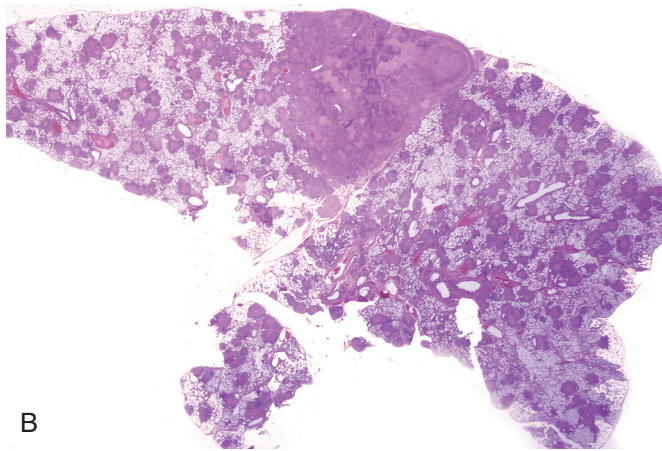
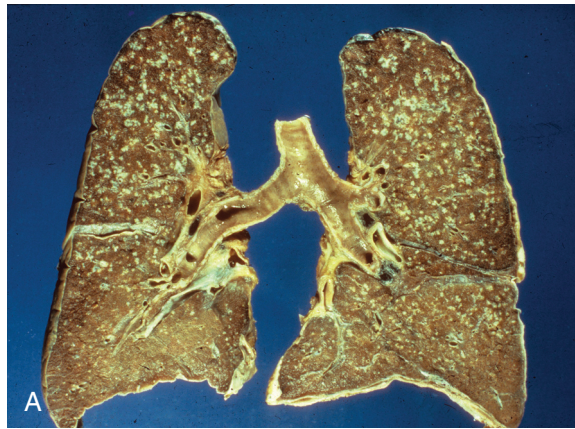
#### Runyon Group IV

*M. fortuitum*  
*M. chelonae*  
*M. abscessus*

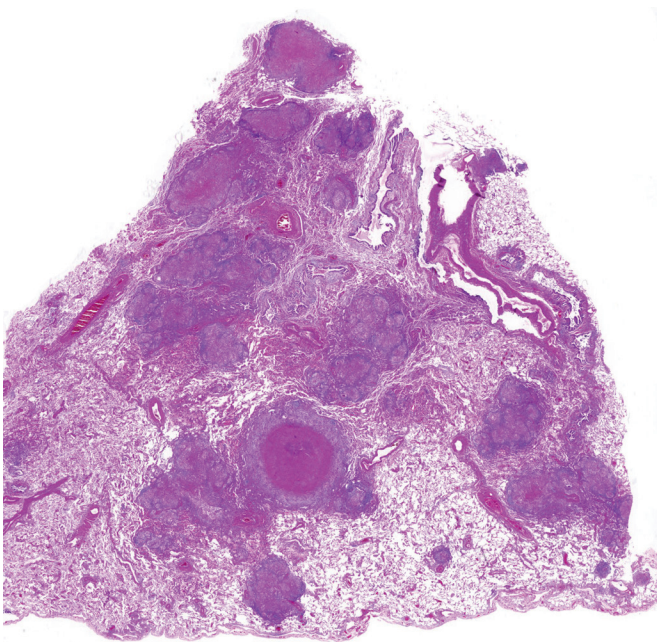
*intracellulare* or *Mycobacterium avium* complex (MAC) can attack the lung in a variety of clinical settings.<sup>63</sup> Patients immunosuppressed by HIV/AIDS can develop virulent infections with features that mimic tuberculosis. When adaptive T cell-mediated immunity is severely compromised, the host response may be limited to foamy histiocytes that have ingested large numbers of mycobacteria.<sup>64</sup> MAC can be demonstrated by both AFB and PAS stains, and clinical signs of both tuberculosis and MAC disease may only be recognized following treatment with antivirals, the so-called *immune reconstitution syndrome*.

In the immunocompetent host, MAC tends to affect older women (Lady Windermere disease) and patients with bronchiectasis or bullous emphysema. It is commonly seen in the right middle lobe syndrome due to bronchiectasis and chronic atelectasis. The lesions of MAC infection are detected radiographically as “tree-in-bud” opacities reflecting terminal bronchiolar infection (Fig. 8.67A), together with nodules that may be either solid or cavitory. Histologically the pathology often shows extensive areas of nonnecrotizing epithelioid histiocytes and is highly characteristic (see Fig. 8.67B). The causative mycobacteria are indistinguishable from *M. tuberculosis* and only culture or PCR can accurately establish the diagnosis.

A recently described variant of MAC infection is “hot tub” lung. In these cases the lung shows a microgranulomatous



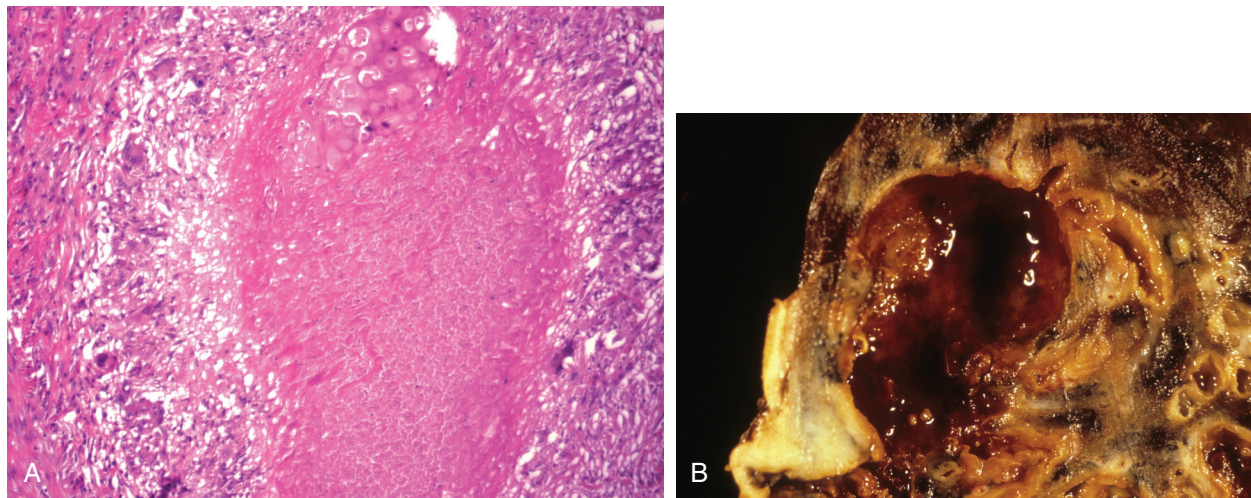
• **Figure 8.60** **A**, Miliary tuberculosis in lung reflects the failure to contain either primary or reactivation infection by the host. **B**, Innumerable millet-sized nodules are seen in lung with focus of necrotizing pneumonia. **C**, The response in miliary tuberculosis included poorly formed granulomas. With profound immunodeficiency, granulomatous changes may be absent.



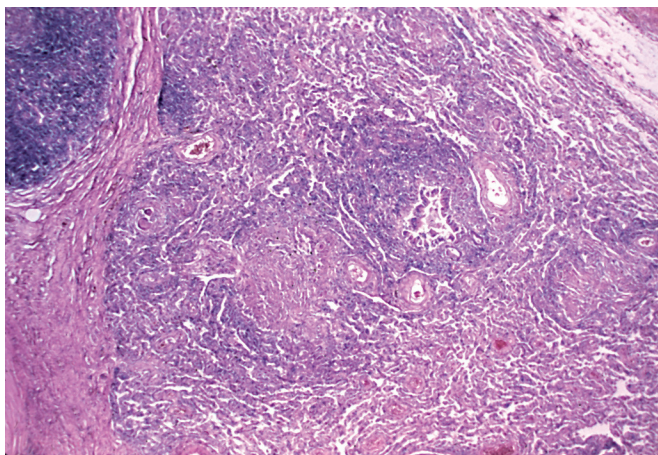
• **Figure 8.61** Geographic infiltrates of necrotizing acinar-nodose tuberculosis.



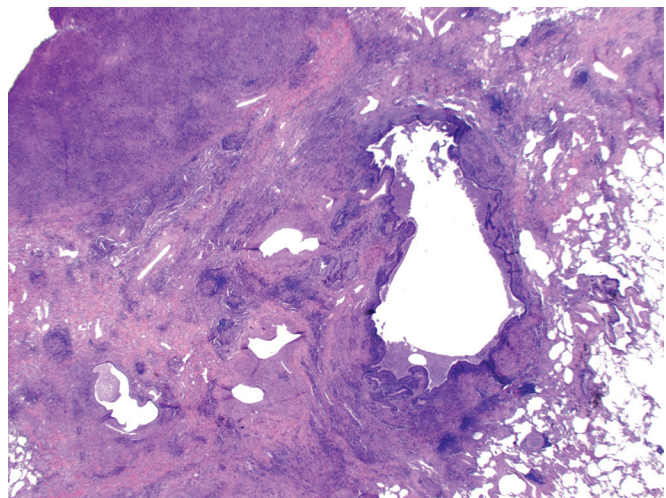
• **Figure 8.62** Localized tuberculoma.



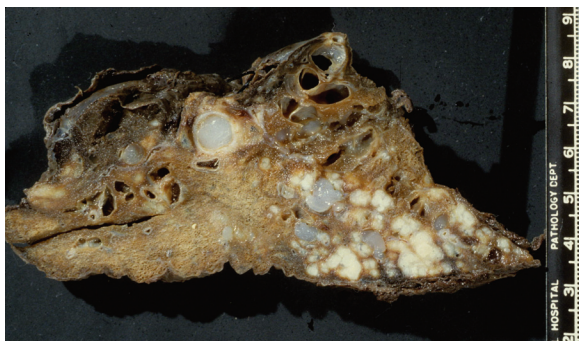
• **Figure 8.63** **A**, Cavitary tuberculosis. **B**, Erosion of a cavity into an adjacent pulmonary artery can produce a *Rasmussen aneurysm* and lead to fatal pulmonary hemorrhage.



• **Figure 8.64** Tracheobronchial tuberculosis. These lesions can mimic Wegener granulomatosis, but the presence of tuberculoid granulomas is a distinguishing diagnostic feature because they are rarely seen in Wegener granulomatosis.



• **Figure 8.66** Necrotizing granulomas in area of old calcified focus of bronchiectasis were due to atypical mycobacterial infection.

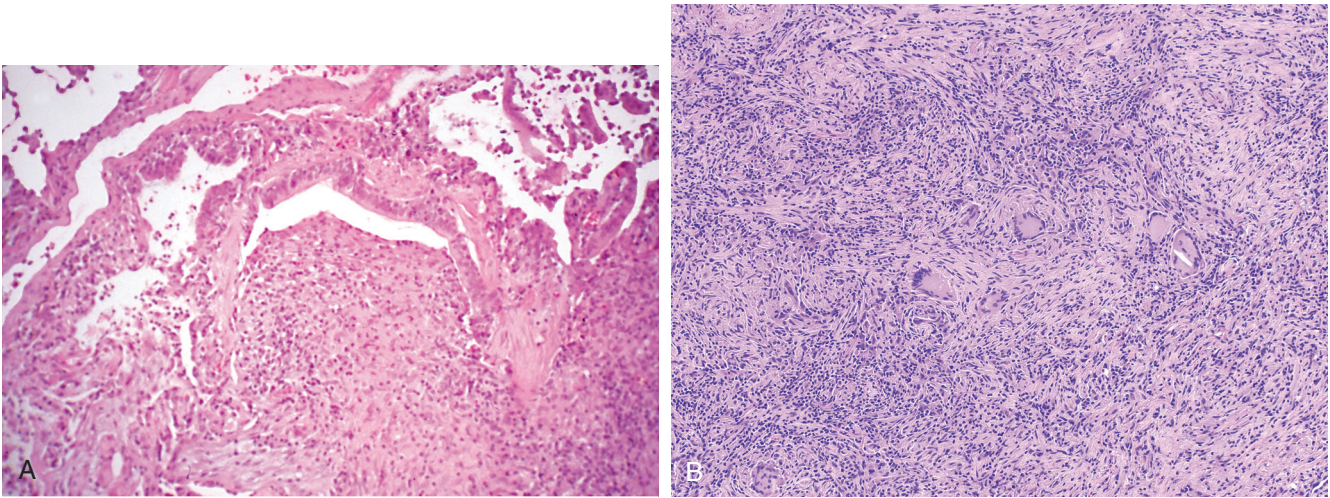


• **Figure 8.65** Bronchiectasis in tuberculosis.

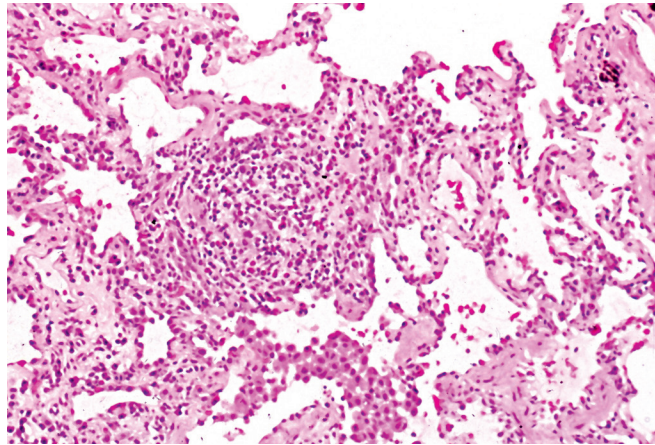
hypersensitivity pneumonitis that may be accompanied by necrotizing granulomatous inflammation. The pathology appears to represent primarily a cell-mediated hypersensitivity response to mycobacterial antigens, with a possible element of direct infection as well (Fig. 8.68).

An unusual presentation of MAC infection in the immunosuppressed host is the *pseudosarcomatous* nodule.<sup>65</sup> This can develop in the lung or in soft tissues and hematopoietic tissues. The nodules are composed of spindle cells and may be mistaken for a low-grade spindle-cell neoplasm (Fig. 8.69A). However, examination reveals the foamy appearance of the spindle cells, which prove to be CD68<sup>+</sup> macrophages containing large numbers of ingested mycobacteria, (see Fig. 8.69B), and the absence of mitotic activity. Within the spectrum of unusual mesenchymal reactions seen in the immunocompromised one must consider inflammatory myofibroblastic tumors that may include foamy histiocytes (Fig. 8.70A) associated with human herpesvirus 8 (HHV-8) infection (see Fig. 8.70B).

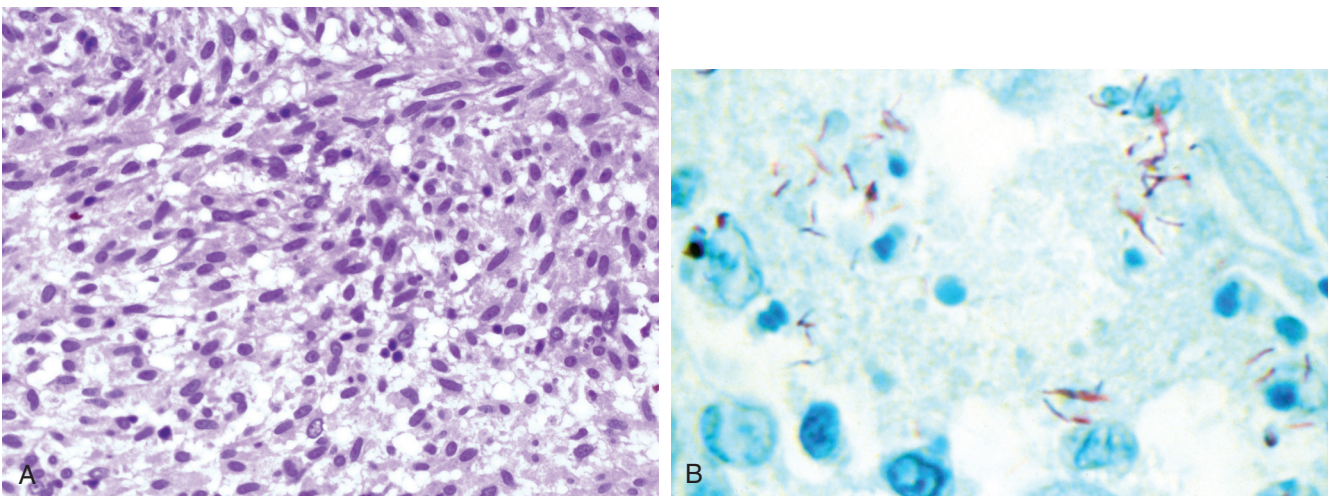
Other mycobacteria also cause pulmonary infection. *Mycobacterium kansasii* is a virulent species of atypical mycobacteria that produces necrotizing infection indistinguishable from tuberculosis. The organism often shows a prominent pattern of “cross-linking” on mycobacterial stains in situ that is characteristic but not diagnostic (Fig. 8.71). Other rapidly growing mycobacteria, including *Mycobacterium abscessus*, infect preexisting areas of



• **Figure 8.67** **A**, Nonnecrotizing granulomatous inflammation ulcerates a small airway in a patient with MAC. **B**, Sheets of epithelioid histiocytes are characteristically seen in MAC infection in nonimmunosuppressed patients with chronic airway disease.

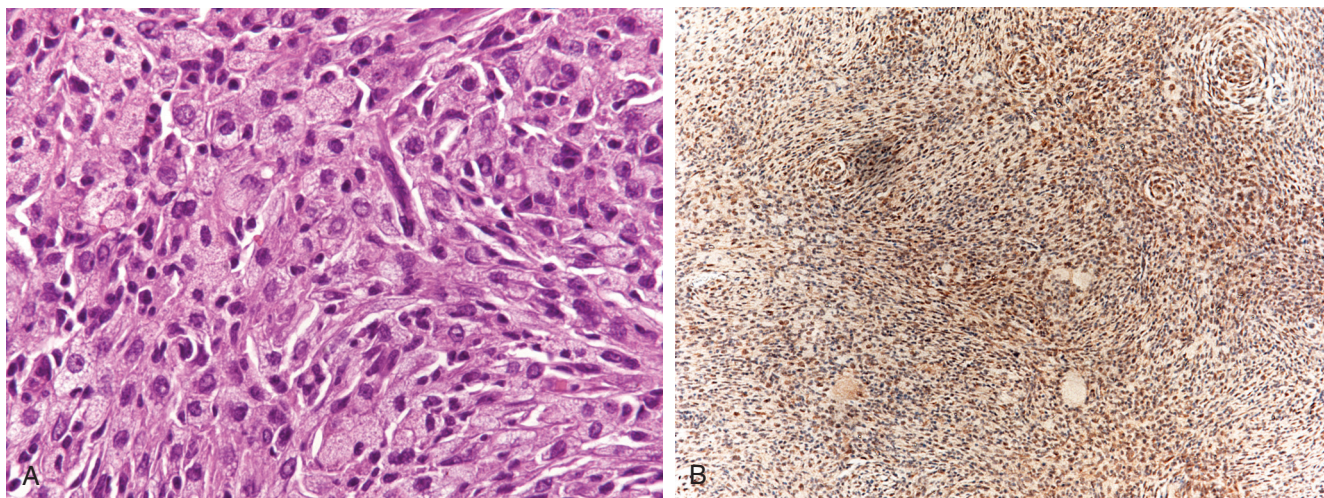


• **Figure 8.68** Micronodular granulomatous inflammation in “hot-tub” lung, a hypersensitivity reaction to MAC.

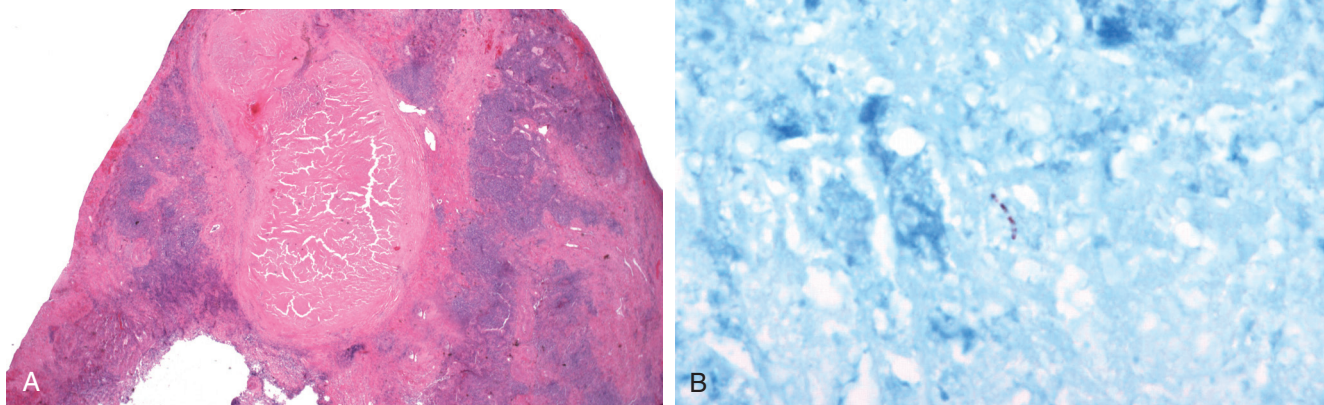


• **Figure 8.69** **A**, A pseudosarcomatous nodule in a patient with human immunodeficiency virus/acquired immune deficiency syndrome due to *Mycobacterium avium* complex. **B**, Large numbers of AFB/periodic acid–Schiff–positive mycobacteria are generally seen in this response.





• **Figure 8.70** **A**, Inflammatory myofibroblastic tumor with foamy histiocytes associated with **(B)** human herpesvirus 8 in patient with acquired immune deficiency syndrome can mimic *Mycobacterium avian* complex infection.



• **Figure 8.71** **A**, *Mycobacterium kansasii* is a virulent organism that produces necrotizing granulomatous inflammation comparable to *M. tuberculosis*. **B**, The elongate bacilli exhibit irregularity in their uptake of AFB stain, producing a characteristic pattern of “cross-linking.”

active bronchiectasis, particularly in cystic fibrosis (Fig. 8.72A), and rarely may involve the lung as miliary blood-borne disease (see Fig. 8.72B). *Mycobacterium fortuitum* produces limited infection in patients with diabetes, HIV/AIDS, and chronic upper gastrointestinal disease; all of the rapid growing nontuberculous mycobacteria, including *Mycobacterium smegmatis*, can complicate pneumonia due to aspiration of lipid-based substances like nose drops.<sup>66</sup>

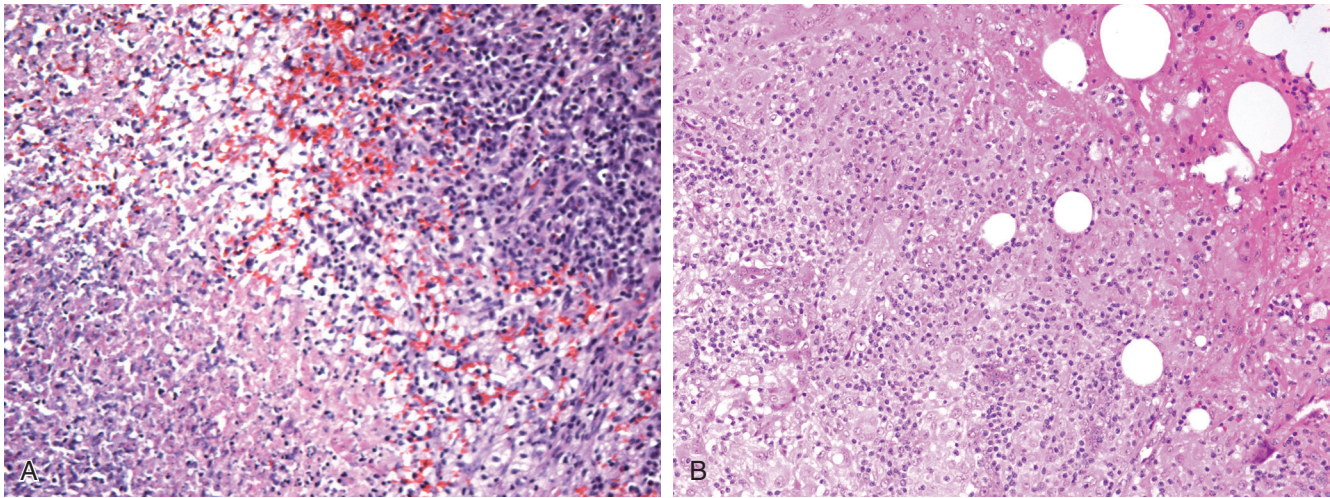
### Melioidosis

Rarely seen outside of Southeast Asia, where it is endemic, chronic infections due to *Pseudomonas pseudomallei* developed in veterans of the Vietnam War many years after they had left the region.<sup>67</sup> Acute melioidosis is a systemic infection that produces widespread coalescent microabscesses, but it may resolve without being recognized only to recur many years later in lung, lymph nodes, and bone. The lung shows necrotizing granulomatous lesions surrounded by a zone of fibrosis, (Fig. 8.73) and regional lymph nodes show stellate necrosis that can mimics “cat-scratch” disease due to *Bartonella henselae*. The offending organism is a

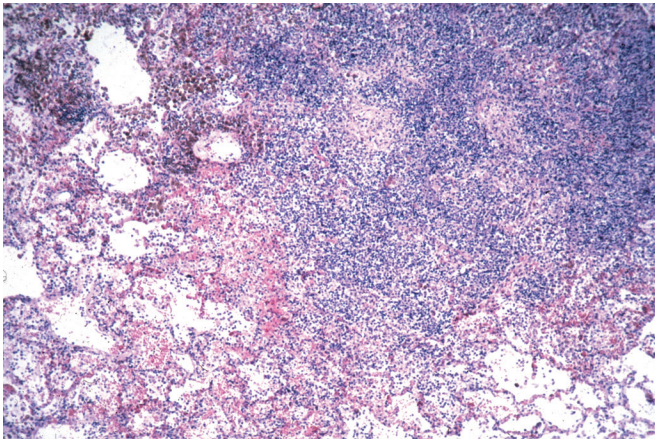
gram-negative motile bacillus that shows bipolar staining that can be difficult to demonstrate in situ.

### Fungal Infection Due to Yeasts

Fungi produce a spectrum of changes in the lung, ranging from benign colonization of airways to malignant angioinvasive infections. Some fungi grow as yeast at body temperatures, whereas others are hyphate molds (Table 8.2). Most fungal yeasts are soil organisms that are topographically distributed in the United States. Although *Histoplasma capsulatum* may be encountered virtually anywhere that soil and water coexist, most cases in the United States are endemic to the Mississippi and Ohio River valleys. *Blastomyces dermatitidis* predominantly affects individuals living in the Great Lakes regions and in the southeastern United States, whereas *Coccidioides immitis* is primarily encountered in the San Joaquin Valley of the Southwest. Despite their usual distribution, modern air travel and a highly mobile population has resulted in the possibility of these infections presenting virtually anywhere, and pathologists must be acquainted with their



• **Figure 8.72** **A**, *M. abscessus* complicates areas of bronchiectasis and may be exceedingly difficult to eradicate fully with antimycobacterial agents. **B**, Miliary *M. abscessus* in a patient with multisystem disease and mycobacteremia.



• **Figure 8.73** *P. pseudomallei*, the cause of melioidosis, may reactivate many years following initial exposure to produce a necrotizing granulomatous pneumonia that resembles tuberculosis.

characteristic histologic appearances. However, it is always prudent to inquire into possible travel prior to diagnosing an “exotic” fungal infection because substantial overlap can exist in fungal morphologies.

### Histoplasmosis

Primary *Histoplasma* infection produces a “viral-like” illness that generally resolves spontaneously.<sup>68</sup> However, if there is a defect in cell-mediated immunity or when the yeast burden is large, progression of infection may ensue.<sup>69</sup> Chronic histoplasmosis tends to develop in the lung apices in areas of bullous emphysema or bronchiectasis. Although most yeast can be identified in H&E-stained sections, *Histoplasma* require special histochemical staining due to their small size. GMS is the stain of choice because PAS at times fails to decorate the yeast.

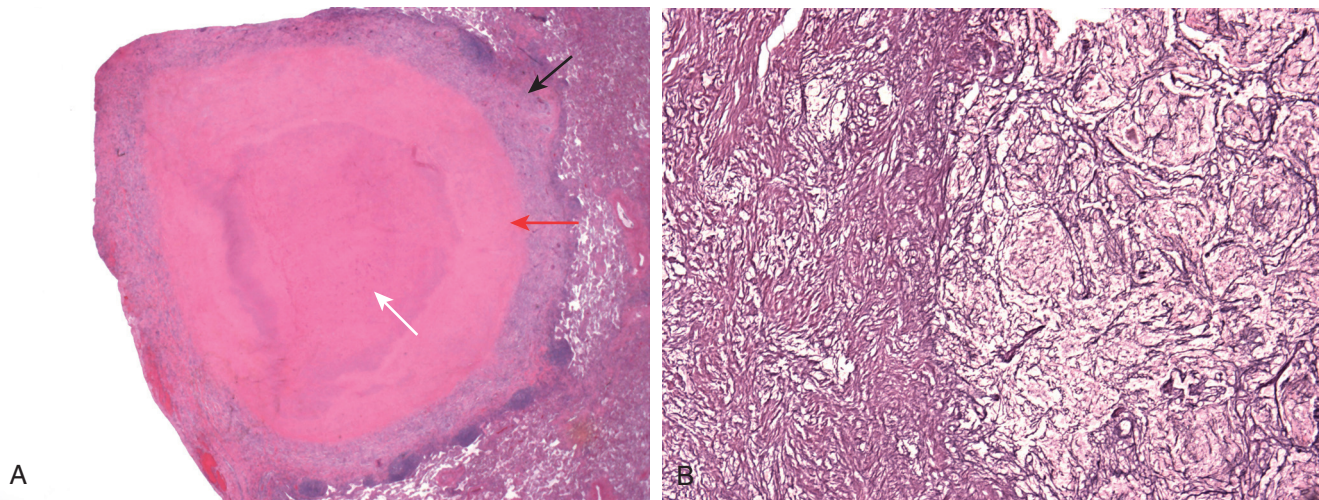
Necrotizing granulomas due to *Histoplasma* spp. show central necrosis often surrounded by regions of mummefactive necrosis in which the “ghost outlines” of the underlying framework of the lung can still be distinguished in H&E- and reticulin-stained sections (Fig. 8.74A and B). The lining of the necrotic granuloma

**TABLE 8.2** Fungal Identification in Tissue

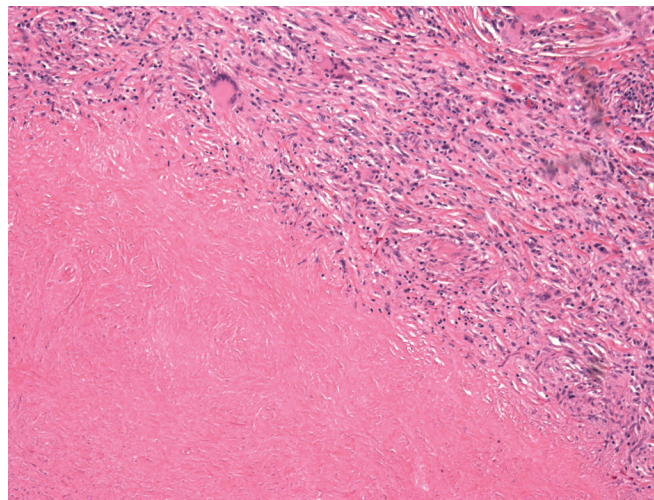
Organism	Size (Width $\mu\text{M}$ )	Defining Morphology
<i>H. capsulatum</i>	2-5	Narrow-neck bud
<i>C. neoformans</i>	5-20	Narrow-neck bud
<i>B. dermatitidis</i>	15-30	Broad-based bud
<i>C. glabrata</i>	3-5	Budding, no pseudohyphae
<i>Candida</i> spp.	2-3	Yeast, pseudohyphae, hyphae
<i>Aspergillus</i> spp.	3-5	Acute-angle branching, septate, conidial head
<i>Zygomycetes</i> spp.	5-8	Right-angle branching, ribbons, pauciseptate
<i>Pseudallescheria</i> spp.	3-4	Acute-angle branch, septate, terminal chlamyospore, pigmented conidia
<i>Fusarium</i> spp.	4-5	Acute- and right-angle branch, septate, narrowed branch points
<i>C. immitis</i>	20-200	Endosporeulation

includes epithelioid histiocytes and giant cells but unlike tuberculosis does not show extensive tubercle granuloma formation, and the wall of the lesion characteristically exhibits paucicellular hyalinized fibrosis (Fig. 8.75).

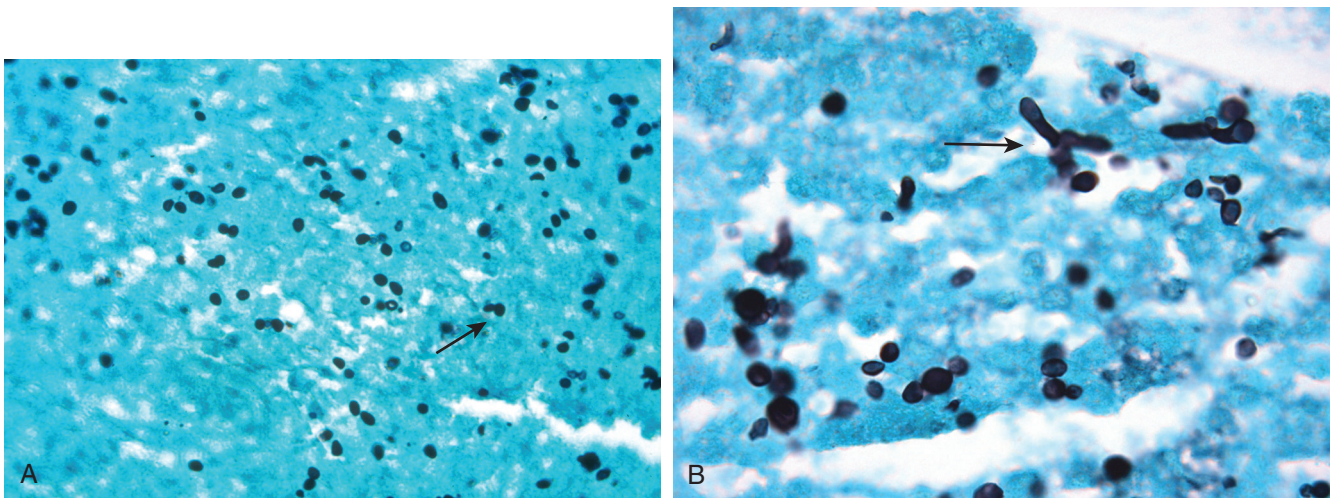
Although they are facultative intracellular pathogens, *Histoplasma* cluster in areas of necrosis and are often seen outside of histiocytes.<sup>70</sup> The 2- to 4- $\mu\text{M}$  yeast show teardrop-shaped forms and reproduce by single, narrow-necked buds whose presence is diagnostic. Despite their name, no capsule is present (Fig. 8.76A). At times, pseudohyphae may be seen, and this should not dissuade the pathologist from making the correct diagnosis (see Fig. 8.76B) when all other diagnostic criteria are met.



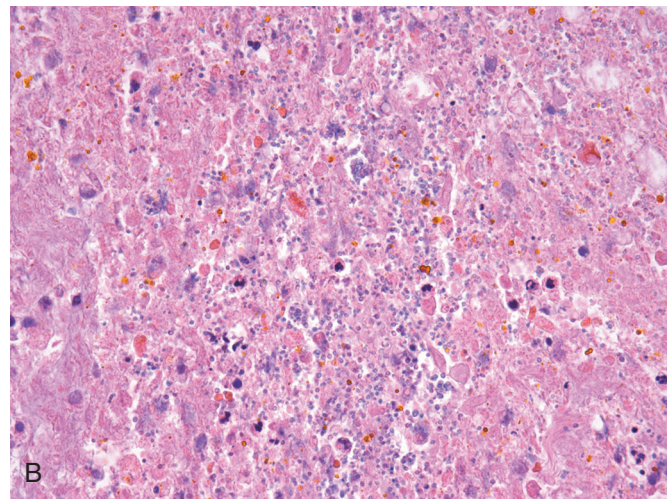
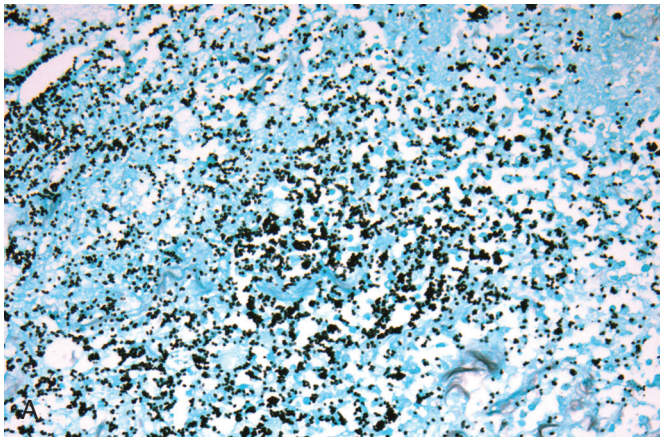
• **Figure 8.74** **A**, Nodular pneumonia due to *H. capsulatum* often shows necrotizing granulomatous inflammation with three zones (*arrows*). The outer capsule encloses an area of mummefactive necrosis that in turn surrounds an area of caseating necrosis findings confirmed by **(B)** reticulin stains.



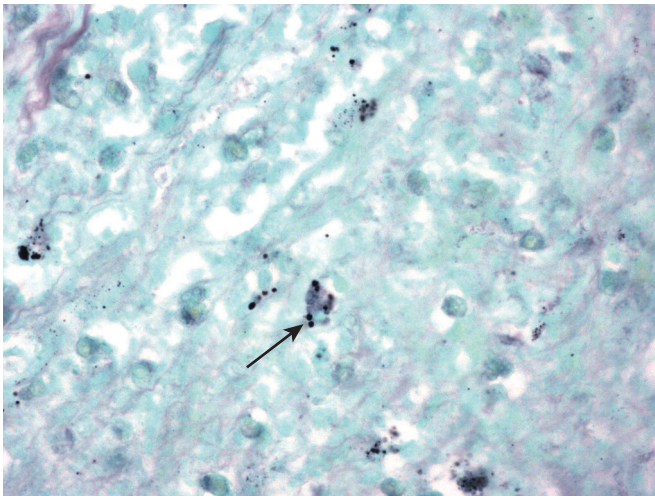
• **Figure 8.75** The wall of the necrotizing granuloma shows poorly formed granulomas and giant cells with a highly characteristic hyalinized basket-weave fibrosis.



• **Figure 8.76** **A**, Narrow necked budding 2 to 4  $\mu\text{m}$  yeast of *H. capsulatum* in Gomori methenamine silver stained section. Periodic acid-Schiff is not reliable for demonstrating this yeast. *Arrow* shows narrow-necked budding yeast. **B**, *H. capsulatum* infection with irregular yeast forms and pseudohyphae. *Arrow* points to pseudohyphal growth.



• **Figure 8.77** A, *C. glabrata* can easily be mistaken for *H. capsulatum* on Gomori methenamine silver stain, but (B) the yeast are amphophilic in hematoxylin and eosin–stained sections and easily differentiated on this basis.



• **Figure 8.78** Microcalcifications (arrow) can closely resemble *H. capsulatum*. At times ultrastructural examination may be required to exclude infection.

The differential diagnosis includes microforms of *Cryptococcus* or *Blastomyces*, *P. jiroveci*, and *Candida glabrata*. In the former, identifying the associated larger yeast forms eliminates the possibility of *H. capsulatum* infection. *P. jiroveci* shows irregularly shaped cysts with pericapsular accentuation on GMS stain and the organisms do not bud; *C. glabrata* can closely mimic the infection in GMS-stained sections, but unlike *Histoplasma*, they also stain amphophilic with H&E and are strongly gram positive (Fig. 8.77 A and B).

However, the most common and greatest difficulties in diagnosis can arise in distinguishing small, regular microcalcifications in GMS-stained sections because they can closely resemble degenerate yeast (Fig. 8.78). The presence of irregular calcifications is a clue to their actual nature, but at times, ultrastructural examination may be required to exclude infection. In the immunosuppressed host, disseminated infection is primarily distributed within interstitial and alveolar macrophages (Fig. 8.79).<sup>71</sup>

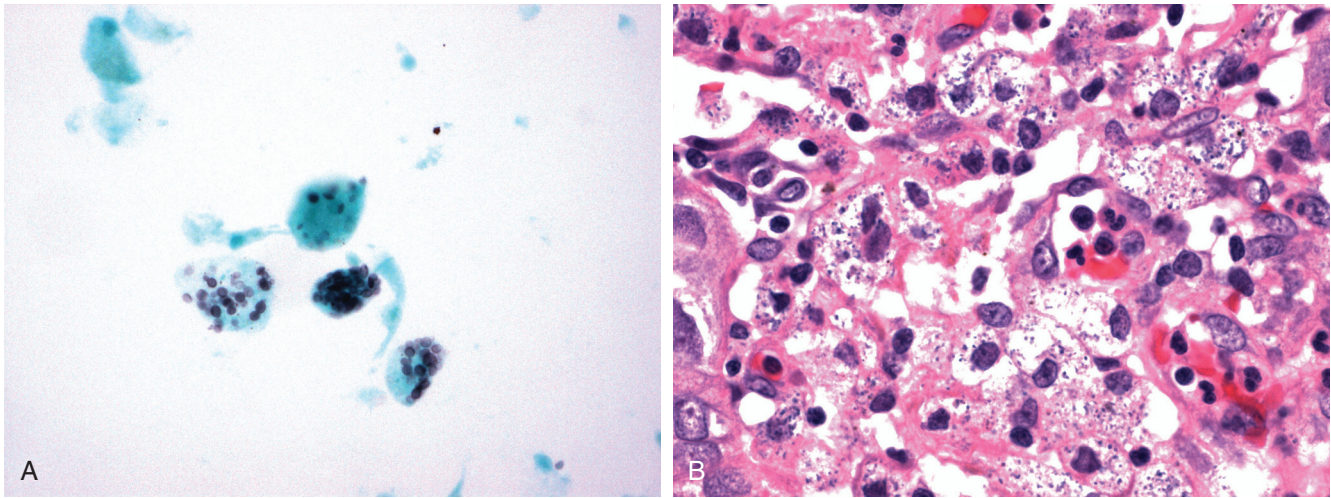
Extension of infection from a peribronchial lymph node can produce *mediastinal granuloma*, a lesion characterized by dense whorled hyaline fibrosis with aggregates of plasma cells (Fig. 8.80A). Organisms are rarely identified in the areas of paucicellular scarring, and this form of the disease appears to be immunologically mediated. At times, necrotizing granulomatous inflammation is concomitantly present and confirms the diagnosis (see Fig. 8.80B). The lesion can entrap the large vessels of the mediastinum, leading to the superior vena caval syndrome and death. Surgical excision is required but not always technically possible.

Remotely infected calcified peribronchial lymph nodes due to histoplasmosis can erode into adjacent airways to be either expectorated or aspirated as broncholiths. Surprisingly, these may show persistently viable yeast forms and colonization by aspirated oropharyngeal bacteria (Fig. 8.81).

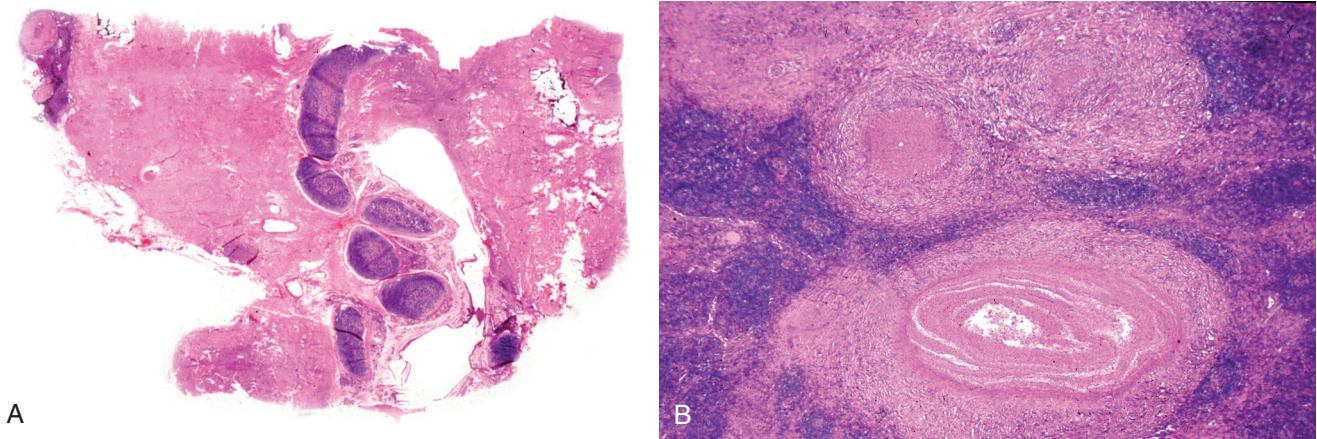
Old calcified granulomas are commonly encountered in surgical resection of lungs for neoplasia.<sup>72</sup> Most of these are due to healed tuberculosis or histoplasmosis, depending on exposure. In the vast majority of cases, no organism will be identified but occasionally nonviable degenerate histoplasma may be seen, although distinguishing them with confidence from microcalcifications can be difficult, and a high threshold for the diagnosis of histoplasmosis should be maintained in this setting.

### **Blastomyces**

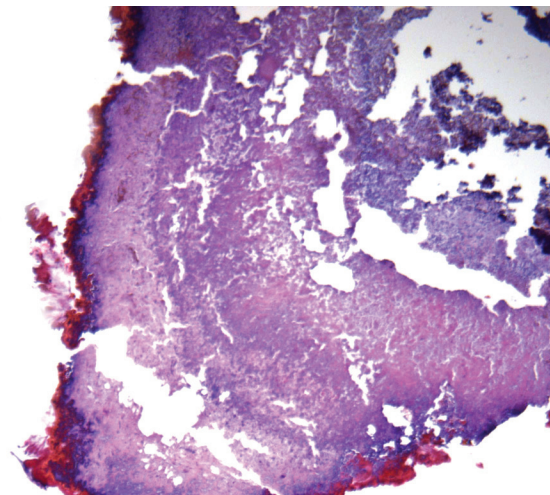
*B. dermatitidis* shows a propensity to infect lung, skin, and bone.<sup>73</sup> The spectrum of pulmonary presentations includes consolidative pneumonia and pulmonary nodules that radiographically may mimic pulmonary carcinoma (Fig. 8.82A). In rare cases, overwhelming infection may lead to acute respiratory failure and death (see Fig. 8.82B).<sup>74</sup> The pulmonary lesion characteristically shows a granulohistiocytic response (Fig. 8.83A). The yeast are large (15 to 30  $\mu\text{M}$ ) and easily identified in H&E sections, where they are distinguished by their thick refractile cell wall (see Fig. 8.83B). The organism is also multinucleate (see Fig. 8.83C) and proliferates via single, broad-based budding (see Fig. 8.83D). Microforms may be present and should not be confused with coinfection by *H. capsulatum*.<sup>75</sup> Giant yeast forms can also occur and may be confused with *C. immitis*.<sup>76</sup>



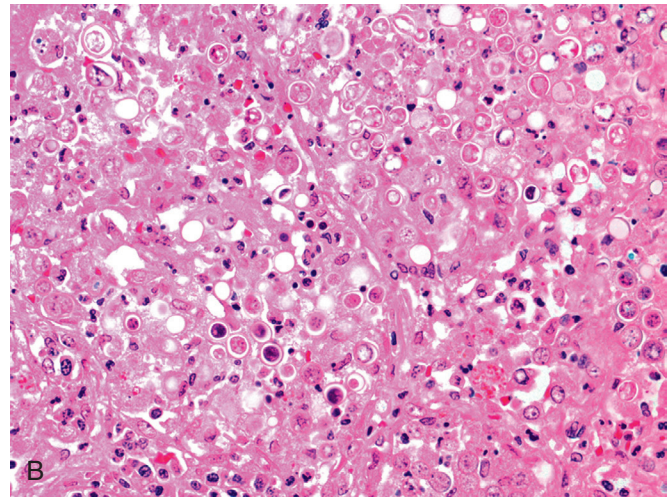
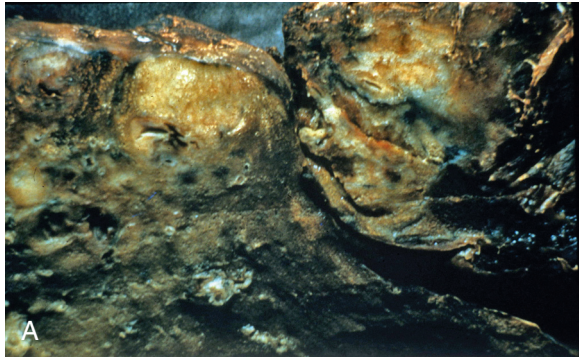
• **Figure 8.79** A, Intracytoplasmic *H. capsulatum* in bronchoalveolar lavage macrophages in patient with disseminated infection and human immunodeficiency virus/acquired immune deficiency syndrome. B, Debris within macrophage phagolysosomes can resemble intracellular yeast.



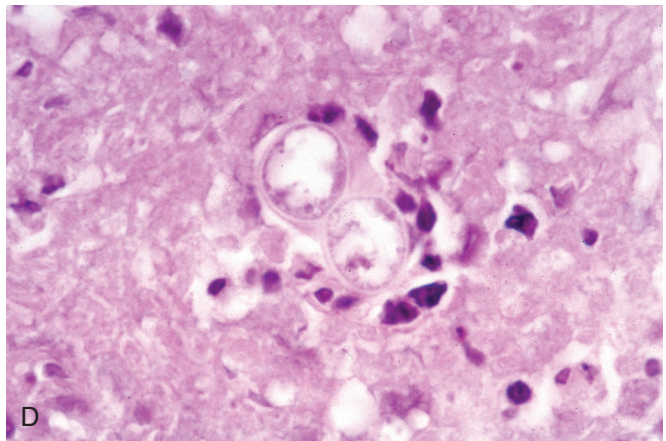
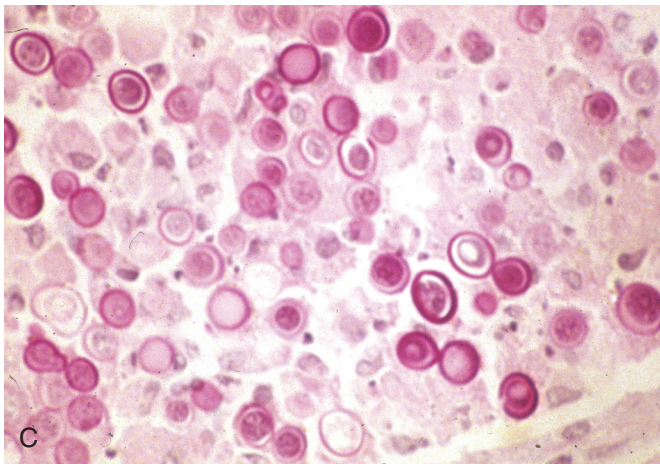
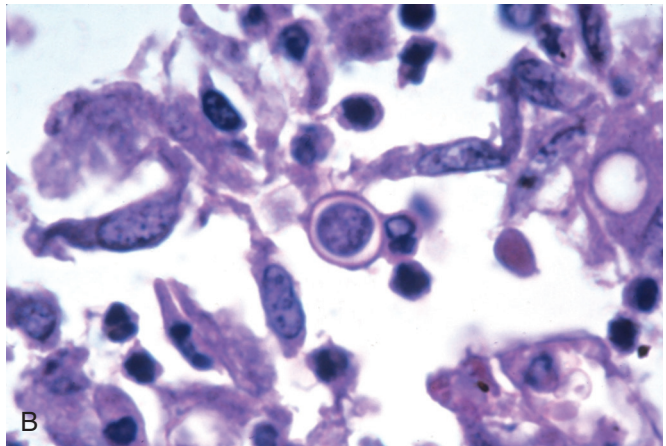
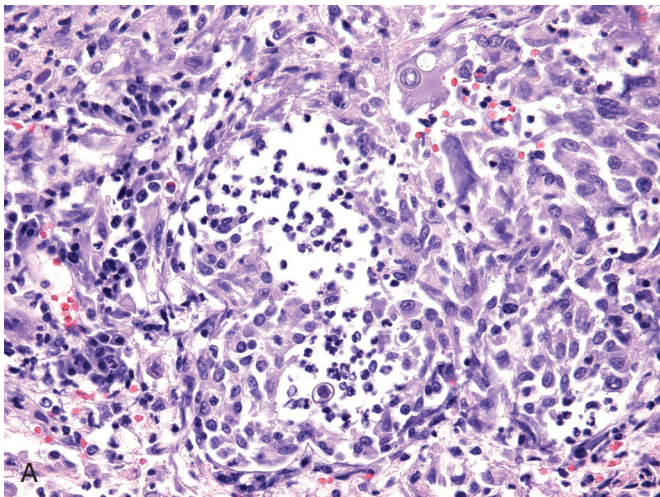
• **Figure 8.80** A, Mediastinal granuloma is a serious complication of pulmonary histoplasmosis. The mediastinum shows paucicellular hyaline scarring and may include (B) foci of necrotizing granulomatous infection.



• **Figure 8.81** Expectorated broncholith due to histoplasmosis.



• **Figure 8.82** **A**, Pulmonary nodule excised as carcinoma due to blastomycosis. **B**, Blastomyces in patients who died from an overwhelming lung infection. Note presence of large numbers of yeast filling alveolar spaces.



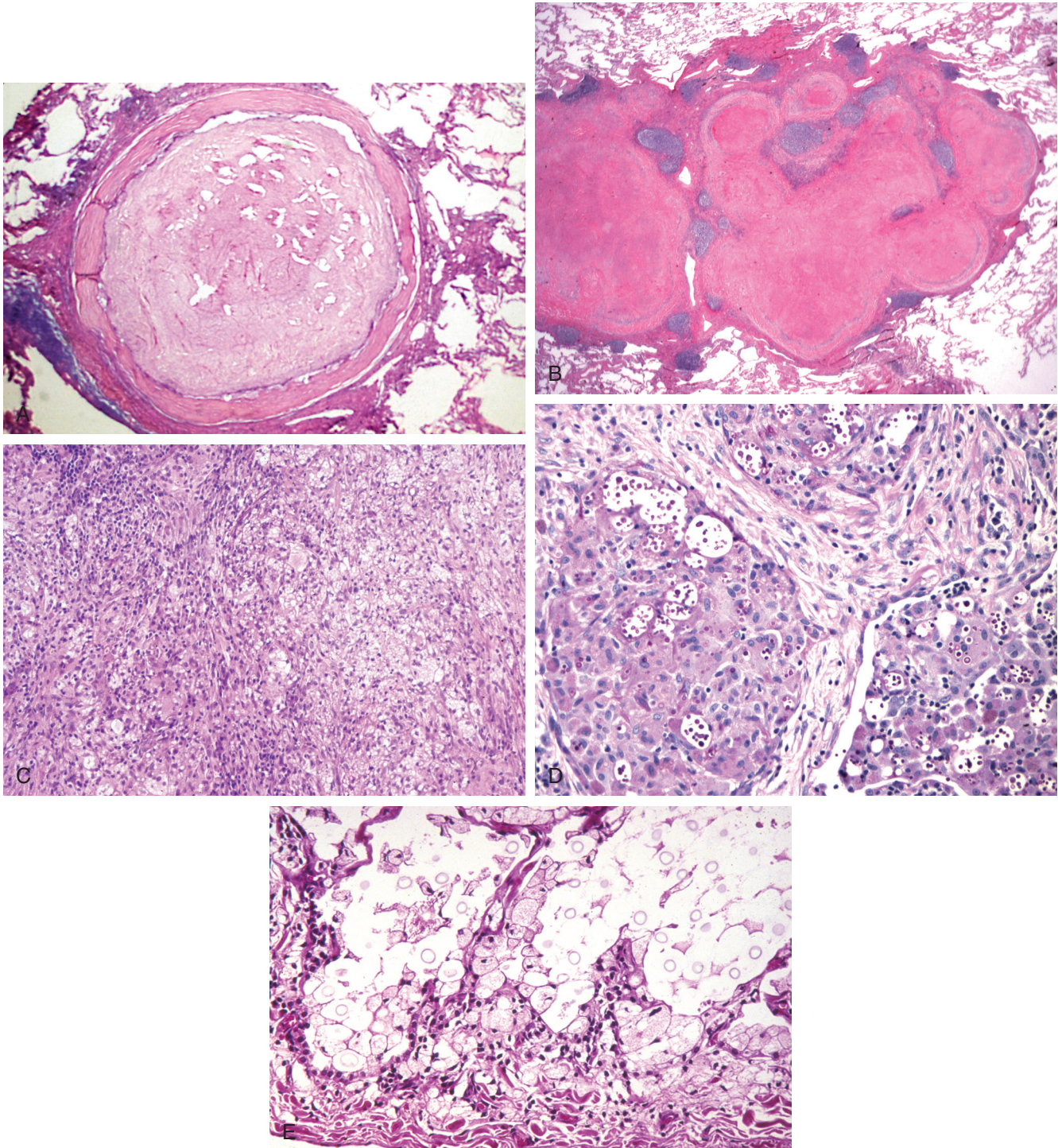
• **Figure 8.83** **A**, Granulohistiocytic response to *B. dermatitidis*. **B**, Yeast of *B. dermatitidis* with refractile cell wall. **C**, *B. dermatitidis* with multinucleation. **D**, *B. dermatitidis* showing broad-based budding.

### Cryptococcus

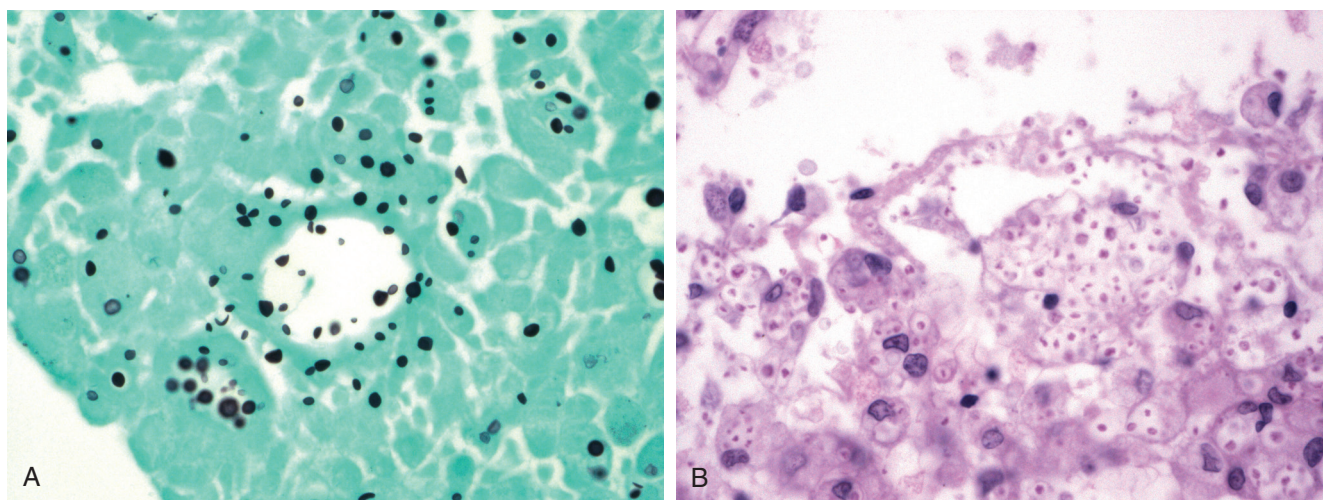
*Cryptococcus neoformans* infects immunocompromised patients but can also be seen in apparently normal hosts.<sup>77</sup> Meningo-encephalitis is the most common clinical presentation, and it represents a complication of subclinical pulmonary infection. *C. neoformans* can produce localized necrotizing cryptococcomas (Fig. 8.84A), confluent bronchopneumonia (see Fig. 8.84B),

granulomatous pneumonia (see Fig. 8.84C), or a null response characterized by “yeast lakes” with minimal inflammation (see Fig. 8.84D). Grossly, the infected lesions are glistening and “slimy.”

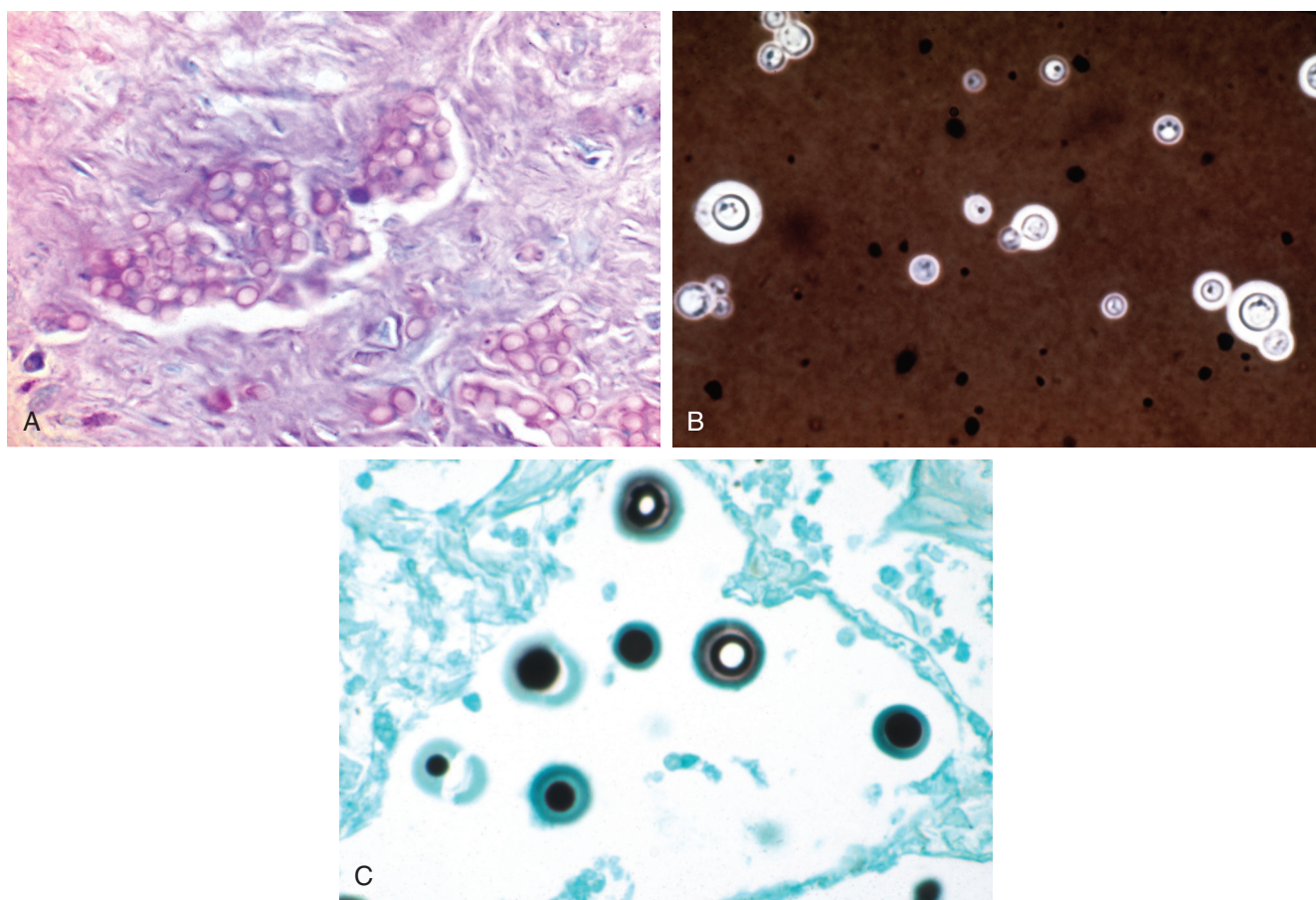
The organism show substantial variability in size (2 to 15  $\mu\text{M}$ ) and shape (Fig. 8.85A), and innumerable microforms can occasionally be seen that must be distinguished from histoplasmosis (see Fig. 8.85B). The yeast proliferate via single, narrow-necked



• **Figure 8.84** A, Nodular cryptococcoma. B, Confluent necrotizing bronchopneumonia. C, Histiocytic response. D, Granulomatous response to *C. neoformans*. E, Yeast lake.



• **Figure 8.85** A, Narrow-necked budding of *C. neoformans* showing variability in size and shapes. B, Microforms of *C. neoformans* within histiocytes must be distinguished from intracellular *H. capsulatum*.



• **Figure 8.86** A, Mucicarmine stains capsule of *C. neoformans*. B, India ink preparation shows capsule of yeast. C, Both Gomori methenamine silver and periodic acid-Schiff stain body of yeast but not its capsule.

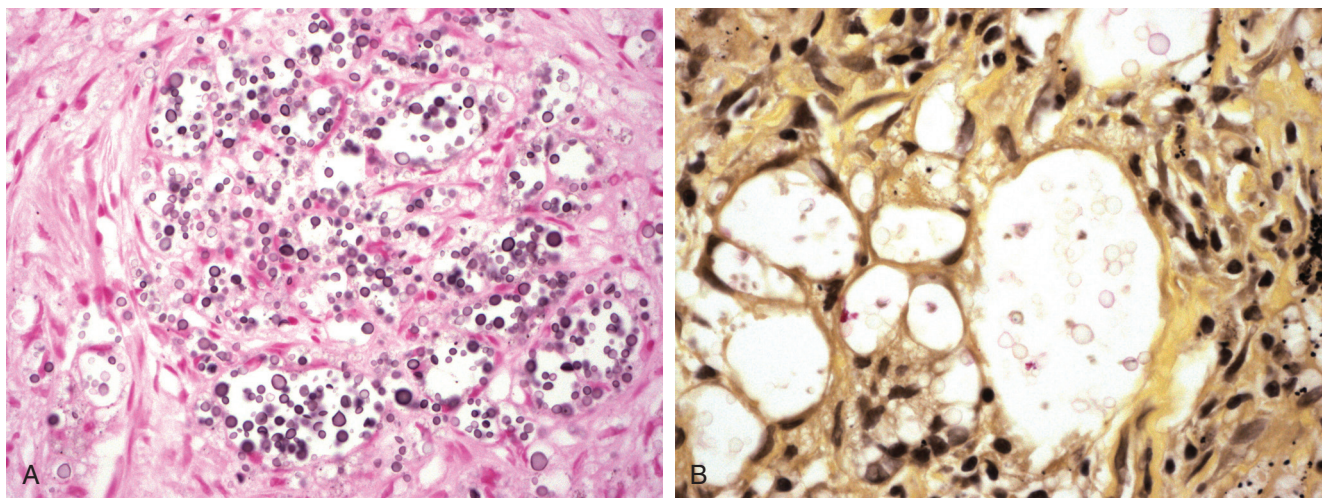
buds (secrete a capsule that is optimally visualized with mucicarmine in situ) (Fig. 8.86A). With GMS, the yeast body stains gray-black and the capsule is not decorated (see Fig. 8.86B). In capsular-deficient organisms the Fontana-Masson stain reacts with a melanin precursor in the yeast wall, highlighting the organisms (Fig. 8.87A), although a careful examination of the mucicarmine

stain will invariably reveal a poorly developed rim of capsular staining (see Fig. 8.87B).<sup>78</sup>

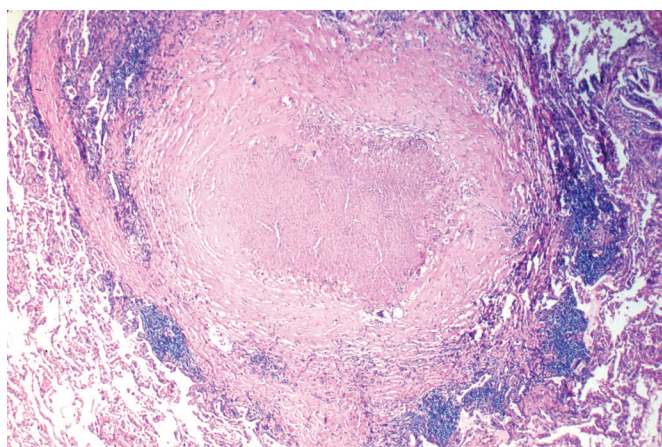
#### *Coccidioides immitis*

Generally affecting patients from the southwestern United States, this organism is distinct from other yeast by virtue of its size (20





• **Figure 8.87** A, “Capsular-deficient” organisms stain with Fontana-Masson. B, “Capsular-deficient” yeast invariably show a faint rim of mucicarmophilic staining.



• **Figure 8.88** Fibrocasseous infection due to *C. immitis*.

to 200  $\mu\text{M}$ ) and its endosporulating mode of reproduction.<sup>79</sup> *C. immitis* produces a spectrum of changes that includes fibrocasseous granulomas, (Fig. 8.88) granulomatous pneumonia, and miliary disease, often accompanied by tissue eosinophilia. The endospores are contained within a spherular capsule and both stain well with GMS (Fig. 8.89A), whereas spherules are variably stained by PAS. The cysts of *C. immitis* have a characteristic tendency to collapse after having discharged their endospores in situ (see Fig. 8.89B).

In endemic areas, *C. immitis* can form fungus balls within preexisting pulmonary cavities (Fig. 8.90A). Because the organism is dimorphic, the presence of the infective hyphal arthroconidia should not be confused with a concomitant mold infection (see Fig. 8.90B).<sup>80</sup>

### Paracoccidioides

*Paracoccidioides braziliensis* infection is endemic in South America, where it produces a range of pulmonary findings comparable to those of blastomycosis, but cases are rare in the United States. The organism is large (10 to 60  $\mu\text{M}$ ) and replicates by multiple narrow-necked buds that produce a “ship’s wheel” appearance that is pathognomonic (Fig. 8.91).<sup>81</sup> However, when this feature is absent, the infection can be confused with other fungi.

### Candida Spp.

Superficial colonization of the upper airways by *Candida* spp. is common in patients treated with inhaled corticosteroids or in chronically ill and diabetic patients (Fig. 8.92). Foci of aspiration pneumonia and abscess cavities may show colonization, but deep pulmonary infection is rarely seen in the absence of fungemia (Fig. 8.93A and B).<sup>82</sup>

*Candida* can have a pleomorphic morphology that includes yeast (blastoconidia), pseudohyphae, and true hyphae, although in some cases, only yeast forms may be present.<sup>83</sup> The organisms can be highlighted by either GMS or PAS and stain strongly gram positive (Fig. 8.94A). At times, blastoconidia of *Candida* spp. can be large and mimic other fungal infections (see Fig. 8.94B). *C. glabrata* (*torula glabrata*)<sup>84</sup> shows multiple, 2- to 5- $\mu\text{M}$  budding yeast that are amphophilic in H&E-stained sections; they are distinct from other *Candida* species because pseudohyphae and hyphae are never present.

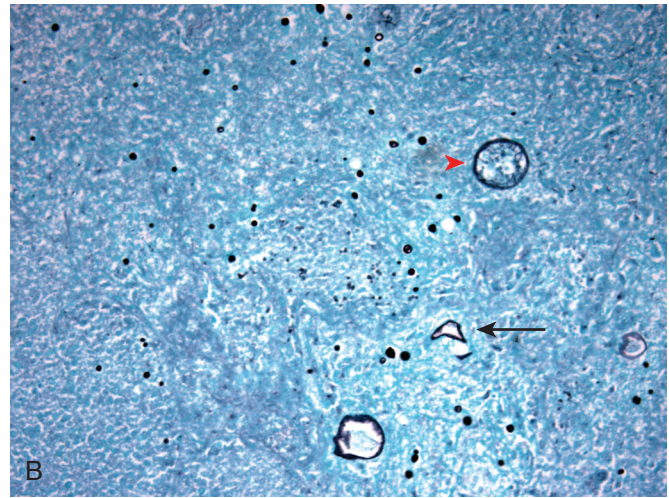
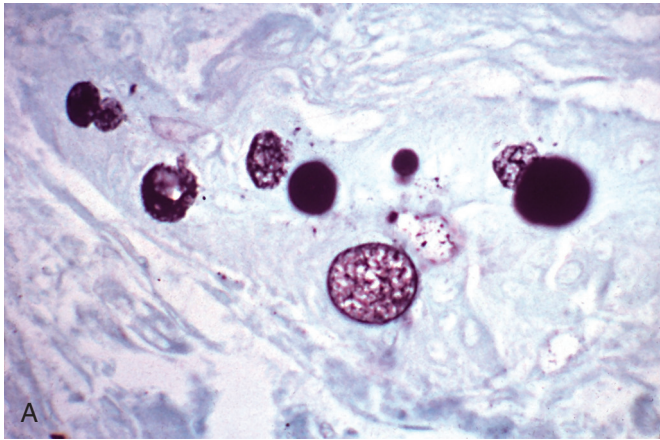
### Hyphate Fungi

Hyphate fungi or “molds” are responsible for a range of pulmonary disorders ranging from colonization of pulmonary airways to angioinvasive, life-threatening infections. *Aspergillus* spp. account for the majority of pulmonary mold infections, but other organisms, including *Zygomycetes*, *Pseudeallescheria*, and *Fusarium*, also produce pulmonary disease.

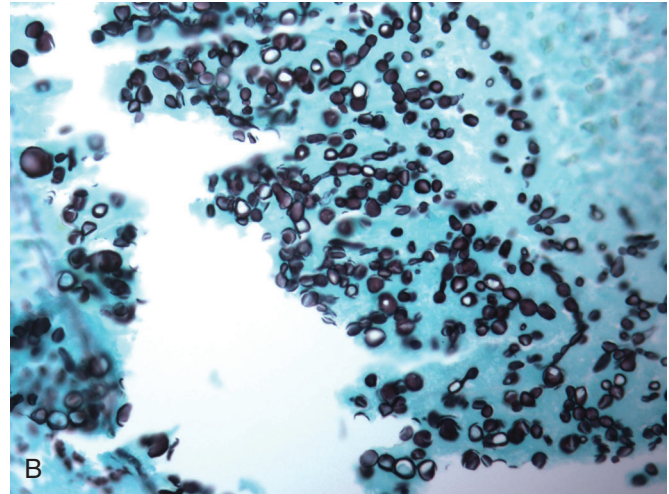
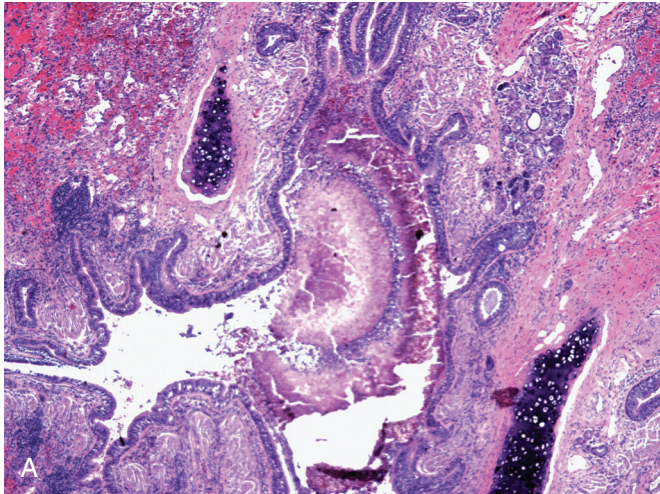
### Aspergillus Spp.

The hyphae of *Aspergillus* spp. range in diameter from 2.5 to 4.5  $\mu\text{M}$  and show frequent septation. *Aspergillus* spp. branch progressively, primarily at acute angles of approximately 45 degrees, mimicking an arborizing tree branch (Fig. 8.95A), but when cut in cross-section may be mistaken for yeast, although the absence of budding suggests the correct diagnosis. In areas of mycelial growth, organisms become tangled, bulbous, and distorted, and it may be impossible to confirm the diagnosis with accuracy, based on morphology (see Fig. 8.95B).

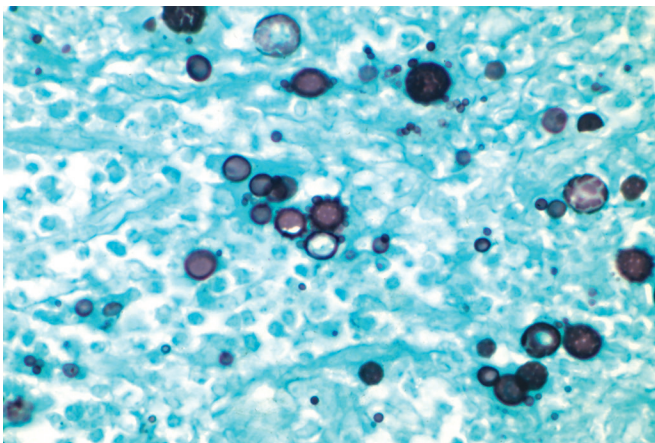
The aspergil, a ritual implement used in the Roman Catholic mass, resembles the fruiting body, and gives the fungus its name (Fig. 8.96A to C). Fruiting bodies develop from mycelia in areas



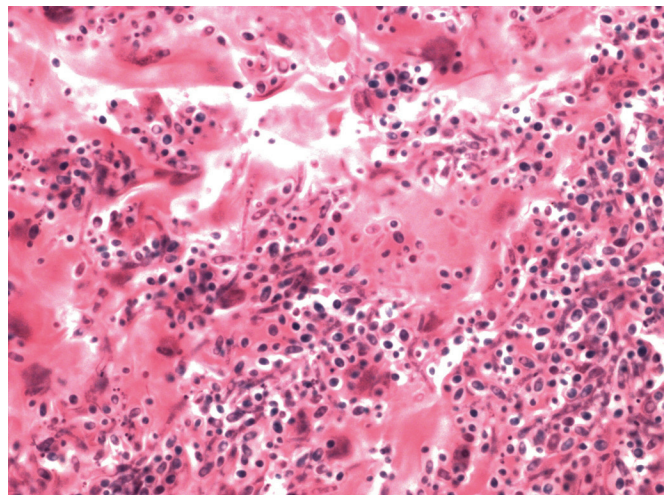
• **Figure 8.89** **A**, Endospores are variably present within periodic acid-Schiff-positive cysts. **B**, Cysts of *C. immitis* have a characteristic tendency to collapse after discharging their contents. **Red arrow** demonstrates intact fungal cyst. **Black arrow** shows a collapsed cyst.



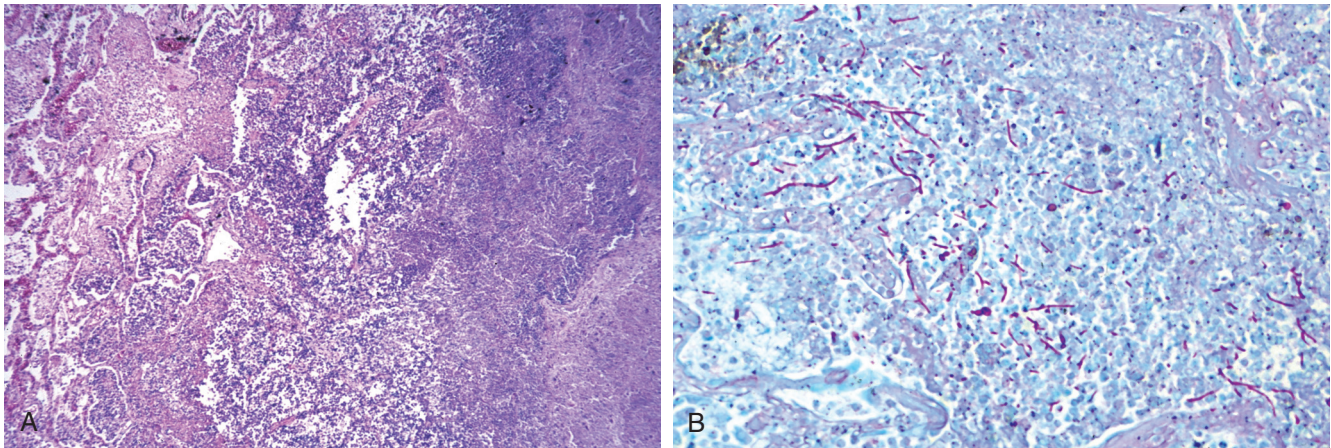
• **Figure 8.90** **A**, Fungus ball due to *C. immitis* with **(B)** yeast and arthroconidia that must not be confused with a concomitant mold infection.



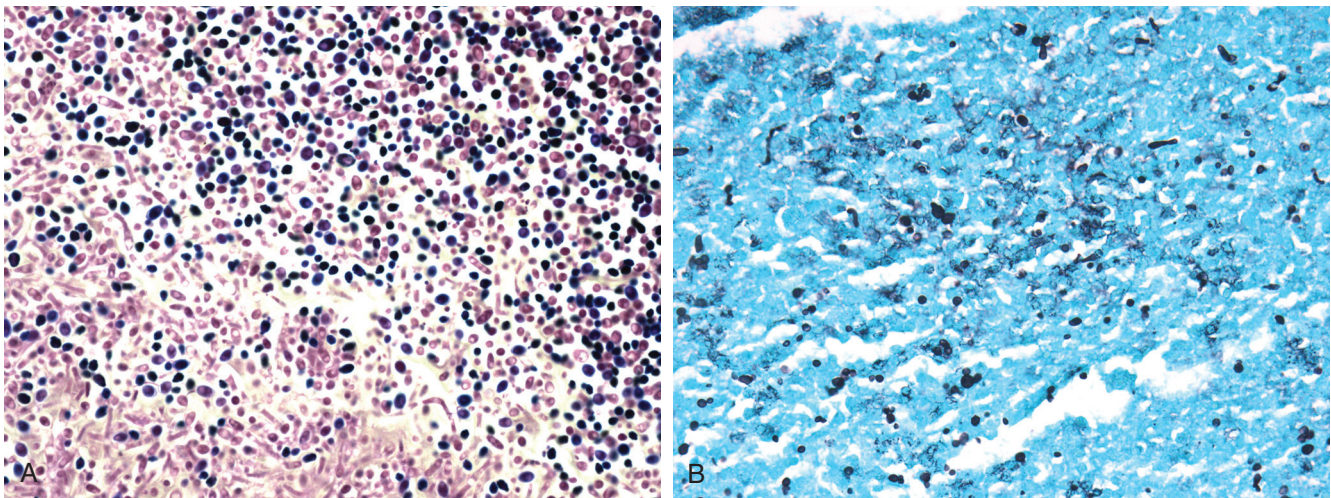
• **Figure 8.91** *Paracoccidioides brazilienses* shows multiple narrow buds that resemble a ship's wheel, but this diagnostic feature is not always present.



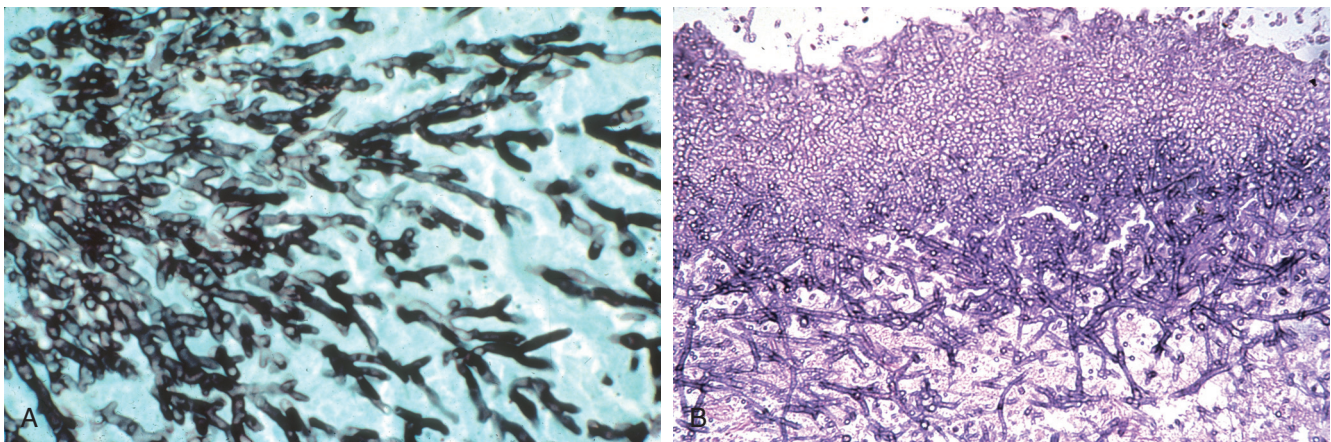
• **Figure 8.92** Dense colonization of airway with *C. albicans* in intubated patient.



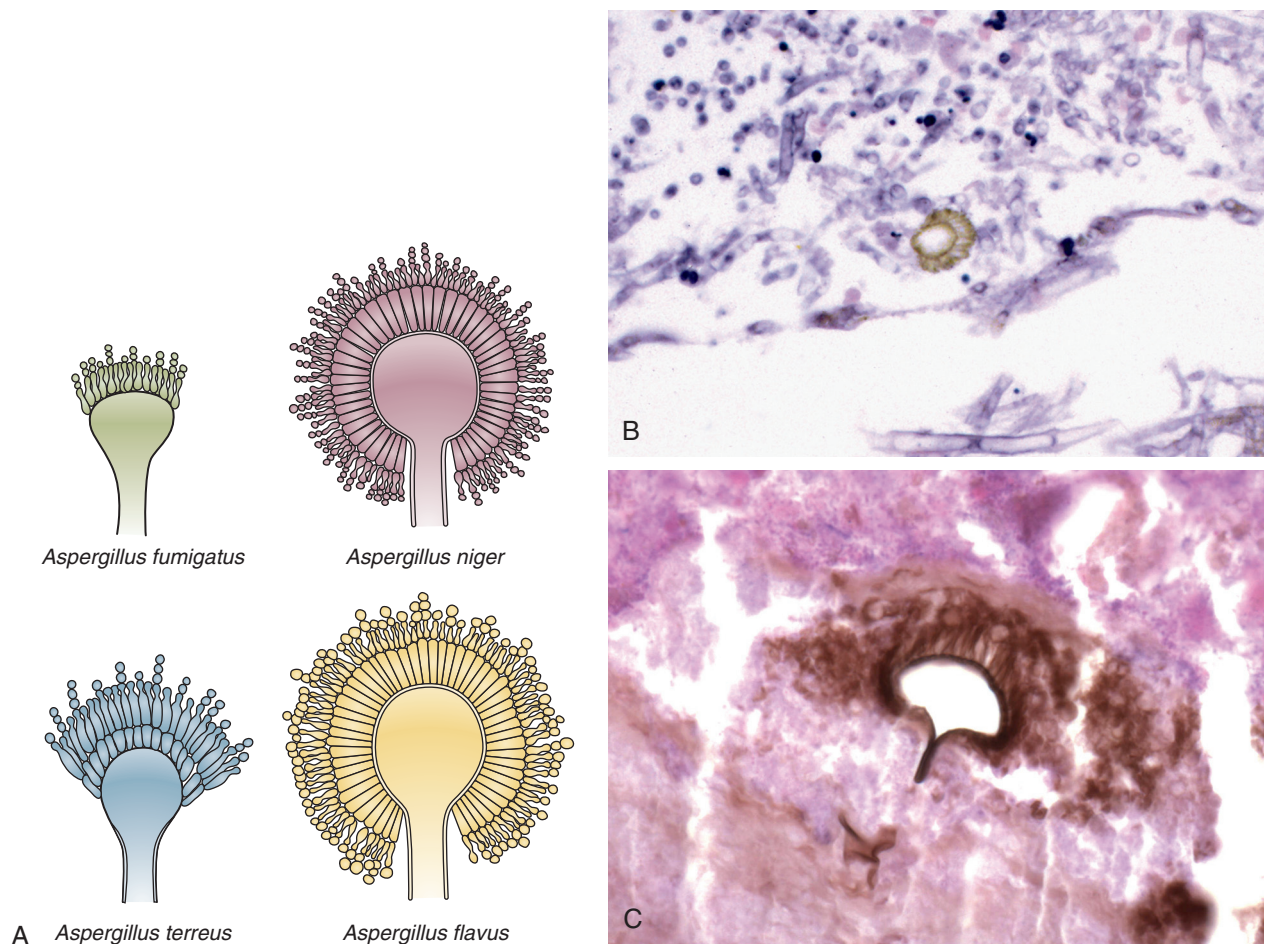
• **Figure 8.93** A, Necrotizing pneumonia due to *C. albicans* in fungemic patient. B, Periodic acid-Schiff stain highlights the organism.



• **Figure 8.94** A, *Candida* yeast are intensely gram-positive. B, Large yeast and pseudohyphae proved to be *Candida tropicalis*.



• **Figure 8.95** A, *Aspergillus* spp. characteristically branch dichotomously and progressively at acute angles. B, Tangled and distorted mycelial growth. It is impossible to speciate fungi based on this morphology.



• **Figure 8.96** A, Morphology of aspergillus fruiting body. B, Gram stain shows fruiting body of *Aspergillus fumigatus* with innumerable gram-positive conidia. C, *A. niger* with innumerable pigmented conidia.

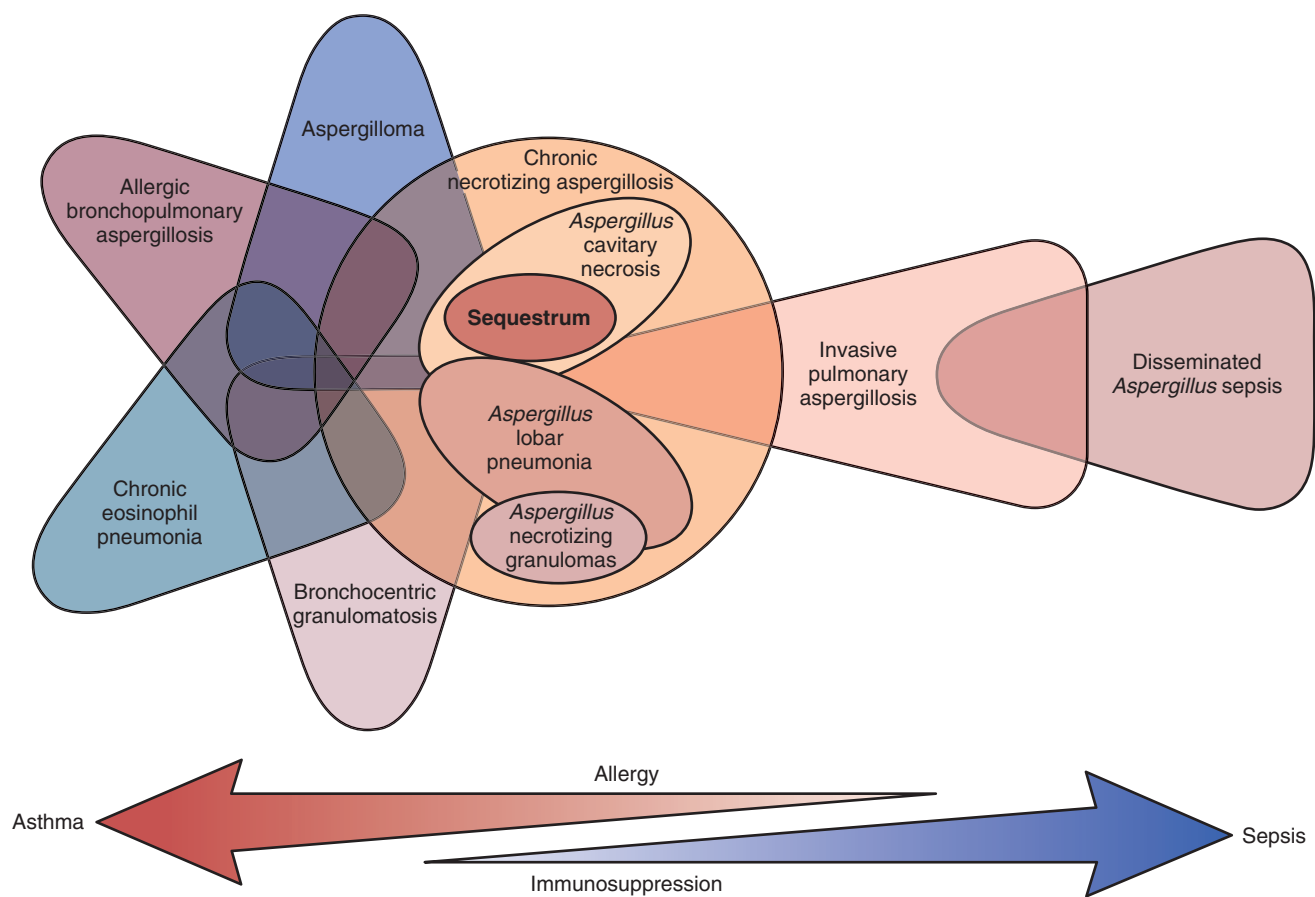
of high oxygen tension, such as lung or sinus cavities but do not develop in tissues. They are composed of a vesicle with one or two layers of phialides that produce the infective conidial spores, and the morphology of the fruiting body allows for accurate speciation in situ. In general, the specific diagnosis of “aspergillosis” should be avoided unless the aspergil is identified because other fungi can be morphologically virtually indistinguishable in tissue. Diagnoses are therefore optimally phrased as “acute-angle branching hyphae consistent with aspergillus.”

**Immune Disorders Due to Aspergillus Infection.** *Aspergillus* spp. give rise to a spectrum of disorders, some reflecting hypersensitivity responses to the organisms, whereas others are the consequence of invasive infection (Fig. 8.97). Distinguishing these is critical for the proper management of these disorders.

**Allergic Bronchopulmonary Aspergillosis.** ABPA shows a range of findings, including intractable asthma, proximal bronchiectasis,<sup>85</sup> and both peripheral blood eosinophilia. It is not certain whether the fungus plays an opportunistic role in exacerbating atopic responses or is primary in its pathogenesis.<sup>86</sup> Patients develop intractable bronchospasm with elevated serum IgE levels specific for *Aspergillus* spp. The pathology includes central cystic bronchiectasis with mucoid impaction (Fig. 8.98A). The impacted mucus is viscid and forms a cast of the airways, a disorder termed *plastic bronchitis*. Microscopically the mucus plugs show layers of degenerating eosinophils interspersed within the mucin (see Fig.

8.98B), and the surrounding lung may show patchy eosinophilic pneumonia. The fragmented fungal hyphae can at times be difficult to identify (see Fig. 8.98C) so that silver stains should be applied routinely to the evaluation of allergic mucus plugs. Whereas the clinical and histologic features of this disorder are most frequently caused by hypersensitivity to *Aspergillus* spp., other fungi (e.g., *Candida* spp.) can yield a comparable syndrome. A subset of patients with cystic fibrosis develops concomitant ABPA, and establishing the diagnosis in this setting can be difficult.<sup>41</sup>

**Bronchocentric Granulomatosis.** Bronchocentric granulomatosis (BCG) appears to reflect an abnormal cell-mediated response to *Aspergillus* spp. and less commonly other fungi (e.g., *Candida* spp. and *C. immitis*), in which small-caliber airways develop circumferential granulomatous inflammation, loss of the normal lining respiratory epithelium, and impaction of the airway lumen by granular basophilic mucin admixed with cellular debris (Fig. 8.99A to C). The disorder may be first noted radiographically as isolated or multiple airway-centered nodules.<sup>87</sup> BCG may be seen as part of the spectrum of findings in ABPA or as an isolated disorder. As in ABPA, fragmented hyphae may be difficult to identify and surrounding areas of eosinophilic pneumonitis are common. When the disease is suspected clinically, it can be treated noninvasively with corticosteroids; however, definitive resection may be undertaken to exclude neoplasia.



• **Figure 8.97** Spectrum of disease due to *Aspergillus* spp.

**Hypersensitivity Pneumonitis.** Hypersensitivity pneumonitis reflects a combined abnormality of humoral and cell-mediated immunologic responses to organic antigens. Most cases of hypersensitivity pneumonitis are caused by thermophilic actinomycetes, but hypersensitivity to *Aspergillus* spp. is well documented. Upper lobe predominance is the rule, and this can be a helpful feature in establishing the diagnosis.

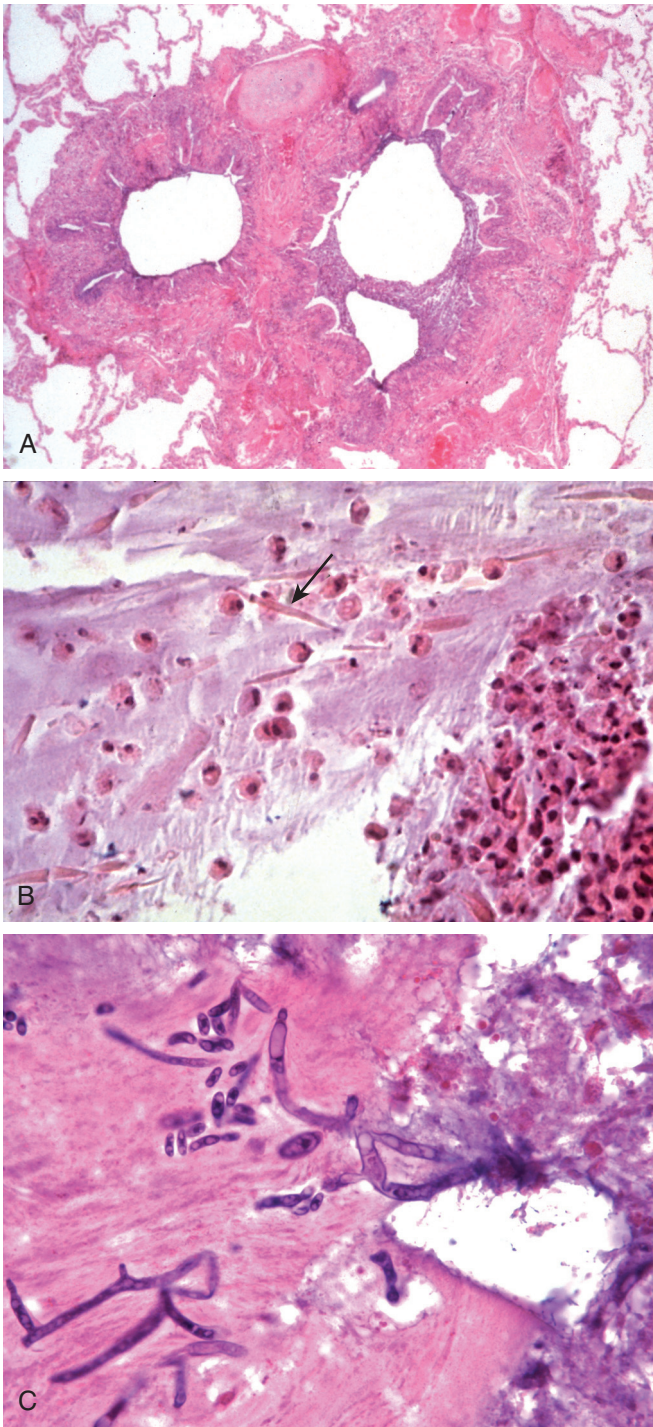
The diagnosis of hypersensitivity pneumonitis is based primarily on establishing a historical link between antigen exposures and the clinical findings, but lung biopsies can establish the diagnosis. Microscopically the lung shows bronchiolocentric, lymphohistiocytic interstitial infiltrates with poorly formed microgranulomas (Fig. 8.100) and giant cells that may contain birefringent crystals and cholesterol crystals. Whereas CD8<sup>+</sup> lymphocytes characteristically predominate in BAL fluid specimens, immunostains will reveal dominance of either CD4<sup>+</sup> or CD8<sup>+</sup> lymphocytes in situ. In addition, other histopathologies, including nonspecific cellular interstitial pneumonitis (NSIP), organizing pneumonia, lymphoid interstitial pneumonitis (LIP), and nonnecrotizing granulomatous inflammation resembling sarcoidosis, can be caused by hypersensitivity pneumonitis. The presence of interstitial and alveolar eosinophils is characteristically seen in hypersensitivity pneumonitis due to *Aspergillus* antigens and is less common in response to other antigens.

**Aspergillus Bronchitis and Chronic Necrotizing Aspergillosis.** The presence of primary airway infection by *Aspergillus* spp. is a poorly recognized entity. It is generally seen in the setting of modest immunosuppression accompanying such disorders as

diabetes mellitus or the use of aerosolized steroids in asthmatics. In some cases, it is a precursor lesion for invasive disease. Fungal hyphae can be seen filling the lumen of airways (Fig. 8.101A) without evidence of frank tissue invasion. Elastic stains are helpful in determining whether organisms have begun to transgress normal tissue barriers (see Fig. 8.101B). Centrally necrotic lesions (Fig. 8.102A) of chronic necrotizing aspergillosis can resemble those due to mycobacteria and other fungi (see Fig. 8.102B).

**Fungus Balls.** The colonization of old fibrocavitary disease (e.g., areas of bronchiectasis due to healed tuberculosis and sarcoidosis, or emphysematous bullae by *Aspergillus* spp.) is the most common cause of a pulmonary fungus ball (Fig. 8.103A and B).<sup>88</sup> The term mycetoma should not be applied to intracavitary fungal mycelial growth because it accurately applies only to soft tissue infections. Patients may be asymptomatic or alternatively present with episodes of hemoptysis, at times massive and requiring emergent bronchial arterial embolization or definitive resection.

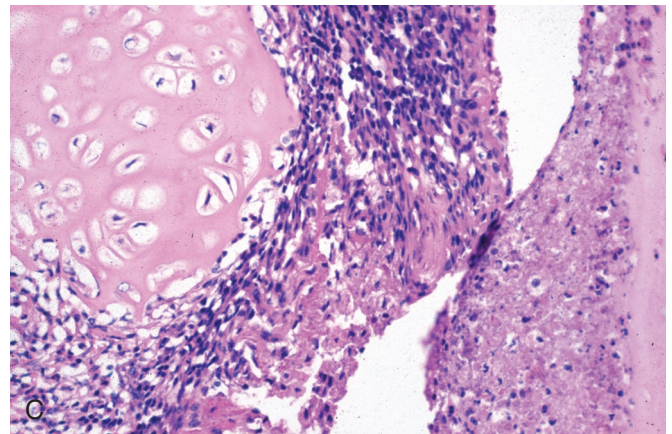
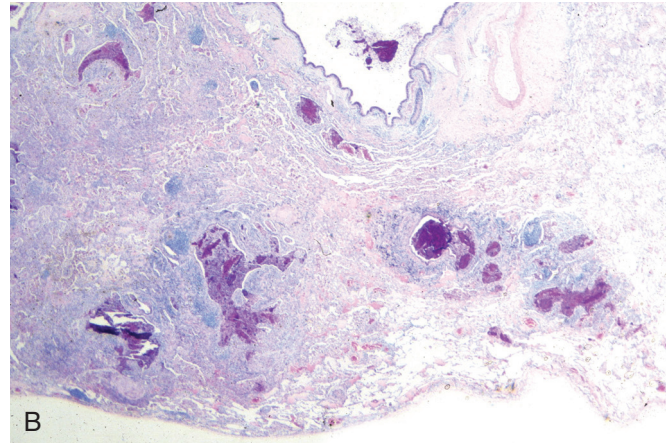
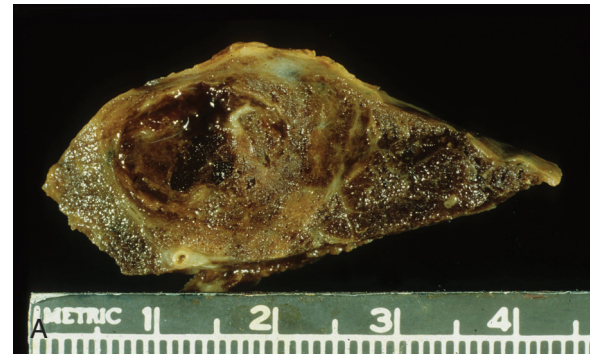
The morphology of the hyphae in a fungus ball is frequently distorted, and it can be impossible to identify diagnostic septate acute angle branching forms. *Aspergillus* fungus balls show heterogeneous staining intensity (see Fig. 8.103C), giving the impression of alternating zones of growth. The wall of the fungus ball frequently shows increased numbers of tissue eosinophils (see Fig. 8.103D). The *Splendore-Hoeppli* phenomenon is often present and is reassuring evidence that angioinvasion is unlikely, unless there has been a recent supervening cause of immunosuppression or neutropenia. The walls of the cavity are lined with granulation tissue, granulomatous inflammation, or metaplastic squamous



• **Figure 8.98** **A**, Central bronchiectasis with dense peribronchiolar scarring in a patient with allergic bronchopulmonary aspergillosis. **B**, Expectorated “allergic” mucus plug with eosinophils and Charcot-Leyden crystals. *Arrow* points to Charcot-Leyden crystal. **C**, *Aspergillus* hyphae in mucus plug.

epithelium, depending on the activity of the disease. The occasional presence of germinative fruiting bodies of *Aspergillus* spp. with characteristic phialides and conidial forms allows definitive speciation.

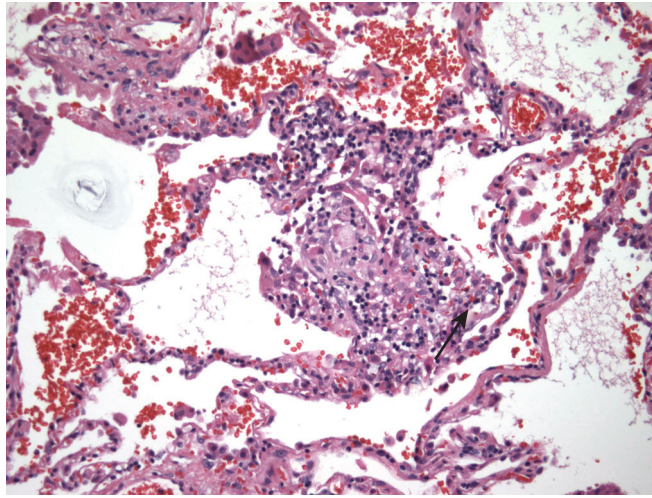
One may rarely see rapid expansion of a cavity due to vascular thrombosis induced by calcium oxalate crystal deposition, a disorder termed *chronic pulmonary oxalosis*.<sup>89</sup> Oxalic acid is



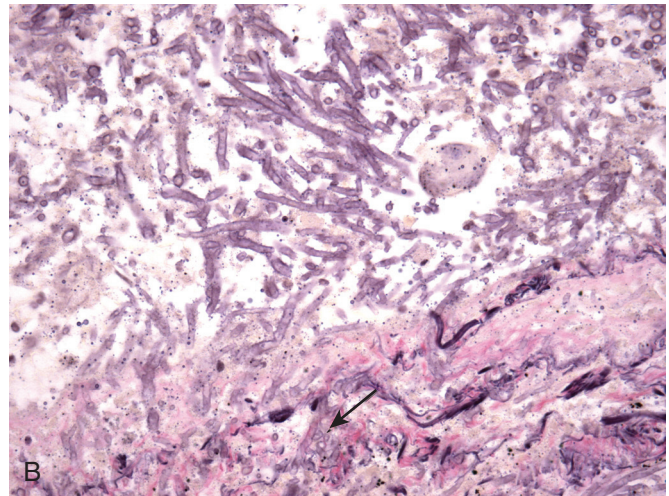
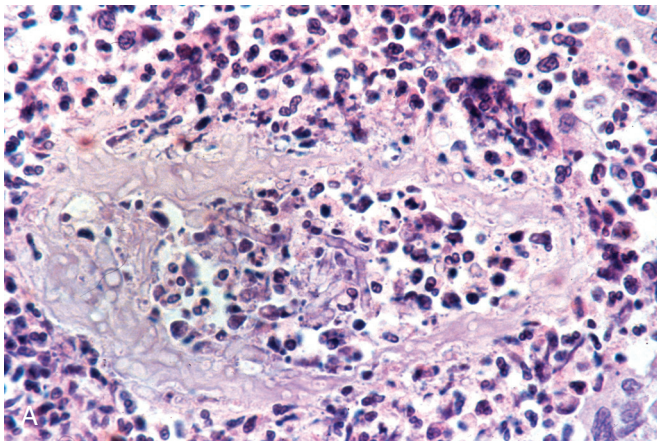
• **Figure 8.99** **A**, Gross appearance of bronchocentric granulomatosis showing **(B)** exquisite bronchocentric distribution in periodic acid-Schiff-stained section. **C**, The lining of a small airway is replaced by granulomatous inflammation, and the lumen is filled with a granular basophilic exudate.

produced by a variety of *Aspergillus* spp. but is most commonly a feature of *Aspergillus niger* infection (Fig. 8.104A). Diffusion of oxalate into surrounding blood vessels is prothrombotic and can lead to extensive ischemic necrosis (see Fig. 8.104B and C). Oxalate crystal deposition in the renal tubules may also be seen. Emergency resection of the fungus ball is the only effective treatment.

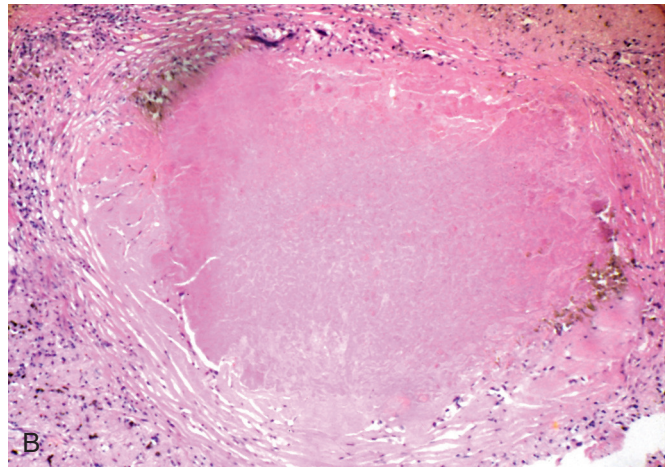
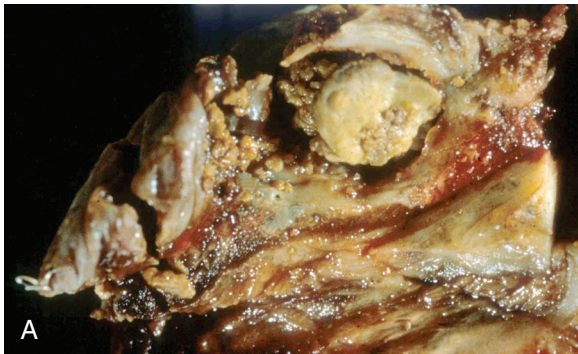
**Angioinvasive Aspergillosis.** This life-threatening infection is seen in patients who have been chronically immunosuppressed and/or neutropenic. It is a complication of bone marrow and solid organ transplantation, as well as of antileukemic chemotherapies. Angioinvasive aspergillosis is an uncommon complication of



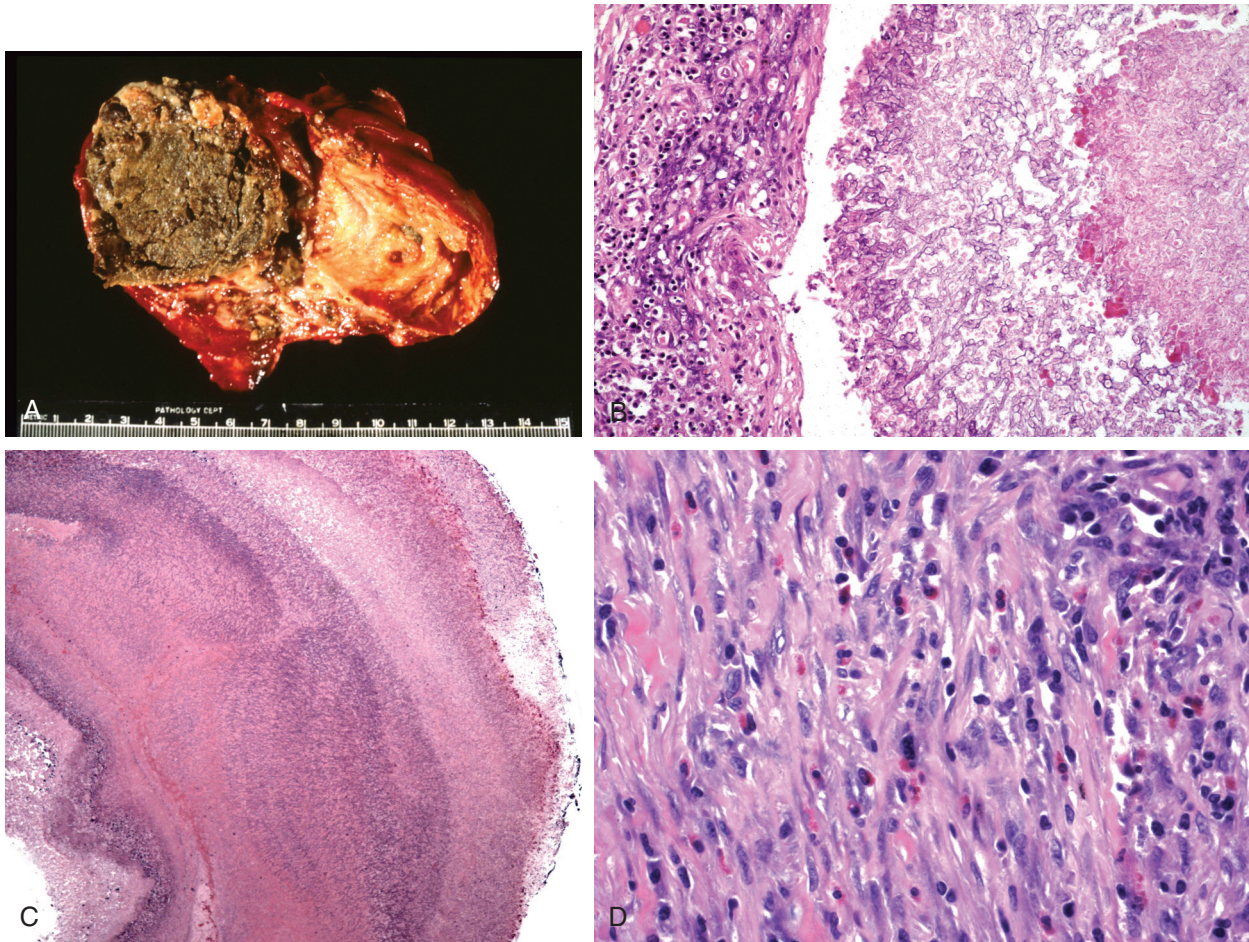
• **Figure 8.100** The microgranulomatous hypersensitivity response to aspergillus often includes tissue eosinophils.



• **Figure 8.101** **A**, Aspergillus bronchitis/bronchiolitis is a precursor to invasive disease. **B**, Elastic stains can determine whether tissue invasion has occurred (*arrow*).



• **Figure 8.102** **A**, Necrotizing lesions due to aspergillus can (**B**) resemble mycobacterial or yeast infection.



• **Figure 8.103** **A**, Fungus ball growing in an old bronchiectatic cavity due to sarcoidosis. **B**, Histology shows tangled mass of hyphae and the Splendore-Hoeppli phenomenon. **C**, Fungus balls often show alternating “zones” of staining intensity with hematoxylin and eosin (and Gomori methenamine silver). **D**, Fungus balls frequently contain eosinophils in their wall.

HIV/AIDS, despite the associated profound immune deficiency. Grossly the lung shows “targetoid” lesions showing central thrombosed vessels secondary to angioinvasion, surrounded by a rim of consolidated lung, confluent bronchopneumonia, or lobar consolidation (Fig. 8.105A), and microscopically a necrotizing pneumonia (see Fig. 8.105B) at times featuring giant cells (see Fig. 8.105C) may be present.<sup>90</sup> Angioinvasion is identified microscopically and may be enhanced with silver and elastic stains (Fig. 8.106A and B). Rarely, foci of infarcted lung can produce an infected nonviable pulmonary sequestrum (Fig. 8.107).

The fungal hyphae tend to invade blood vessels and to “metastasize” to other organs. The presence of sunburst vasculocentric hyphal growth is diagnostic of a “metastatic” focus of infection (Fig. 8.108), and virtually any organ may be secondarily involved. Circulating *Aspergillus* spp. can also seed abnormal cardiac valves to produce endocarditis with fatal embolic hemorrhagic infarctions to brain and other vital organs.

**Other *Aspergillus* Species.** *Aspergillus terreus* is an opportunistic fungus that infects patients with chronic granulomatous disease, as well as other immunocompromised hosts.<sup>90</sup> Its hyphae

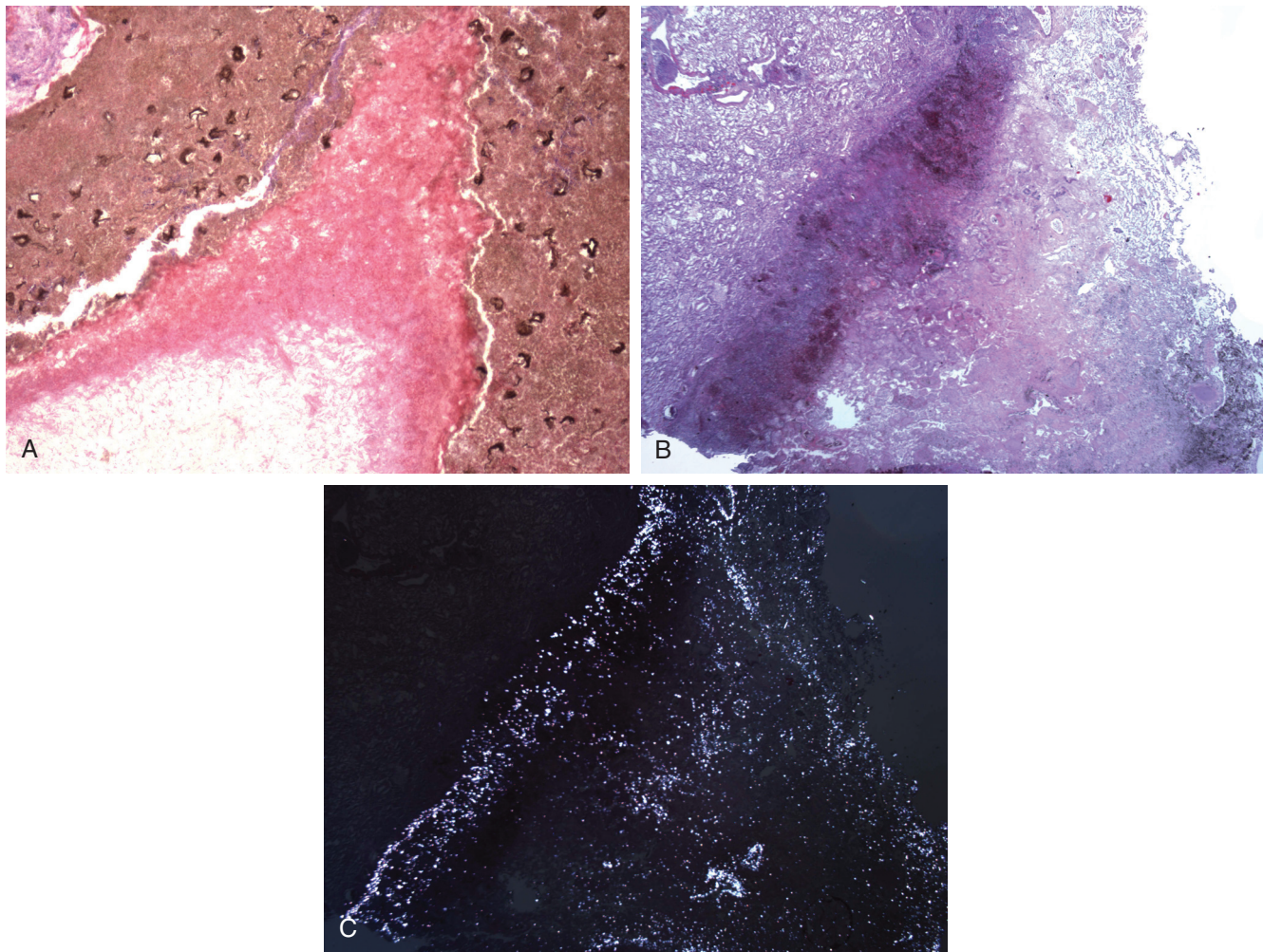
are pyriform with orthogonal branches (Fig. 8.109A and B). Fungus balls due to *Aspergillus nidulans* have a propensity to produce pale-staining, enlarged fungal forms or *Hulle cells* that show Maltese cross birefringence when examined under polarized light (Fig. 8.110A and B).<sup>91</sup>

### Other Hyphate Fungi

Although the majority of acute-angle branching septate hyphae encountered in medical practice prove to be *Aspergillus* spp., exceptions do occur and can be difficult to distinguish in situ. Organisms that closely mimic *Aspergillus* include the *Zygomycetes*, *Pseudallescheria boydii* (*Scedosporium*), and *Fusarium* spp. Pulmonary infection by *Zygomycetes* is due to organisms of the order *Mucorales* (*Mucor*), including *Mucor*, *Rhizopus*, *Absidia*, *Rhizomucor*, and *Apophysomyces*.<sup>92</sup> Infection generally occurs in immunosuppressed hosts and in patients with diabetic ketoacidosis or disorders of iron metabolism. As treatment invariably includes surgical resection, establishing an accurate diagnosis is critical.

The histologic responses to infection are comparable to those caused by angioinvasive aspergillosis. The hyphae of the *Zygomycetes*





• **Figure 8.104** **A**, Fungus ball due to *A. niger*. **B**, Extensive local ischemic infarction of lung and **(C)** deposition of calcium oxalate crystals are seen with polarized light.

are broad (5 to 25  $\mu\text{M}$ ), pauciseptate, tending to branch at right angles (Fig. 8.111A), although acute-angle branching does occur and its presence should not dissuade one from the correct diagnosis. The hyphae of the *Zygomycetes* are well stained by hematoxylin, and they have a proclivity to produce ribbonlike structures (see Fig. 8.111B), but caution in diagnosis is required because treated aspergillus can assume this appearance. The fungus rapidly invades vessels, perineural lymphatics, and cartilage and tends not to respect tissue boundaries. *Zygomycetes*, as well as all other hyphate fungi, can rarely form noninvasive fungus balls in the lung.

**Pseudallescheria (Scedosporium).** The hyphae of *Pseudallescheria* are smaller (2 to 4  $\mu\text{M}$ ) than those of *Aspergillus* spp.; the fungus branches predominantly at acute angles but, unlike *Aspergillus*, tends to branch haphazardly rather than progressively, and terminal chlamydoconidia mimicking a “tennis racket” may be apparent (Fig. 8.112). Although it is a hyaline fungus, the conidia produced by *Pseudallescheria* in fungus balls are ovoid and pigmented.<sup>11</sup>

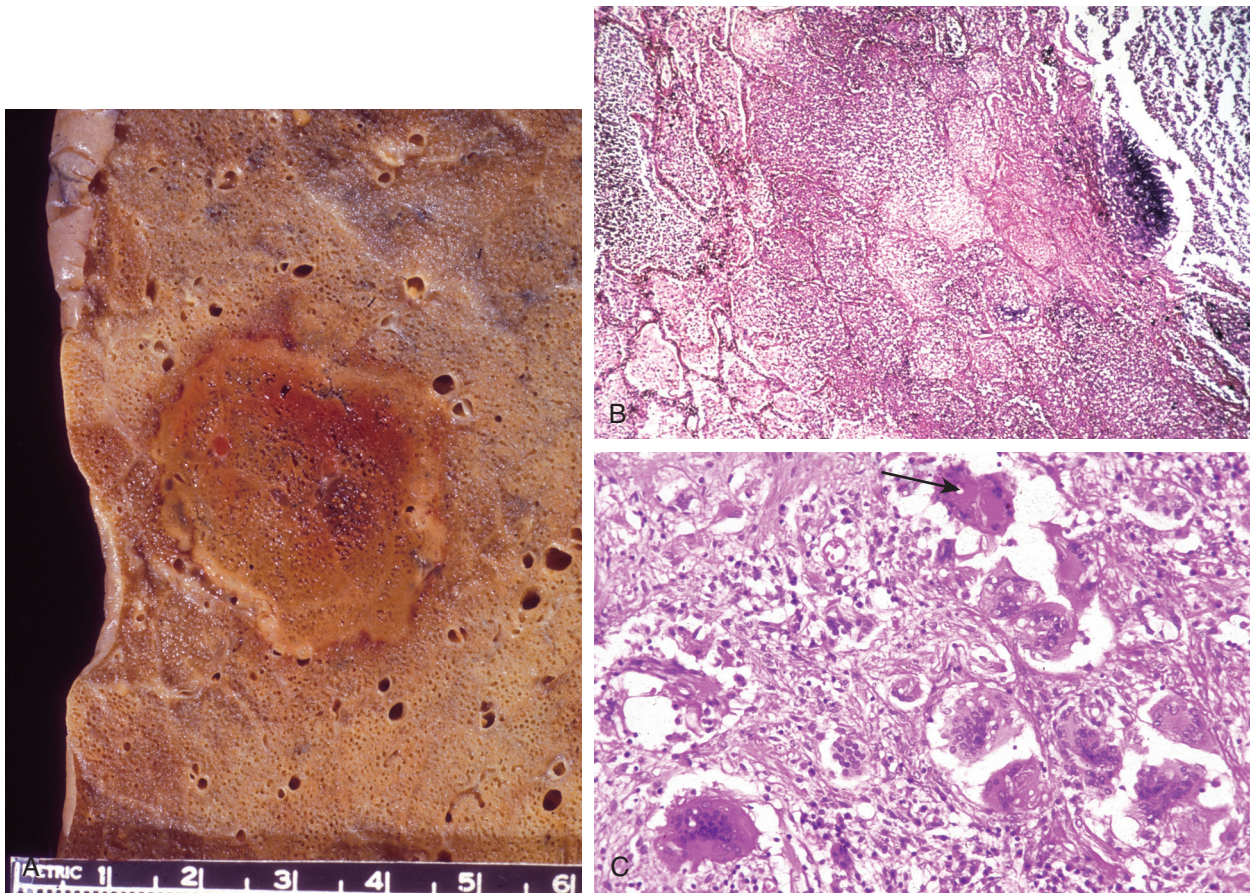
**Fusarium.** *Fusarium* is an opportunistic infection of lung that is seen in patients who are severely immunosuppressed. The

septate hyphae of *Fusarium* spp. branch irregularly and at right angles, showing constrictions at branch points (Fig. 8.113).<sup>11</sup>

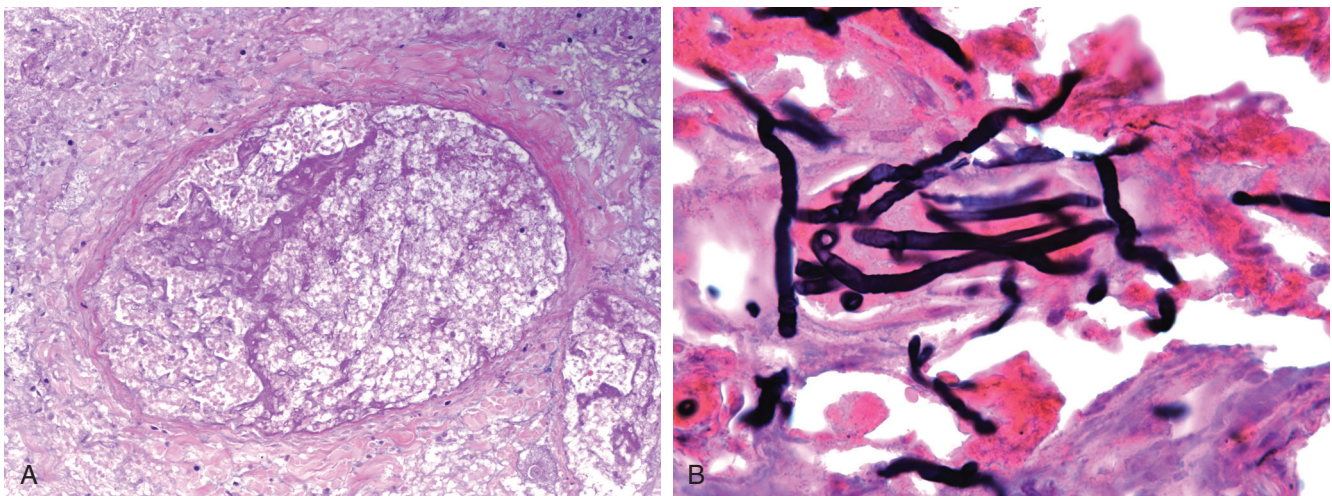
#### Differential Diagnosis

Whereas distinguishing hyphate fungal pathogens from one another in tissue can be exceedingly difficult, it is important because the efficacy of available fungal antibiotics depends on the diagnosis. The galactomannan assay is relatively specific for invasive aspergillosis and is rarely positive in mucormycosis, which can be helpful in distinguishing them noninvasively. The sensitivity is somewhat higher in the BAL than is serum.<sup>93</sup> However, this test should not be used to screen patients for aspergillus infection because its sensitivity in the nonimmunosuppressed and noninvasive disease is limited.

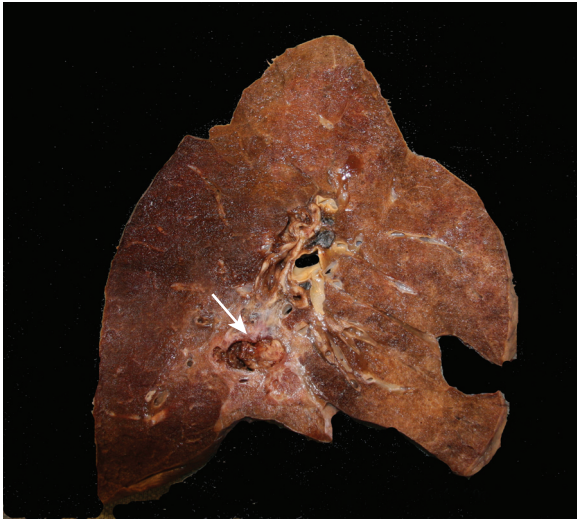
Whereas both *Aspergillus* spp. and *Pseudallescheria* are sensitive to voriconazole, *Pseudallescheria* is resistant to amphotericin. The sensitivity of *Fusarium* spp. to most antifungal antibiotics appears to be both unpredictable and limited. In all cases, culture remains the gold standard for diagnosis. Immunohistochemical reagents that can distinguish between hyphate fungi exist but are not



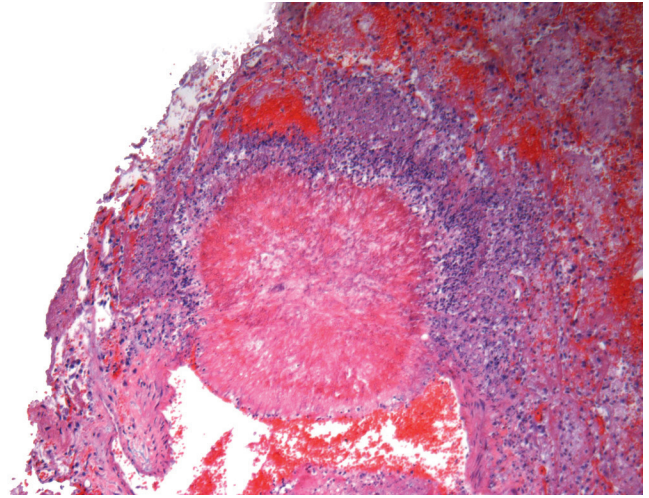
• **Figure 8.105** **A**, Angioinvasive aspergillosis with targetoid lesion due to vascular thrombosis, ischemic infarction, and fungal invasion into surrounding tissues. **B**, Necrotizing pneumonia due to angioinvasive aspergillosis with mycelial fungal growth developing at surface of cavitory lesion. **C**, Giant cells in pneumonia due to *A. fumigatus*. Arrow points to giant cells in inflammation.



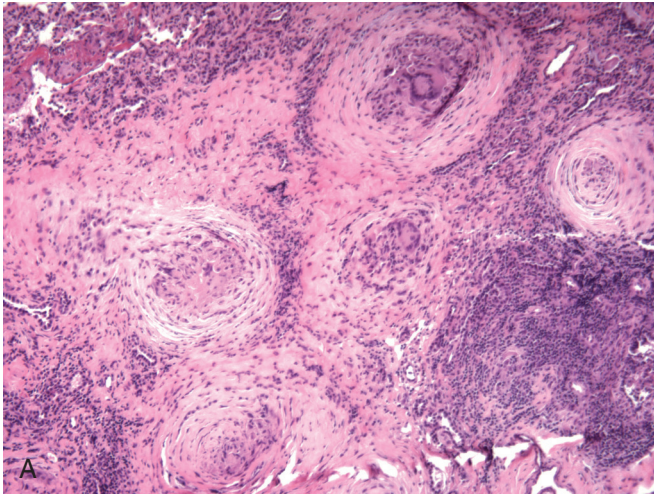
• **Figure 8.106** **A**, Blood vessel invasion may be seen with hematoxylin and eosin (H&E) and to better advantage in **(B)** section costained with Gomori methenamine silver and H&E.



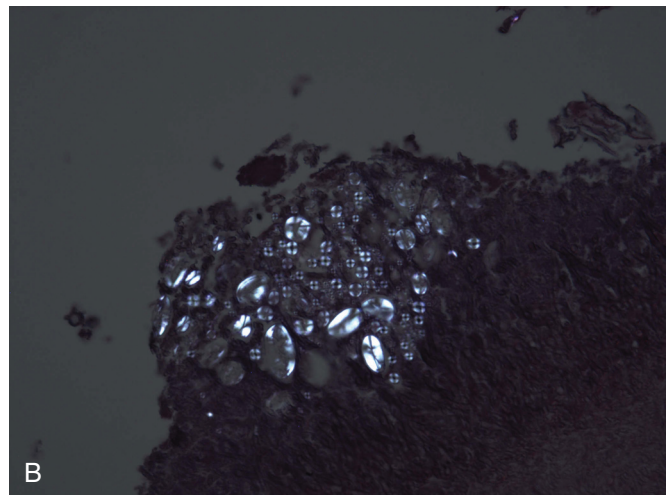
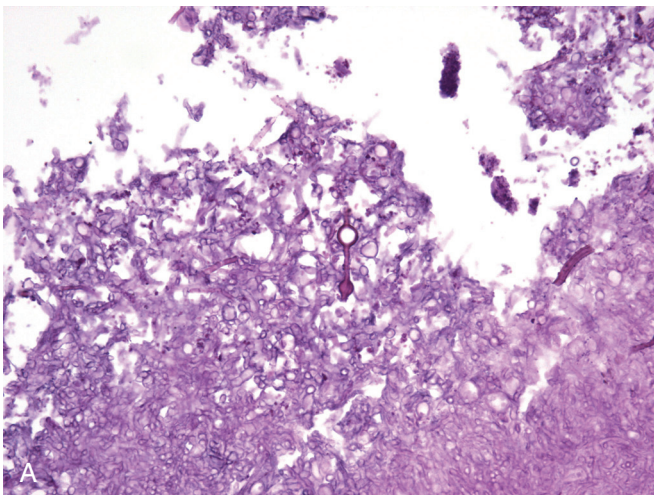
• **Figure 8.107** Area of nonviable lung (sequestrum) due to angioinvasive aspergillosis (arrow).



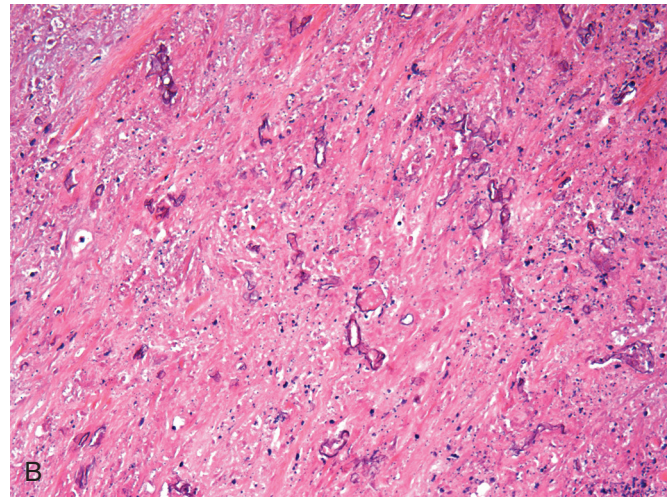
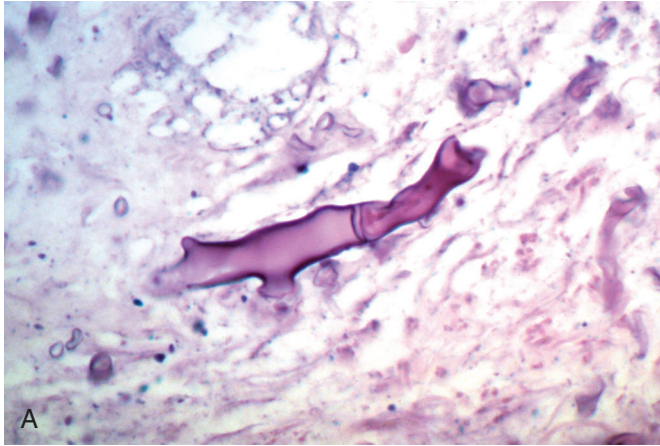
• **Figure 8.108** Focus of "metastatic" fungal infection showing sunburst pattern of growth out of blood vessel.



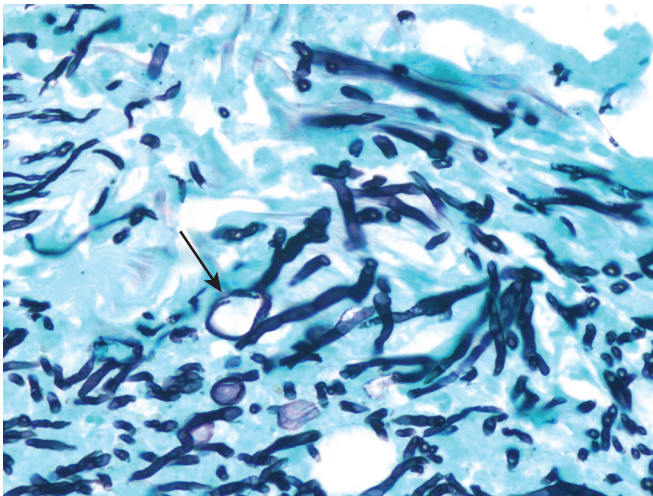
• **Figure 8.109** A, *A. terreus* infection in patient with chronic granulomatous disease showing (B) fragmented pyriform hyphae branching at right angle.



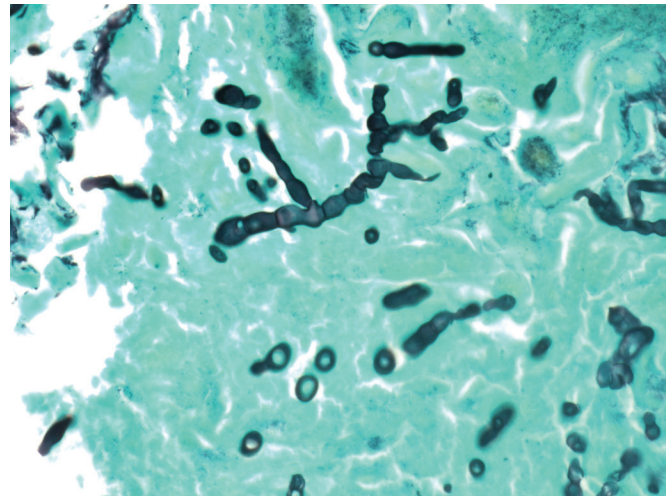
• **Figure 8.110** A, Fungus ball due to *A. nidulans* with Hülle cells that (B) show Maltese cross configuration when examined with polarized light.



• **Figure 8.111** A, *Zygomycetes* spp. hyphae are broad, pauciseptate, and tend to branch at right angles. B, Area of necrotizing angioinvasive disease with ribbonlike hyphae that stain well with hematoxylin.



• **Figure 8.112** *P. boydii* are slightly smaller than *Aspergillus* spp. and tend to grow randomly with prominent terminal chlamydospores (arrow). Definitive diagnosis is generally not possible based solely on morphology in tissue sections.

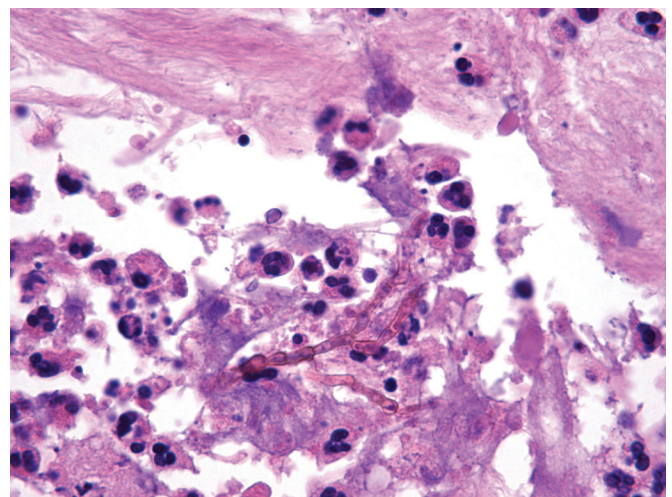


• **Figure 8.113** *Fusarium* tend to branch at right angles with narrow-branch points, but definitive classification is generally not achieved in tissue sections.

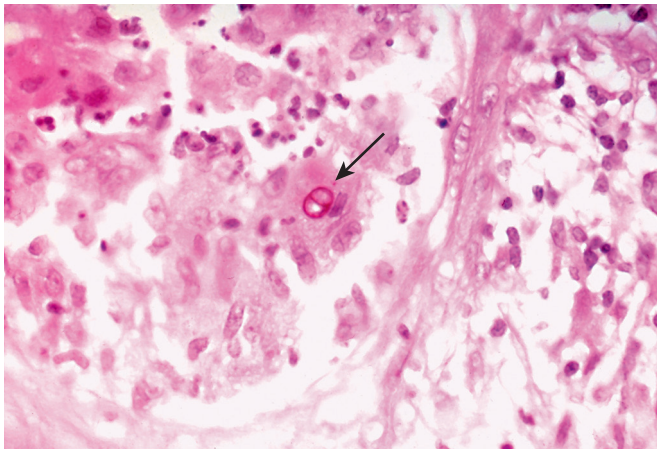
commercially widely available, and all reagents must be carefully tested with appropriate controls. The PCR assay is presently not an effective diagnostic approach.

### Dematiaceous (Pigmented) Fungi

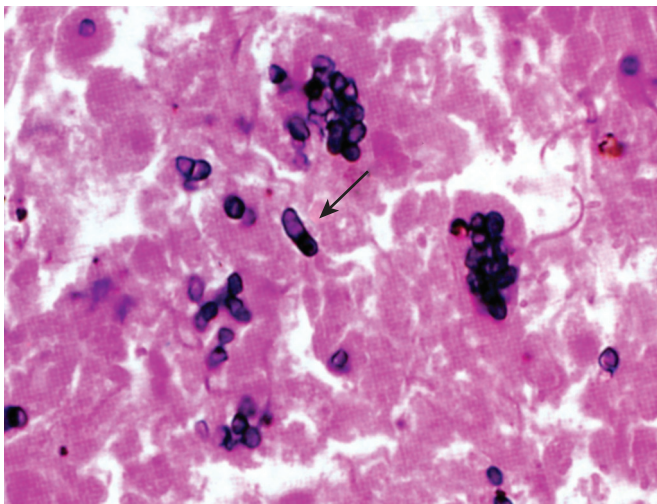
Pigmented fungi can be divided into those forming yeast (chromoblastomycosis) and those due to hyphate fungi (phaeohyphomycosis).<sup>94</sup> The specific organisms producing disease cannot be diagnosed morphologically, and isolation in culture is required. The Fontana-Masson stain can be applied when questions exist as to whether a fungus seen in H&E sections is pigmented. *Bipolaris*, *Curvularia*, *Alternaria*, and others are pigmented hyphate fungi that cause allergic pulmonary disorders mimicking those due to *Aspergillus* spp. (Fig. 8.114). The correct diagnosis is suggested by the presence of pigmented hyphae within allergic mucus or within fungus balls. *Chromoblastomycosis* is appreciated by the presence of sclerotic (Medlar) bodies. These are clusters of pigmented yeast that show characteristic multiaxial septa (Fig. 8.115).



• **Figure 8.114** Phaeohyphomycosis show pigmented fungal hyphae. Subclassification requires microbiologic culture.



• **Figure 8.115** Chromblastomycosis shows pigmented yeast forms with characteristic “sclerotic” Medlar bodies with multiaxial septation (arrow).



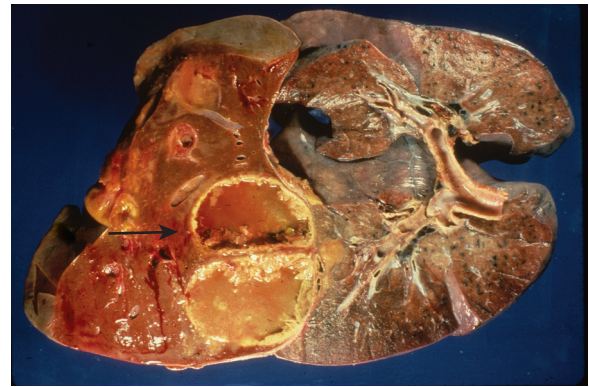
• **Figure 8.116** *P. marneffei* is a dimorphic fungus that is often seen within histiocytes and has a “sausage” shape with characteristic septation (arrow).

### *Penicillium marneffei*

Pulmonary infection due to *P. marneffei* is rarely seen outside of patients from Southeast Asia with HIV/AIDS, but it is a significant cause of necrotizing bronchopneumonia in this region. The organism is a small (2 to 5  $\mu\text{M}$ ) dimorphic fungus with an elongate sausage shape showing a characteristic septum. The organisms can be identified free within areas of necrosis or within foamy histiocytes (Fig. 8.116). The infection may also disseminate, commonly to involve the skin. Other fungi, including *Geotrichum* and *Sporothrix*, are rare causes of pulmonary infection.<sup>95</sup>

### Parasites

The lung can be host to a variety of parasitic infections. Whereas many are seen primarily in tropical climates, others occur in temperate climes or as the result of immunosuppression. As previously noted, the current ease of global travel has greatly increased encounters with tropical diseases.



• **Figure 8.117** Amebic abscess with “anchovy paste” gross appearance. Arrow points to hematin pigment in cecum of schistosome.

### Protozoa

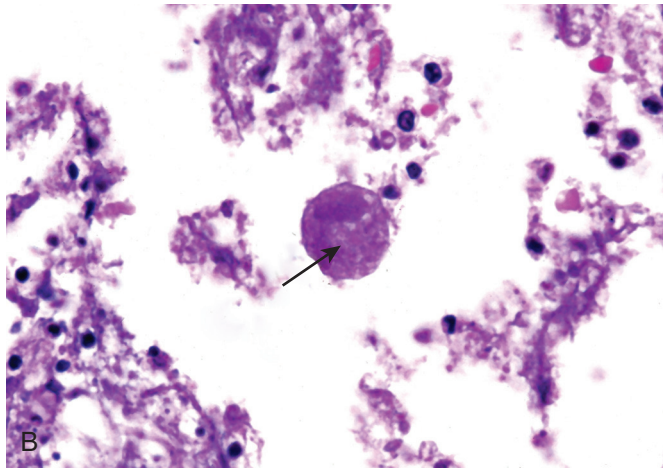
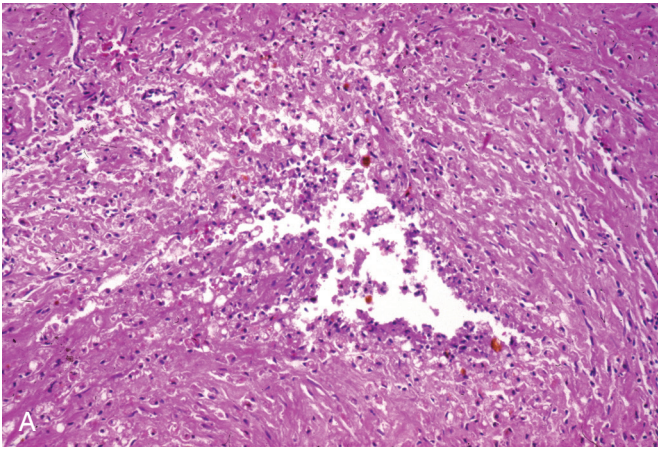
**Ameba.** Several species of protozoa can produce pulmonary infection. *Entamoeba histolytica* affects the lung secondary to the transdiaphragmatic extension of a hepatic amebic abscess or less commonly as the result of blood-borne spread from an intestinal source.<sup>96</sup> A pulmonary amebic abscess may extend to the pleura or rupture into an airway, leading to intrapulmonic dissemination. The amebic abscess shows liquefactive necrosis that grossly resembles “anchovy paste” (Fig. 8.117). The histologic response in areas of necrosis primarily includes neutrophils, but the margins of the lesion will show a polymorphous infiltrate of macrophages, lymphocytes, and plasma cells, and tissue eosinophilia is uncommon (Fig. 8.118A). Amebae can be distinguished from macrophages by their larger size, amphophilic bubbly cytoplasm, a sharply defined nuclear karyosome, (see Fig. 8.118B) and in the case of *E. histolytica*, by the ingestion of erythrocytes.

Free-living amebae, including *Acanthamoeba*, *Balamuthia*, and *Naegleria*, rarely affect the lung and primarily cause meningoencephalitis. However, in immunosuppressed patients, infection may spread beyond the confines of the nervous system to include the lung.

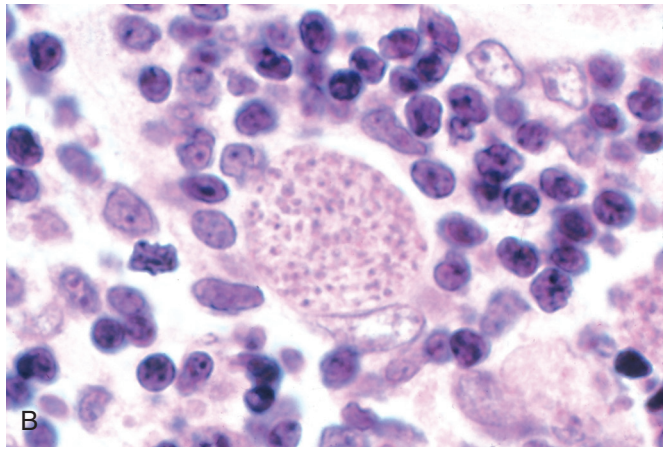
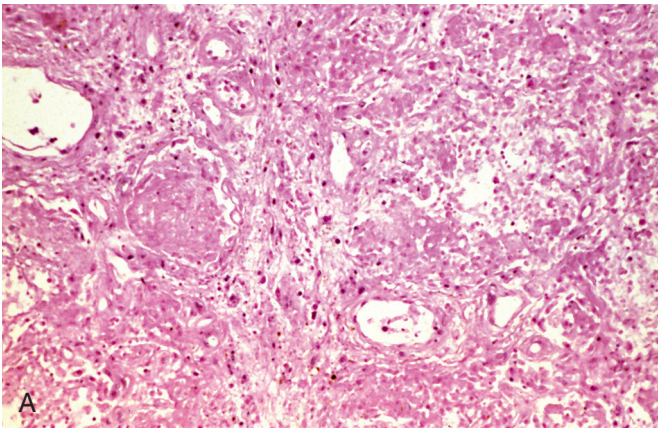
**Toxoplasma.** *Toxoplasma gondii* produces pneumonia in patients who are immunosuppressed, most often with HIV/AIDS.<sup>97</sup> Whereas *Toxoplasma* is a common infection of the central nervous system (CNS) and retina in HIV/AIDS, pulmonary infection is rare. When present, it includes a fibrinopurulent pneumonitis with areas of necrosis (Fig. 8.119A). The organisms are obligate intracellular parasites and are identified either as engorged pseudocysts containing crescent-shaped tachyzoites and/or GMS- and PAS-positive true cysts containing bradyzoites (see Fig. 8.119B).

**Cryptosporidium.** *Cryptosporidium parvum* is a water-borne opportunistic infection that affects patients with HIV/AIDS but has also been seen as outbreaks among children in daycare centers.<sup>98</sup> The disease primarily affects the small bowel, leading to cholera-like watery diarrhea. In patients with HIV/AIDS the infection can spread to the hepatobiliary tree, as well as to the pulmonary airways.

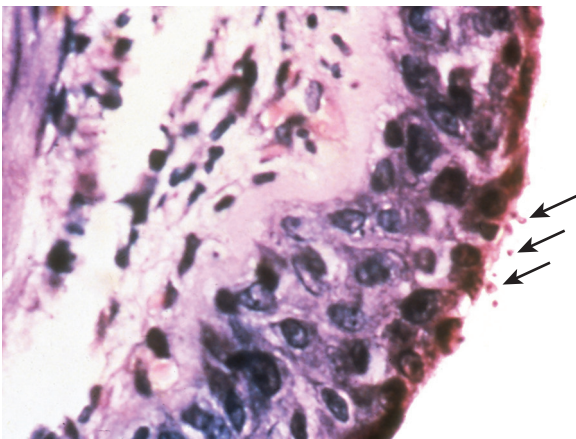
The diagnosis is made by identifying the amphophilic spores (3 to 5  $\mu\text{M}$ ) of *Cryptosporidia* along the surface of infected respiratory epithelium (Fig. 8.120). Although apparently extracellular by light microscopic determination, ultrastructural analysis demonstrates that the cysts are actually intracytoplasmic and invested by apical cytoplasm. The underlying mucosa shows a mild lymphocytic



• **Figure 8.118** A, Liquefactive necrosis in lung abscess due to (B) *E. histolytica* showing ingestion of erythrocyte (arrow).



• **Figure 8.119** A, Necrotizing pneumonia in a patient with human immunodeficiency virus/acquired immune deficiency syndrome due to *T. gondii*. B, High power demonstrates bradyzoites within macrophage.



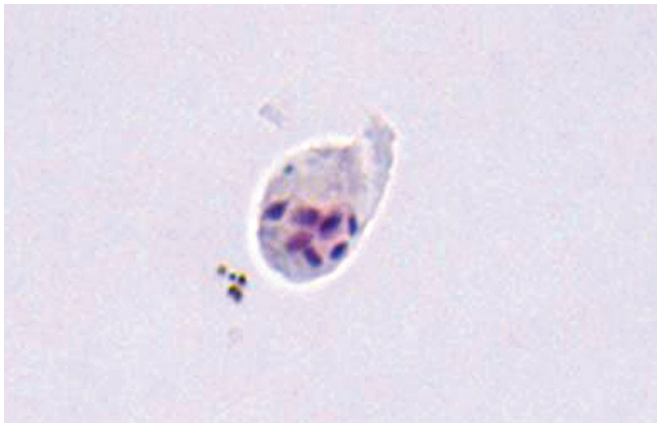
• **Figure 8.120** *C. parvum* seen along the surfaces of ciliated pulmonary epithelium (arrows). The cysts are actually invested by apical cytoplasm.

infiltrate. Although well seen with H&E, the cysts are also stained by GMS, modified AFB, and Giemsa. The diagnosis is obvious once considered but can easily go unnoticed unless considered in the differential diagnosis.

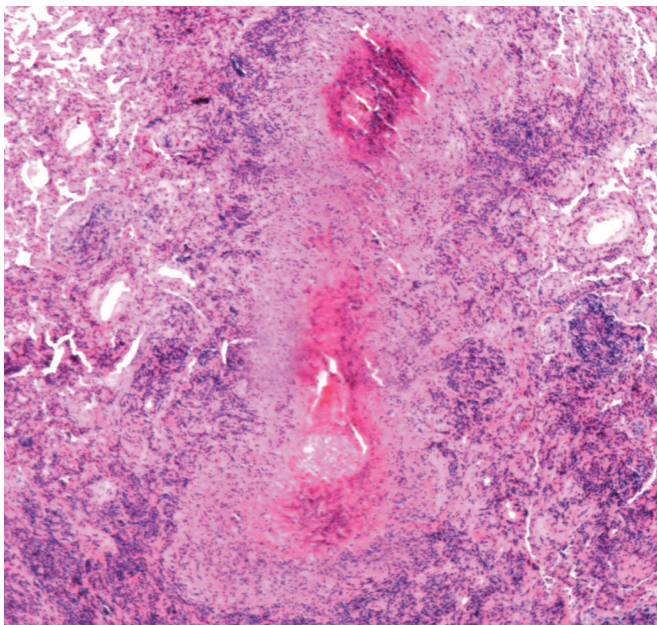
**Microsporidia.** Microsporidia are spore-forming protozoa that, like *Cryptosporidium*, infect immunosuppressed patients to produce a watery diarrheal illness. Extraintestinal disease, including bronchial involvement, is uncommon but has been observed. The organisms are intracytoplasmic and generally located within the apical cytoplasm.<sup>99</sup> Because of their small size (1 to 2  $\mu\text{M}$ ), they may be exceedingly difficult to detect, especially when the organism load is low. Special stains, including tissue Gram stain, trichrome, Warthin-Starry, and GMS, can assist in their identification (Fig. 8.121). Further speciation requires ultrastructural examination.

### **Nematodes (Round Worms)**

Several nematodes (round worms) have a larval developmental phase in the lung (Box 8.7).<sup>100</sup> The larvae of *Ascaris*, *Necator*, *Ancylostoma*, and *Strongyloides* migrate through the airways towards the mouth, where they are swallowed or expectorated. This process can evoke wheezing, migratory pneumonia, and



• **Figure 8.121** Bronchoalveolar lavage macrophage contains *Microsporidium* spp. demonstrated by Brown-Hopps stain.



• **Figure 8.122** Necrotizing granulomatous and eosinophilic inflammation due to *S. mansoni*.

### • BOX 8.7 Nematodes With Pulmonary Larval Phase

*Ascaris lumbricoides*  
*S. stercoralis*  
*Necator americanus*  
*Ancylostoma duodenale*

blood eosinophilia, a complex termed Loeffler syndrome. The presence of track-like necrotizing granulomatous bronchitis and bronchopneumonia with prominent eosinophilic infiltrates should alert the pathologist to the presence of a migratory parasitic pulmonary infection (Fig. 8.122).

*Strongyloides stercoralis* is most often seen in the tropics; however, cases are endemic to the southeastern United States. Patients receiving high doses of corticosteroids are susceptible to

infection and what is termed “hyperinfection.” In hyperinfection, filariform organisms exit the gut and migrate to the lungs, where they may be found in airways, alveoli, and blood vessels, and produce a hemorrhagic and eosinophilic pneumonia. When normal pathways of maturation are inhibited, the filariform larvae mature to egg-laying adults that give rise to rhabditiform larvae, and the presence of expectorated ova indicates hyperinfection (Fig. 8.123A). Parasitemia predisposes to gram-negative sepsis that can lead to concomitant DAD (see Fig. 8.123B).

**Dirofilaria.** In temperate climates, *Dirofilaria immitis* is a zoonosis that causes canine “heartworm.” Mosquitoes transfer microfilariae into subcutaneous tissues, where they mature silently and enter the systemic venous circulation. From there, they travel to the right heart, but in humans they do not mature further. Pulmonary disease reflects embolism of a nonviable helminth from the heart into the pulmonary circulation, where it generally lodges in a small muscular artery to produce an area of localized rounded infarction with a chronic immunologic reaction to the dead worm.<sup>101</sup> The embolic event itself may be clinically silent or associated with chest pain, fever, chills, hemoptysis, and peripheral blood eosinophilia. The disease is often first recognized as a solitary pulmonary nodule that is resected to exclude neoplasia.

Microscopically one sees a rounded area of pulmonary infarction (Fig. 8.124A). The diagnosis is facilitated by identifying the coiled nematode within an occluded muscular pulmonary artery. The area of surrounding necrosis is surrounded by a zone of granulomatous inflammation with lymphocytes, plasma cells, and variable degrees of tissue eosinophilia, all contained within a dense fibrous capsule. Trichrome, elastic, and reticulin stains highlight the features of the helminth and help to localize it in a vessel (see Fig. 8.124B and C). *Dirofilaria* are distinguished from other nematodes by their prominent muscular lateral cords and a striated cuticle that bulges inward in the region of the lateral cords, yielding a bat wings appearance.

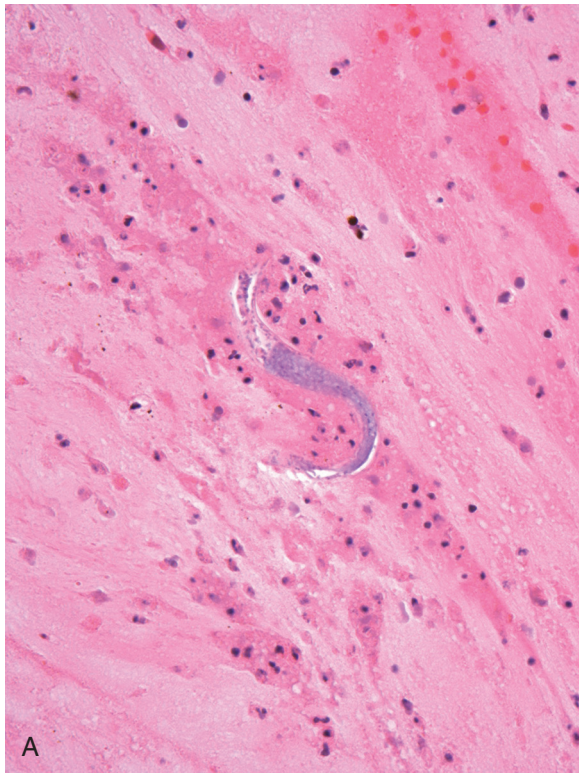
### Trematodes (Flukes)

A number of trematodes produce pulmonary disease that can present as solitary pulmonary nodules, pulmonary infarctions, necrotizing granulomas, or eosinophilic pneumonia. The most frequent fluke infection in the United States is *Schistosomiasis*, due to its wide distribution in both the Eastern and Western hemispheres.

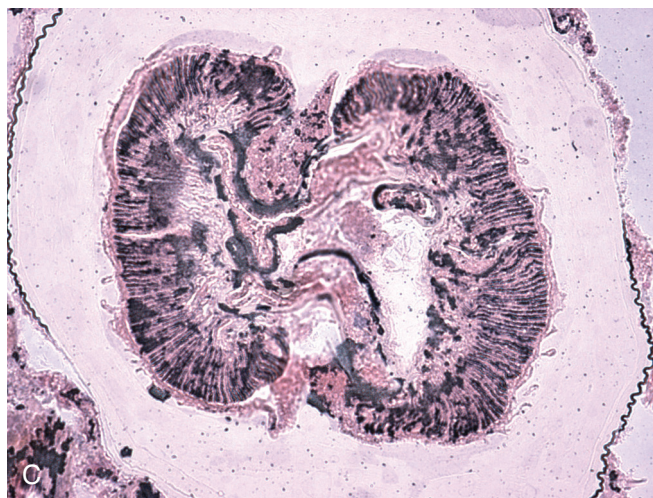
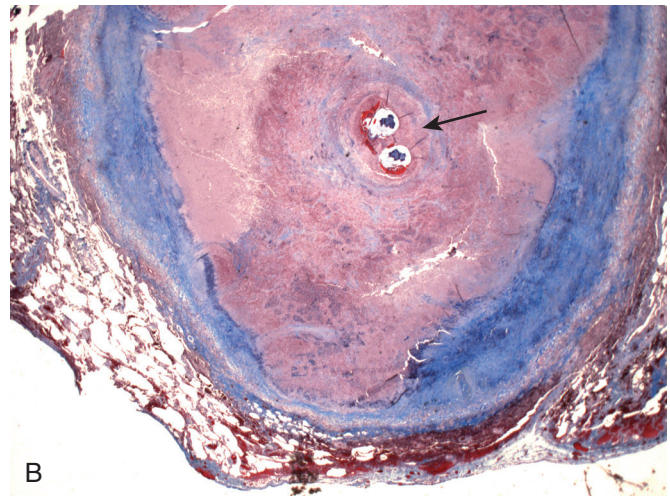
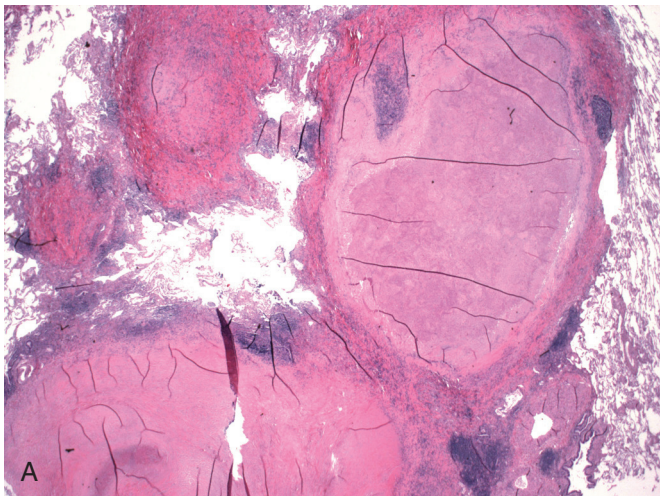
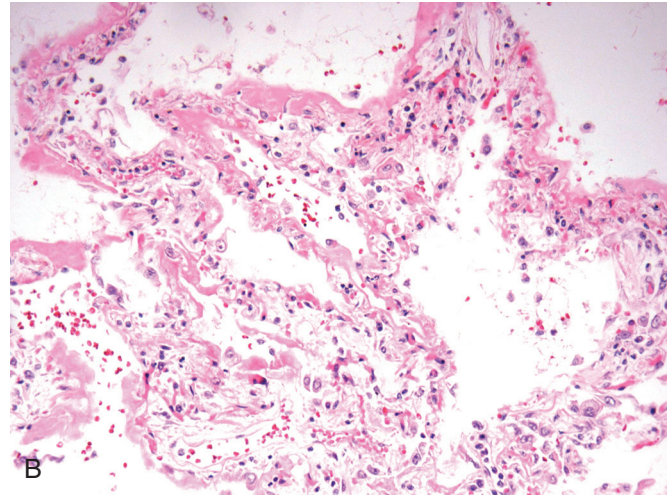
Pulmonary involvement reflects aberrant migration of adult worms into the lung, where they are found within pulmonary vessels (Fig. 8.125A). The helminth evokes an intense granulomatous and eosinophilic response, and extravascular refractile ova may be present and, like the helminth, can evoke granulomatous and eosinophilic reactions.

The ova are large (70 to 170  $\mu$ M) depending on the species. The ova of *Schistosomiasis mansoni*, which produces most cases of pulmonary disease, show a prominent lateral spine that can be seen with H&E and that is highlighted by modified acid-fast stains, although the latter finding is inconstant (see Fig. 8.125B). Other species, including *Schistosomiasis hematobium* and *Schistosomiasis japonicum*, rarely cause pulmonary disease, and their ova show either a prominent or inconspicuous terminal spine, respectively.

*Schistosomiasis* can also produce a granulomatous pulmonary hypertensive arteriopathy due to the presence of either ova or migrating schistosomules within small-caliber pulmonary arteries and arterioles (Fig. 8.126).<sup>102</sup> The thickened vascular walls show epithelioid histiocytes and giant cells with adventitial fibrosis and

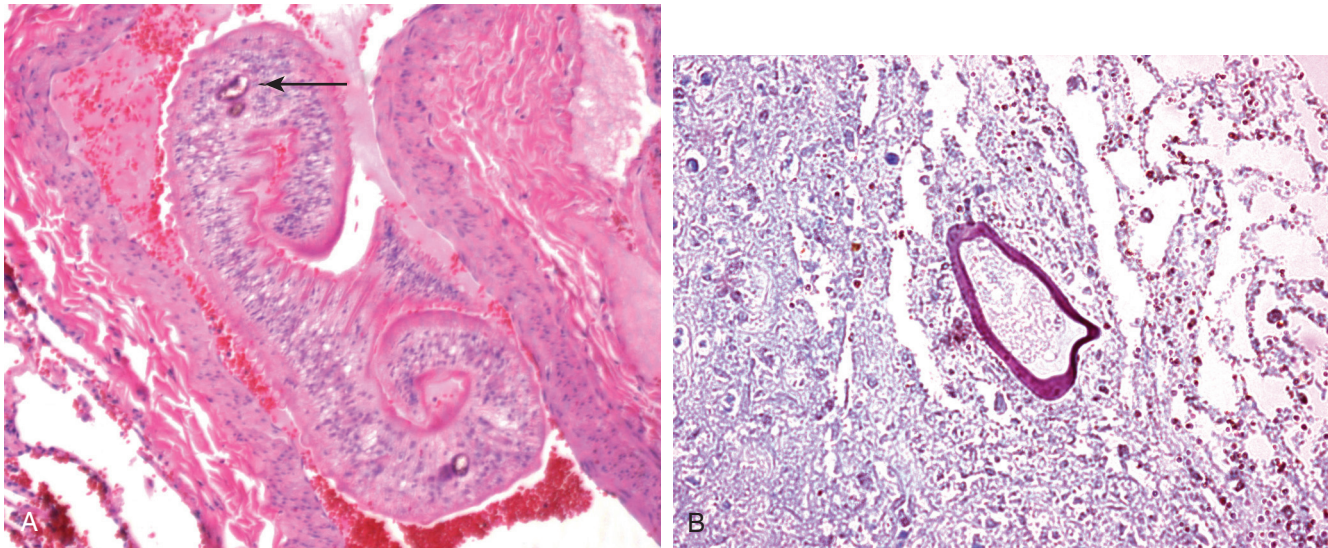


• **Figure 8.123** **A**, Rhadbitiform larval form of *S. stercoralis* in a patient with hyperinfection. **B**, Patient died from diffuse alveolar damage due to superimposed gram-negative sepsis.

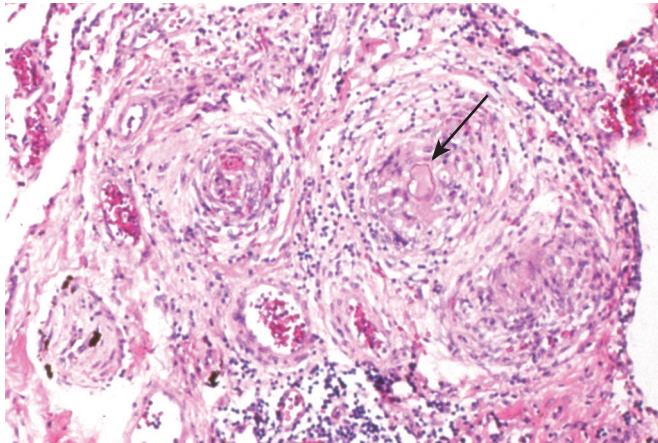


• **Figure 8.124** **A**, Nodular pulmonary infarction due to *D. immitis* seen in **(B)** trichrome and **(C)** reticulin stains. Nematode shows muscular lateral chords with invagination of overlying cuticle.





• **Figure 8.125** **A**, Coiled tuberculated schistosome within pulmonary artery. **B**, Large lateral spine and cortex of *S. mansoni* ovum is decorated by modified AFB stain.



• **Figure 8.126** Granulomatous pulmonary arteritis due to *S. mansoni*. Both eggs (arrow) and schistosomules can be found in vessels, although their demonstration may require the examination of multiple sections.

eosinophils. This disorder usually arises from infection by *S. mansoni* or less commonly *S. japonicum* that has already produced pipestem hepatic fibrosis and presinusoidal portal hypertension, leading to shunting of portal blood into the systemic venous circulation, with ova swept into the pulmonary arterial bed, where they evoke the pathologic response.

**Paragonimiasis.** *Paragonimus*, often referred to as the “lung fluke,” is a globally distributed trematode, with human disease limited to endemic regions.<sup>103</sup> Most cases in Asia are due to *Paragonimus westermani*, but other species are responsible for disease seen in Africa and Central and South America. Zoonotic forms of human infection rarely occur in North America secondary to *Paragonimus kellecotti* that affects rodents and cats.

The organism is a freshwater species that infects crabs and crayfish as intermediate hosts; the disease is transmitted to humans via ingestion of these crustaceans, although cases may be seen that are due to ingestion of contaminated seaweed or watercress. The larvae mature in the bowel and migrate through the diaphragm to infect the lung. Patients present with pulmonary infiltrates,

fever, weight loss, and malaise. Hemoptysis is common. Pleural involvement is present in approximately half of patients. Peripherally located cystic lesions develop in the lung, together with areas of pneumonic consolidation, and concomitant bacterial and mycobacterial infections may be present.

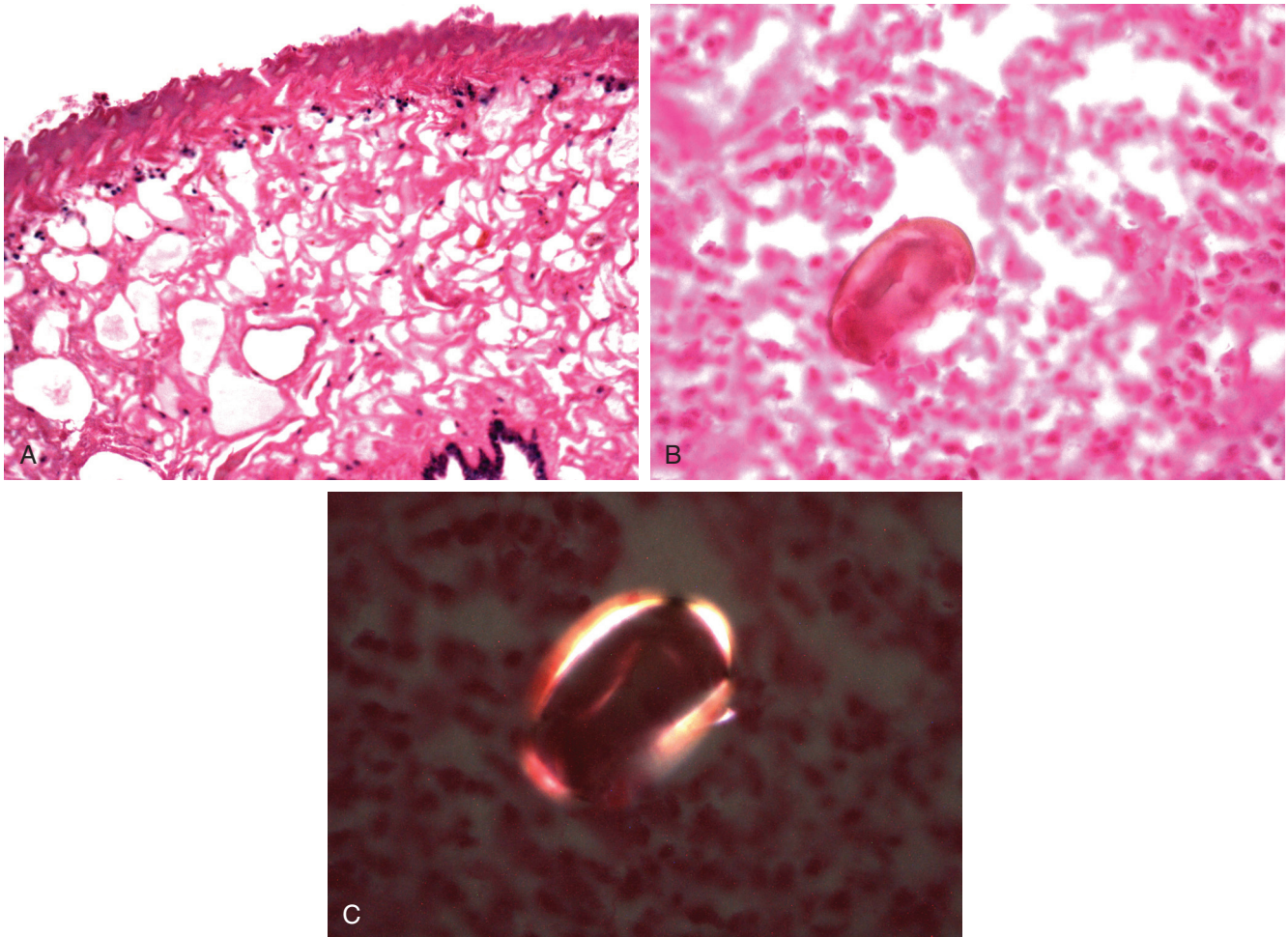
Grossly, *Paragonimus* is a large, 10-mm, reddish fluke. Its wall consists of a tegument with prominent spiny projections best seen on high-power examination of trichrome-stained sections (Fig. 8.127A). It exhibits prominent oral and ventral suckers and a loose internal stroma. The worm evokes a cystic necrotizing granulomatous and fibrotic response with tissue eosinophilia. The ova of *Paragonimus* are approximately 80  $\mu\text{m}$  and show a flattened operculum (see Fig. 8.127B). They are also intensely birefringent under polarized light, and this is an important distinguishing factor with respect to schistosome ova (see Fig. 8.127C).

### Cestodes (Tapeworms)

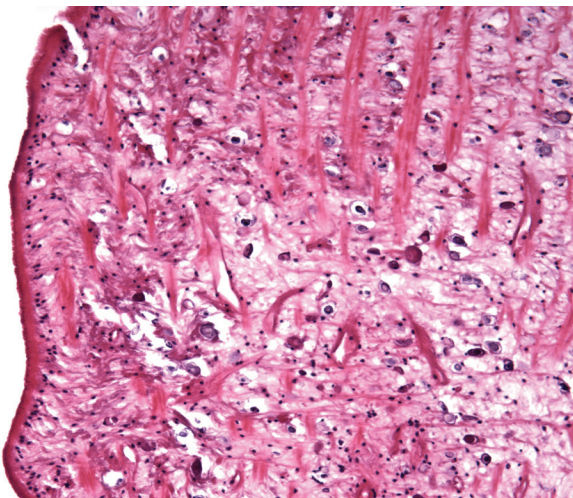
The most common cestode pathogen in the lung is *Echinococcus*, although other tapeworm larvae, including *Cysticercus* and *Sparaganum* can rarely infect the lung (Fig. 8.128).<sup>104</sup> The adult tapeworm lives attached to the wall of the small intestine of carnivorous canids. Intermediate hosts are the grazing ungulates, including sheep, goats, deer, and bison. In the continental United States, the disease is endemic to midwestern and western states.

Pulmonary disease is generally the result of preexisting hepatic involvement by *Echinococcus granulosus*, although other species, including *Echinococcus vogeli* and *Echinococcus multilocularis*, are also pathogenic.<sup>105</sup> The appearance of the disease is characteristic on chest radiographs that show single or multiple large fluid-filled cysts (Fig. 8.129). These cysts can be asymptomatic or cause symptoms due to compression of the surrounding airways and lung. Rupture into an airway can lead to suppurative pneumonia, the proliferation of new cysts, and generate fatal anaphylactic reactions.

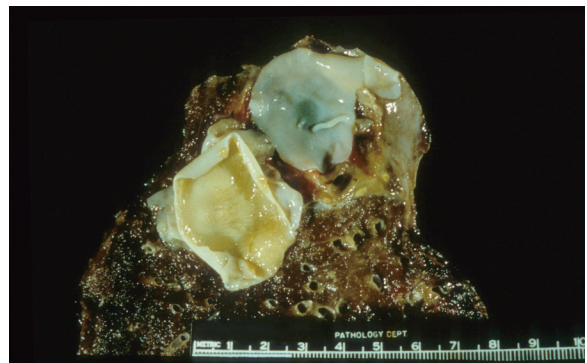
The cyst wall shows contributions from the cestode, as well as from the host. The inner germinative layer of the lamellar cyst wall is the matrix for protoscolices that detach to form secondary brood capsules (Fig. 8.130A). The rostellum of the attachment



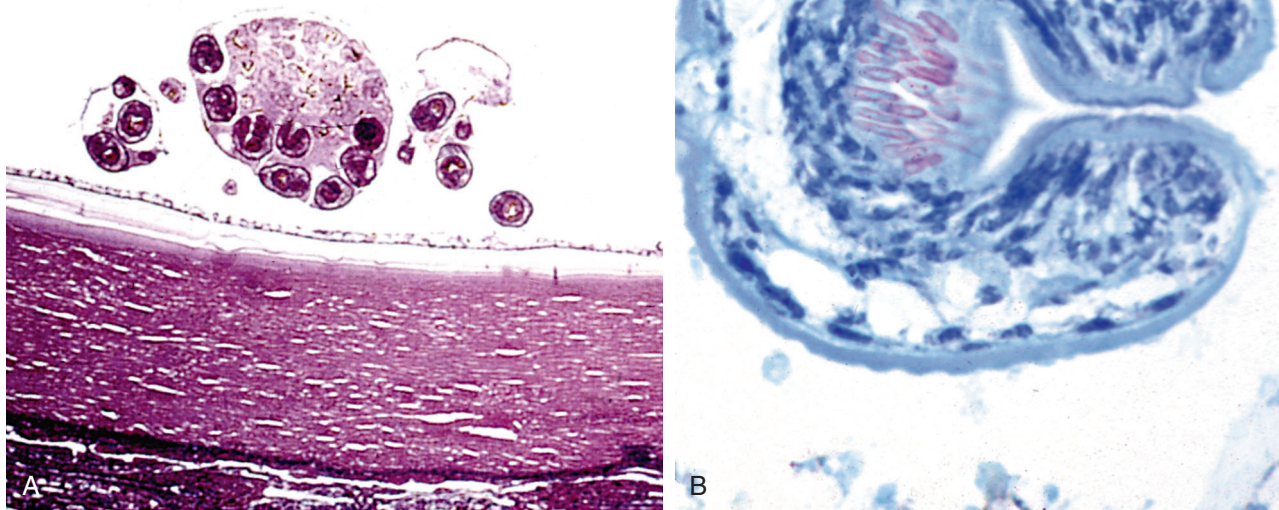
• **Figure 8.127** A, *Paragonimus* spp. are trematodes that show characteristic surface tegumental spikes. B, The ova of *Paragonimus* spp. are operculated, refractile, and (C) show diagnostic birefringence with polarized light.



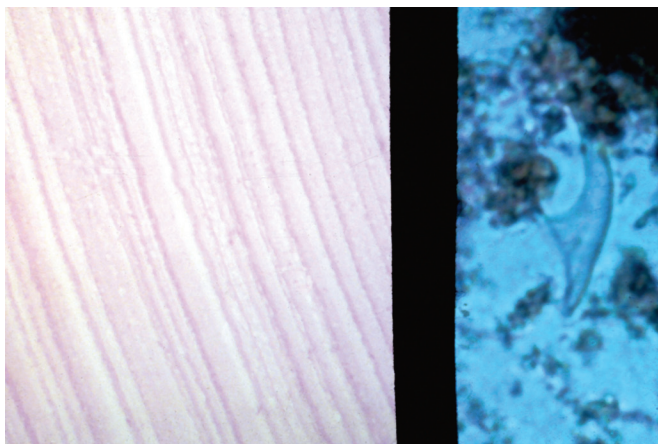
• **Figure 8.128** A cestode larval *sparganum* removed from lung.



• **Figure 8.129** Pulmonary cyst due to *E. granulosus*.



• **Figure 8.130** A, Germinative layer of echinococcal cyst giving rise to protoscolices. B, Rostellum and hooklets of a protoscolex stain with modified AFB.



• **Figure 8.131** Chitinous cyst wall (left panel) and refractile hooklet of *E. granulosus* (right panel).

apparatus of the protoscolex contains rows of hooklets that are refractile and stain with modified AFB (see Fig. 8.130B). The cestode component is acellular chitinous lamellar wall that is apparent with H&E and further highlighted with GMS, and within the cyst wall, detritus and hooklets give rise to so-called hydatid sand (Fig. 8.131).

### Microbes Associated With Bioterrorism

Recent world events have prompted interest in biological agents that can potentially be used as weapons of mass destruction. Several of these produce pneumonia and depend on dissemination

via aerosolized secretions to achieve their ignominious goal. Whereas most of these infections are naturally virulent, they tend to occur under situations that are no longer commonly encountered in modern societies. Their adoption by bioterrorists may include the need to bioengineer the organisms to promote their attack rate.

### Anthrax

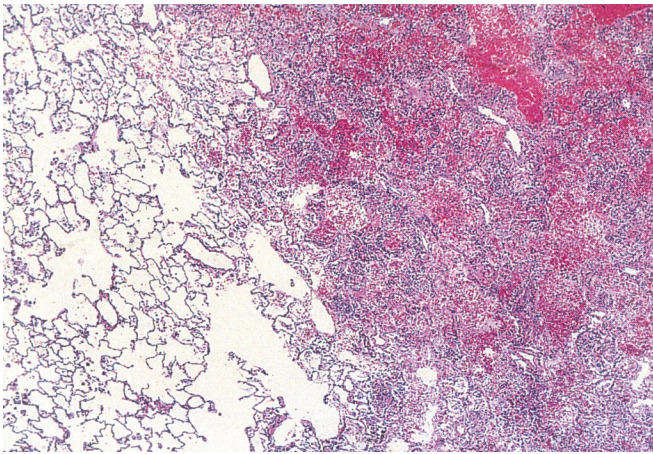
*Bacillus anthracis*, a toxin-producing gram-positive bacillus, was first isolated by Robert Koch as the cause of anthrax, a disease that primarily involved sheep and other farm animals. However, transmission to humans from infected animals has been recognized from antiquity as a complication of wool sorting (wool sorter's disease). An epidemic of inhalational anthrax occurred in 1979 at a biofacility in Sverdlovsk, in the former Union of Soviet Socialist Republics (USSR), and in 2001 there was a limited epidemic of anthrax due to contaminated letters sent through the US mail service by an unidentified terrorist.<sup>106</sup>

Cutaneous penetration by the bacillus produces a necrotic eschar with rapid extension to blood vessels, resulting in bacteremia, sepsis, meningitis, and death. However, the most deadly form of infection is pulmonary. In these cases the bacilli are inhaled, which evokes a localized hemorrhagic pneumonia and associated pleural effusion. Organisms proliferate rapidly in the lung, where they produce a localized hemorrhagic pneumonia with scant neutrophilic reaction, (Fig. 8.132) and spread via the pulmonary lymphatics to the regional lymph nodes to produce hemorrhagic mediastinitis, followed by bacteremia, toxic shock, and death in a high percentage of cases. The diagnosis must be suspected and treated early to be curable. However, it has most

often first been recognized at autopsy, where tissues prove to be teeming with bacteria.

### *Yersinia pestis* (Plague Pneumonia)

Plague has played an important role in world history. The causative agent is *Y. pestis*, a gram-negative rod that is carried by animal fleas.<sup>107</sup> Infection occurs as the result of contact with infected animals via aerosol or direct contact with infected secretions. Throughout history, the black rat, *Rattus rattus*, has been most responsible worldwide for the persistence and spread of plague in urban epidemics, but any rodent can mechanically transmit infected fleas. Although *Y. pestis* has not yet been seen as a bioterrorist agent, it has received attention as a potential weapon of mass destruction because as few as 1 to 10 bacilli are sufficient to cause infection when introduced via the oral, intradermal, subcutaneous, or intravenous routes.



• **Figure 8.132** Hemorrhagic pneumonia due to anthrax.

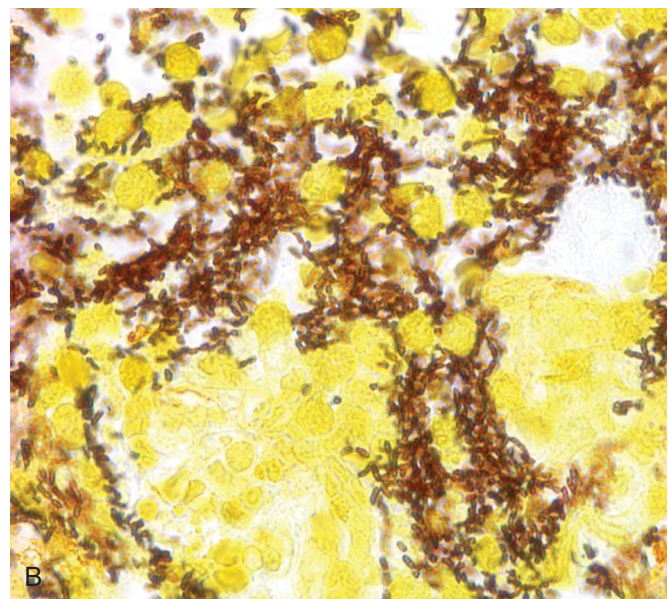
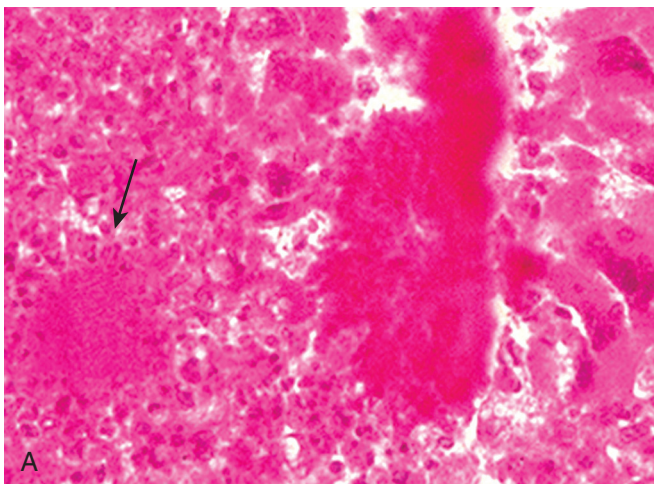
*Yersinia* produces a necrotizing hemorrhagic pneumonia and large numbers of extracellular organisms that can be seen with H&E (Fig. 8.133). Pulmonary infection leads rapidly to bacteremia and to death by sepsis.

### *Francisella tularensis* (Tularemia Pneumonia)

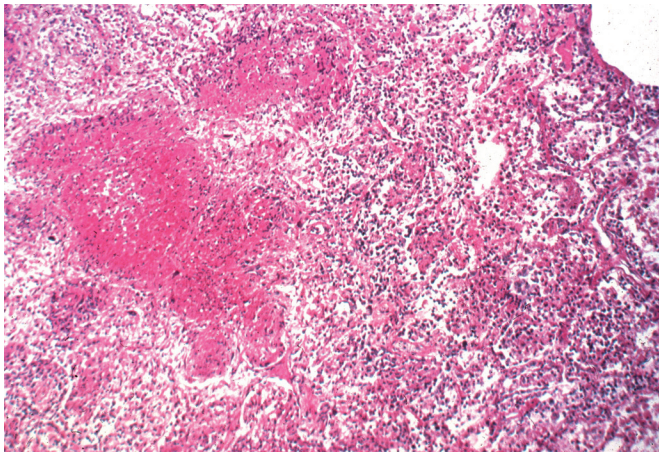
Tularemia causes a necrotizing bronchopneumonia that leads to sepsis and death. However, the gram-negative bacillus is less virulent than either anthrax or plague, and it produces a relatively slow progression of disease, a fact that limits its potential role as an agent of bioterrorism.<sup>108</sup> The histologic response in the lung is polymorphic and includes an early hemorrhagic granulohistiocytic response with microabscess formation (Fig. 8.134), followed by granulomatous inflammation. When these coexist, the appearance of this infection is characteristic. The short coccobacillary forms require silver impregnation to be visualized in tissues.

### Pleural Infection

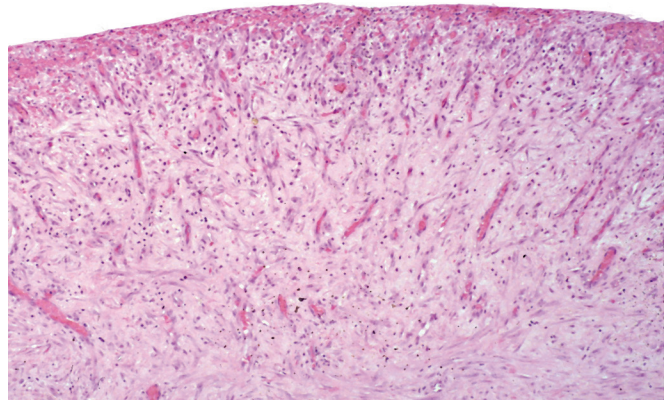
Parapneumonic effusions can complicate bacterial pneumonias, but they are rarely biopsied unless they lead to a restrictive rind around the lung requiring decortication (Fig. 8.135). Both gram-positive and gram-negative bacteria can produce empyema (i.e., abscess in the pleural space) (Fig. 8.136A and B). Mycobacteria (Fig. 8.137), actinomyces (Fig. 8.138), fungi (Fig. 8.139), and parasites can all produce pleural disease, and the nature of the inflammatory response will substantially assist in narrowing the differential diagnosis, even when organisms cannot be identified. Tuberculosis can result years later in a fibrothorax, often with dystrophic calcification, but with no residual granulomatous response. Pleural eosinophilia can be a clue to the presence of an underlying parasitic infection (Fig. 8.140) but can also be seen in fungal and mycobacterial infections, in response to drugs and pleural metastases, and following pneumothorax.



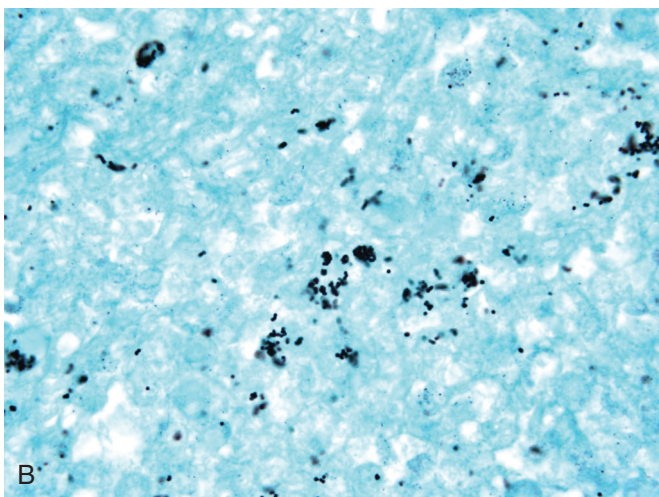
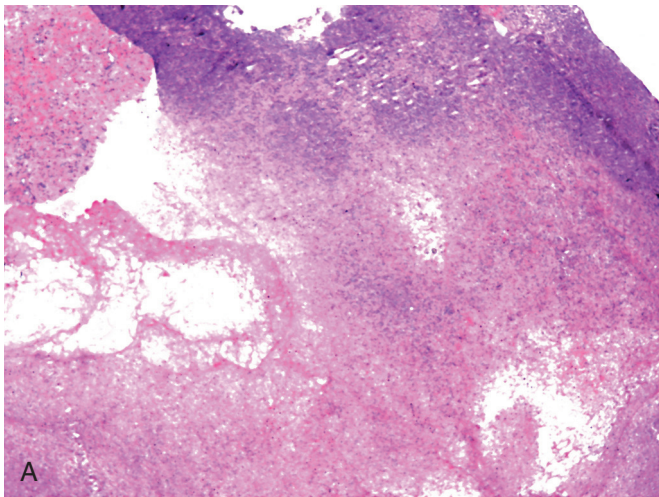
• **Figure 8.133** A, Necrotizing hemorrhagic pneumonia due to plague (*Y. pestis*). Organisms are seen both in hematoxylin and eosin— (arrow) and (B) silver-stained sections.



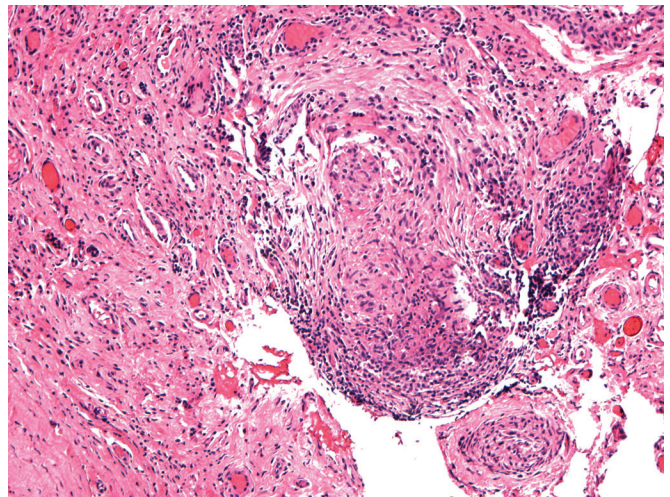
• **Figure 8.134** Granulomatous pneumonia due to tularemia.



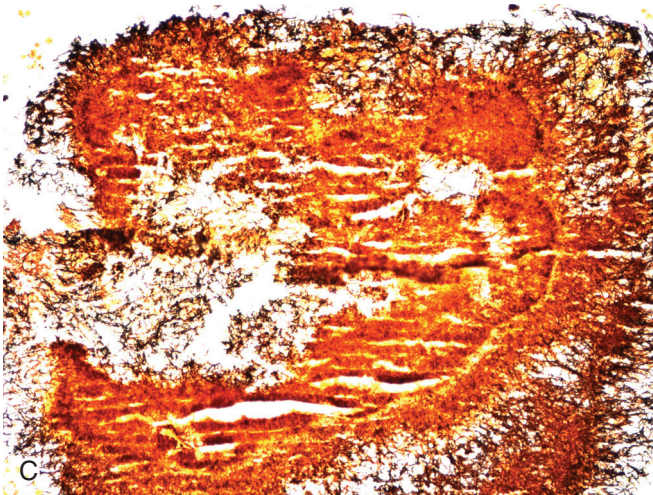
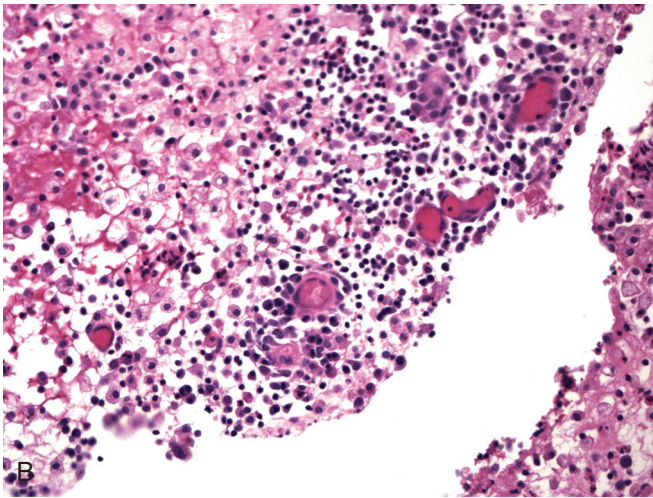
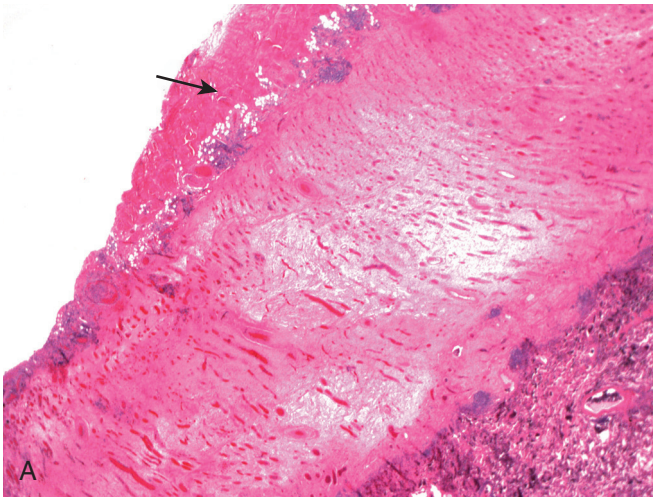
• **Figure 8.135** Organizing fibrinous pleuritis due to pneumococcal pneumonia. Patient had parapneumonic effusion.



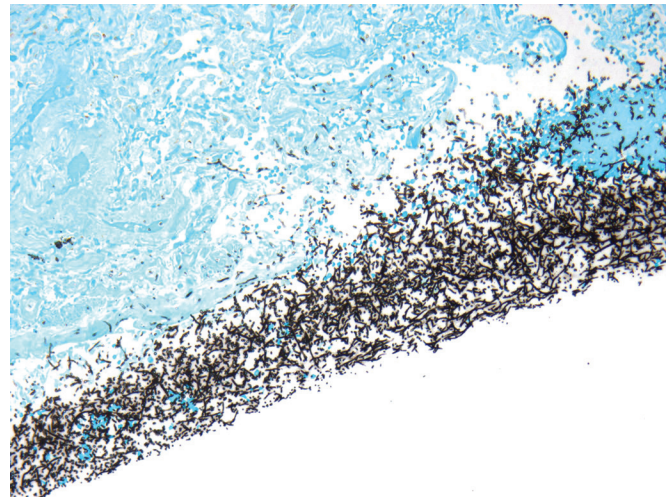
• **Figure 8.136** A, Empyema secondary to staphylococcal pneumonia. B, Clusters of cocci are stained by Gomori methenamine silver.



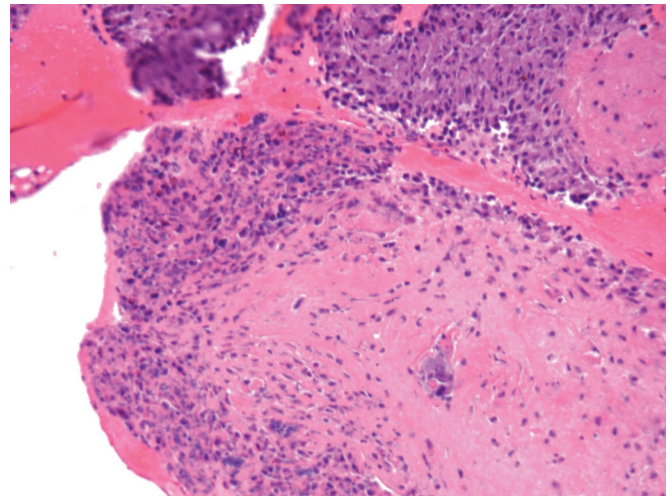
• **Figure 8.137** Granulomatous pleuritis in tuberculosis.



• **Figure 8.138** **A**, Dense pleural adhesion transgressing diaphragm (arrow). **B**, Abscess cavity with granulohistiocytic inflammation. **C**, Steiner stain shows filamentous bacteria in sulfur granule. Organisms were also positive with tissue Gram stain and Gomori methenamine silver.



• **Figure 8.139** Aspergillus pleuritis.



• **Figure 8.140** Eosinophilic calcifying pleuritis in a patient with underlying *Trichuris* infection.

## References

1. Marr K, Patterson T, Denning D. Aspergillosis. Pathogenesis, clinical manifestations, and therapy. *Infect Dis Clin North Am*. 2002;16:875-894.
2. Toledo-Pereyra L. Benefit of open lung biopsy in patients with previous non-diagnostic transbronchial lung biopsy: a guide to appropriate treatment. *Chest*. 1980;77:647-650.
3. Vélez L, Correa LT, Maya MA, et al. Diagnostic accuracy of bronchoalveolar lavage samples in immunosuppressed patients with suspected pneumonia: analysis of a protocol. *Respir Med*. 2007;101:2160-2167.
4. Jaffe J, Maki D. Lung biopsy in immunocompromised patients: one institution's experience and an approach to management of pulmonary disease in the compromised host. *Cancer*. 1981;48:1144.
5. Nasuti J, Gupta P, Baloch Z. Diagnostic value and cost-effectiveness of on-site evaluation of fine needle aspiration specimens: review of 5,688 cases. *Diagn Cytopathol*. 2002;27:1-4.
6. Harkin TJ, et al. Transbronchial needle aspiration in patients infected with HIV. *Am J Respir Crit Care Med*. 1998;157:1913-1919.
7. Navan N, Molyneaux PL, Breen RA, Connell DW, Jepson A, Nankvell M. Utility of endobronchial ultrasound-guided transbronchial needle aspiration in patients with tuberculous intrathoracic lymphadenopathy: a multicentre trial. *Thorax*. 2011;66:889-893.
8. McKenna R, Mountain C, McMurtey M. Open lung biopsy in immunocompromised patients. *Chest*. 1984;86:671.
9. Leslie K, Will M. *Practical Pulmonary Pathology*. Philadelphia: Churchill Livingstone; 2005.
10. Koneman E, Gade W. Mycology at a distance. *Clin Lab Sci*. 2002;15:131-135.
11. Kradin R, Mark E. Pathology of pulmonary disorders due to aspergillus spp. *Arch Pathol Lab Med*. 2008;132:606-614.
12. Kradin R. Pulmonary immune response. In: Kradin R, Robinson B, eds. *Immunopathology of the Lung*. Boston, MA: Butterworth-Heinemann; 1996:1-13.
13. MacLean JA, Xia W, Pinto CE, Zhao L, Liu HW, Kradin RL. Sequestration of inhaled particulate antigens by lung phagocytes. A mechanism for the effective inhibition of pulmonary cell-mediated immunity. *Am J Pathol*. 1996;148:657-666.
14. O'Donnell WJ, Kradin RL, Evins AE, Wittram C. Case records of the Massachusetts General Hospital. Weekly clinicopathological exercises. Case 39-2004. A 52-year-old woman with recurrent episodes of atypical pneumonia. *N Engl J Med*. 2004;351:2741-2749.
15. Mandal RV, Mark EJ, Kradin RL. Organizing pneumonia and pulmonary lymphatic architecture in diffuse alveolar damage. *Hum Pathol*. 2008;39:1234-1238.
16. Gerberding JL, Morgan JG, Shepard JA, Kradin RL. Case records of the Massachusetts General Hospital. Weekly clinicopathological exercises. Case 9-2004. An 18-year-old man with respiratory symptoms and shock. *N Engl J Med*. 2004;350:1236-1247.
17. Neumann G, Noda T, Kawaoka Y. Emergence and pandemic potential of swine-origin H1N1 influenza virus. *Nature*. 2009;459:931-939.
18. Yeldandi AV, Colby TV. Pathologic features of lung biopsy specimens from influenza pneumonia cases. *Hum Pathol*. 1994;25:47.
19. Oseasohn R, Adelson L, Kaji M. Clinicopathologic study of the thirty-three fatal cases of Asian influenza. *N Engl J Med*. 1959;260:509.
20. Franks TJ, Chong PY, Chui P, et al. Lung pathology of severe acute respiratory syndrome (SARS): a study of 8 autopsy cases. *Hum Pathol*. 2003;34:743-748.
21. Memish ZA, Zumla AI, Al-Hakeem RF, Al-Rabeeh AA, Stephens GM. Family cluster of middle east respiratory syndrome coronavirus infections. *N Engl J Med*. 2013;368:2487-2494.
22. Groothuis JR, Gutierrez KM, Lauer BZ. Respiratory syncytial virus infection in children with bronchopulmonary dysplasia. *Pediatrics*. 1988;82:199.
23. Nicholls JM, Poon LL, Lee KC, et al. Lung pathology of fatal severe acute respiratory syndrome. *Lancet*. 2003;361:1773-1778.
24. Kipps A, Kaschula R. Virus pneumonia following measles: a virological and histological study of autopsy material. *S Afr Med J*. 1976;50:1083-1088.
25. Ohori NP, Michaels MG, Jaffe R, Williams P, Yousem SA. Adenovirus pneumonia in lung transplant recipients. *Hum Pathol*. 1995;26:1073-1079.
26. Drew WL. Cytomegalovirus infection in patients with AIDS. *Clin Infect Dis*. 1992;4:608.
27. Strickler JG, Manivel JC, Copenhaver CM, Kubic VL. Comparison of in situ hybridization and immunohistochemistry for detection of cytomegalovirus and herpes simplex virus. *Hum Pathol*. 1990;21:443-448.
28. Ramsey PG, Fife KH, Hackman RC, Meyers JD, Corey L. Herpes simplex virus pneumonia: clinical, virologic, and pathologic features in 20 patients. *Ann Intern Med*. 1982;97:813.
29. Graham BS, Snell JD Jr. Herpes simplex virus infection of the adult lower respiratory tract. *Medicine (Baltimore)*. 1983;62:384.
30. Shenoy ES, Lai PS, Shepard JA, Kradin RL. Case records of the Massachusetts General Hospital. Case 39-2015. A 22-year-old man with hypoxemia and shock. *N Engl J Med*. 2015;373:2456-2466.
31. Sargent EN, Carson MJ, Reilly ED. Roentgenographic manifestation of varicella pneumonia with post-mortem correlation. *Am J Roentgenol Radium Ther Nucl Med*. 1967;98:305-317.
32. Duchin JS, Koster FT, Peters CJ, et al. Hantavirus pulmonary syndrome: a clinical description of 17 patients with a newly recognized disease. *N Engl J Med*. 1994;330:949.
33. Nolte KB, Feddersen RM, Foucar K, et al. Hantavirus pulmonary syndrome in the United States: a pathological description of a disease caused by a new agent. *Hum Pathol*. 1995;26:110.
34. Rollins S, Colby T, Clayton F. Open lung biopsy in *Mycoplasma pneumoniae* pneumonia. *Arch Pathol Lab Med*. 1986;110:34-41.
35. Marzouk K, Corate L, Saleh S, Sharma OP. Epstein-Barr-virus-induced interstitial lung disease. *Curr Opin Pulm Med*. 2005;11:456-460.
36. Weber WR, Askin FB, Dehner LP. Lung biopsy in *Pneumocystis carinii* pneumonia. A histopathologic study of typical and atypical features. *Am J Clin Pathol*. 1977;67:11.
37. Amin MB, Mezger E, Zarbo RJ. Detection of *Pneumocystis carinii*. Comparative study of monoclonal antibody and silver staining. *Am J Clin Pathol*. 1992;98:13.
38. Travis WD, Pittaluga S, Lipschik GY, et al. Atypical pathologic manifestations of *Pneumocystis carinii* pneumonia in the acquired immune deficiency syndrome. Review of 123 lung biopsies from 76 patients with emphasis on cysts, vascular invasion, vasculitis, and granulomas. *Am J Surg Pathol*. 1990;14:615.
39. Vawter GG, Shwachman H. Cystic fibrosis in adults: an autopsy study. *Pathol Annu*. 1979;14:357-382.
40. Polosa R, Cacciola RR, Prosperini G, Spicuzza L, Morjaria JB, Di Maria GU. Endothelial-coagulative activation during chronic obstructive pulmonary disease exacerbations. *Haematologica*. 2008;93:1275-1276.
41. Stevens DA, Moss RB, Kurup VP, et al. Allergic bronchopulmonary aspergillosis in cystic fibrosis—state of the art: Cystic Fibrosis Foundation Consensus Conference. *Clin Infect Dis*. 2003;37:S225.
42. Branson D. Identification of Micrococcaceae in clinical bacteriology. *Appl Microbiol*. 1968;16:906-911.
43. Yousem SA. The historical spectrum of chronic necrotizing forms of pulmonary aspergillosis. *Hum Pathol*. 1997;28:650.
44. Tuomanen E, Austrian R, Masure H. Pathogenesis of pneumococcal pneumonia. *N Engl J Med*. 1995;332:1280-1284.
45. Barnham M. Rapidly fatal group B and G streptococcal infections in adults. *J Infect*. 1980;2:279-281.

46. Gilet Y, Issartel B, Vanheims P. Association between strains carrying gene for Panton-Valentine leukocidin and highly lethal necrotising pneumonia in young immunocompetent patients. *Lancet*. 2002;359:753-759.
47. Pierce AK, Edmonson EB, McGee G, Ketchersid J, Loudon RG, Sanford JP. An analysis of factors predisposing to gram-negative bacillary necrotizing pneumonia. *Am Rev Respir Dis*. 1966;94:309-315.
48. Kirtland SH, Corley DE, Winterbauer RH. The diagnosis of ventilator-associated pneumonia. *Chest*. 1997;112:445-457.
49. le Roux B, Mohlala M, Odell J, Whitton I. Suppurative diseases of the lung and pleural space. Part I: empyema thoracis and lung abscess. *Curr Probl Surg*. 1986;23:1-89.
50. Brown JR. Human actinomycosis—a study of 181 subjects. *Hum Pathol*. 1973;4:319.
51. Winslow DJ. Botryomycosis. *Am J Pathol*. 1959;35:153.
52. Beaman BL, Burnside J, Edwards B, Causey W. Nocardial infections in the United States, 1972–1974. *J Infect Dis*. 1976;134:286.
53. Winn WC, Myerowitz RL. The pathology of the *Legionella* pneumonias. A review of 74 cases and literature. *Hum Pathol*. 1981;12:401-422.
54. Harvey RL, Sunstrum JC. *Rhodococcus equi* infection in patients with and without human immunodeficiency virus infection. *Rev Infect Dis*. 1991;13:139.
55. Kwon KY, Colby TV. *Rhodococcus equi* pneumonia and pulmonary malakoplakia in acquired immunodeficiency syndrome: pathologic features. *Arch Pathol Lab Med*. 1994;118:744.
56. Lozupone C, Cota-Gomez A, Palmer BE, et al. Widespread colonization of the lung by *Tropheryma whippelii* in HIV Infection. *Am J Respir Crit Care Med*. 2013;187:1110-1117.
57. Dobbins W. Diagnosis of Whipple's disease. *N Engl J Med*. 1995;332:390-392.
58. Sepkowitz KA, Raffalli J, Riley L. Tuberculosis in the AIDS era. *Clin Microbiol Rev*. 1995;8:180.
59. Dannenberg AM Jr. Delayed-type hypersensitivity and cell-mediated immunity in the pathogenesis of tuberculosis. *Immunol Today*. 1991;12:228.
60. Kim JH, Langston AA, Gallis HA. Miliary tuberculosis: epidemiology, clinical manifestations, diagnosis, and outcome. *Rev Infect Dis*. 1990;12:583.
61. Lupatkin H, Brau N, Flomenberg P, Simberkoff MS. Tuberculosis abscess in patients with AIDS. *Clin Infect Dis*. 1992;14:1040.
62. Woods GL, Washington JA II. Mycobacteria other than *Mycobacterium tuberculosis*: review of microbiologic and clinical aspects. *Rev Infect Dis*. 1987;9:275.
63. Inderlied CB, Kemper CA, Bermudez LEM. The *Mycobacterium avium* complex. *Clin Microbiol Rev*. 1993;6:266.
64. Strom RL, Gruninger RP. AIDS with *Mycobacterium avium-intracellulare* lesions resembling those of Whipple's disease. *N Engl J Med*. 1983;309:1323.
65. Klatt EC, Jensen DF, Meyer PR. Pathology of *Mycobacterium avium-intracellulare* infection in acquired immunodeficiency syndrome. *Hum Pathol*. 1987;18:709.
66. Greenberger PA, Katzenstein AL. Lipid pneumonia with atypical mycobacterial colonization. Association with allergic bronchopulmonary aspergillosis. *Arch Intern Med*. 1983;143:2003-2005.
67. Piggott J, Hocholzer L. Human melioidosis. *Arch Pathol*. 1970;90:101-111.
68. Goodwin RA Jr, Des Prez RM. Histoplasmosis. *Am Rev Respir Dis*. 1978;117:929.
69. Wheat LJ, Slama TG, Zeckel ML. Histoplasmosis in the acquired immune deficiency syndrome. *Am J Med*. 1985;78:203.
70. Goodwin RA Jr, Des Prez RM. Pathogenesis and clinical spectrum of histoplasmosis. *South Med J*. 1973;66:13.
71. Sarosi GA, Johnson PC. Disseminated histoplasmosis in patients infected with human immunodeficiency virus. *Clin Infect Dis*. 1992;14(suppl 1):S60-S67.
72. Gottridge JA, Meyer BR, Schwartz NS, Lesser RS. The nonutility of chest roentgenographic examination in asymptomatic patients with positive tuberculin test results. *Arch Intern Med*. 1989;149:1660-1662.
73. Tenenbaum MJ, Greenspan J, Kerkering TM. Blastomycosis. *Crit Rev Microbiol*. 1982;9:139.
74. Mansour MK, Ackman JB, Branda JA, Kradin RL. Case records of the Massachusetts General Hospital. Case 32-2015. A 57-year-old man with severe pneumonia and hypoxemic respiratory failure. *N Engl J Med*. 2015;373:1554-1564.
75. Tuttle JG, Lichtwardt HE, Altshuler CH. Systemic North American blastomycosis. Report of a case with small forms of blastomycetes. *Am J Clin Pathol*. 1953;23:890.
76. Watts JC, Chandler FW, Mihalov ML, Kammeyer PL, Armin AR. Giant forms of *Blastomyces dermatitidis* in the pulmonary lesions of blastomycosis: potential confusion with *Coccidioides immitis*. *Am J Clin Pathol*. 1990;93:575.
77. Mitchell TG, Perfect JR. Cryptococcosis in the era of AIDS—100 years after the discovery of *Cryptococcus neoformans*. *Clin Microbiol Rev*. 1995;8:515.
78. Lazcano O, Speights VO Jr, Strickler JG, Bilbao JE, Becker J, Diaz J. Combined histochemical stains in the differential diagnosis of *Cryptococcus neoformans*. *Mod Pathol*. 1993;6:80-84.
79. Stevens DA. Coccidioidomycosis. *N Engl J Med*. 1995;332:1077.
80. Singh VR, Smith DK, Lawrence J, et al. Coccidioidomycosis in patients infected with human immunodeficiency virus: review of 91 cases at a single institution. *Clin Infect Dis*. 1996;23:563.
81. Drut R. Paracoccidioidomycosis: diagnosis by fine-needle aspiration cytology. *Diagn Cytopathol*. 1995;13:52-53.
82. Rose HD, Sheth NK. Pulmonary candidiasis. A clinical and pathological correlation. *Arch Intern Med*. 1978;138:964-965.
83. Okudaira M, Kurata H, Sakabe F. Studies on the fungal flora in the lung of human necropsy cases. A critical survey in connection with the pathogenesis of opportunistic fungus infections. *Mycopathologia*. 1977;61:3-18.
84. Fishman JA, Kubak BM. Clinical cases in transplantation. *Transpl Infect Dis*. 2002;4(suppl 3):62-66.
85. McCarthy DS, Pepys J. Allergic broncho-pulmonary aspergillosis. Clinical immunology. 2. Skin, nasal and bronchial tests. *Clin Allergy*. 1971;1:415.
86. Basich JE, Graves TS, Nasir Baz M, et al. Allergic bronchopulmonary aspergillosis in corticosteroid-dependent asthmatics. *J Allergy Clin Immunol*. 1981;68:98.
87. Gefter WB. The spectrum of pulmonary aspergillosis. *J Thorac Imaging*. 1972;7:56.
88. Smith FB, Beneck D. Localized Aspergillus infestation in primary lung carcinoma. Clinical and pathological contrasts with post-tuberculous intracavitary aspergilloma. *Chest*. 1991;100:554-556.
89. Roehrl MH, Croft WJ, Liao Q, Wang JY, Kradin RL. Hemorrhagic pulmonary oxalosis secondary to a noninvasive *Aspergillus niger* fungus ball. *Virchows Arch*. 2007;451:1067-1073.
90. Stergiopoulou T, Meletiadis J, Roilides E, et al. Host-dependent patterns of tissue injury in invasive pulmonary aspergillosis. *Am J Clin Pathol*. 2007;127:349-355.
91. Segal BH, DeCarlo ES, Kwon-Chung KJ, Malech HL, Gallin JJ, Holland SM. Aspergillus nidulans infection in chronic granulomatous disease. *Medicine (Baltimore)*. 1998;77:345-354.
92. Sugar AM. Mucormycosis. *Clin Infect Dis*. 1992;14(suppl 1):S126.
93. D'Haese J, Theunissen K, Vermeulen E, et al. Detection of galactomannan in bronchoalveolar lavage fluid samples of patients at risk for invasive pulmonary aspergillosis: analytical and clinical validity. *J Clin Microbiol*. 2012;50:1258-1263.
94. Fader RC, McGinnis MR. Infections caused by dematiaceous fungi: chromoblastomycosis and phaeohyphomycosis. *Infect Dis Clin North Am*. 1988;2:925.
95. Sekhon AS, Stein L, Garg AK, Black WA, Glezos JD, Wong C. Pulmonary penicilliosis marneffeii: report of the first imported case in Canada. *Mycopathologia*. 1994;128:3-7.



96. Gutierrez Y. *The Intestinal Amebae*. Philadelphia: Lea and Febiger; 1990.
97. Bertoli F, Espino M, Arosemena JR, et al. A spectrum in the pathology of toxoplasmosis in patients with acquired immunodeficiency syndrome. *Arch Pathol Lab Med*. 1995;119:214.
98. Current WL, Garcia LS. Cryptosporidiosis. *Clin Lab Med*. 1991;11:873.
99. Giang TT, Kotler DP, Garro ML, Orenstein JM. Tissue diagnosis of intestinal microsporidiosis using the chromotrope-2R modified trichrome stain. *Arch Pathol Lab Med*. 1993;117:1249.
100. Gutierrez Y. *Rhabdita-Strongyloides and Other Free Living Nematodes*. Philadelphia: Lea and Febiger; 1990.
101. Echeverii A, Long R, Check W, Burnett C. Pulmonary dirofilariasis. *Ann Thorac Surg*. 1999;67:201-202.
102. Sadigursky M, Andrade Z. Pulmonary changes in schistosomal cor pulmonale. *Am J Trop Med Hyg*. 1982;31:779-784.
103. Bercovitz Z. Clinical studies on human lung fluke disease (Endemic Hemoptysis) caused by *paragonimus westermani* infestation. *Am J Trop Med*. 1937;1937:101-122.
104. Iwatani K, Kubota I, Hirotsu Y, et al. Sparganum mansonii parasitic infection in the lung showing a nodule. *Pathol Int*. 2006;56:674-677.
105. Katz AM, Pam CT. Echinococcus disease in the United States. *Am J Med*. 1958;25:759.
106. Abramova F, Grinberg L, Yampolskaya O, Walker D. Pathology of inhalational anthrax in 42 cases from the Sverdlovsk outbreak of 1979. *Proc Natl Acad Sci U S A*. 1993;90:2291-2294.
107. Pollitzer R. *Plague*. Geneva: World Health Organization; 1954.
108. Guarner J, Jennigan J, Shieh W, et al. Pathology and pathogenesis of bioterrorism-related inhalational anthrax. *Am J Pathol*. 2003; 163:701-709.